Nebraska Laser Eye Associates

Spring 2015

Refractive Update

Ablative photodecomposition

John H. BROPHY, Joel A. SILVER and James L. KINSEY
Department of Chemistry, Massachusetts Institute of Technology, Cambridge, Massachusetts 02139, USA

Received 25 May 1974
Revised manuscript received 11 June 1974

Excimer wavelength photons interact with organic molecules

North-Holland Publishing Company

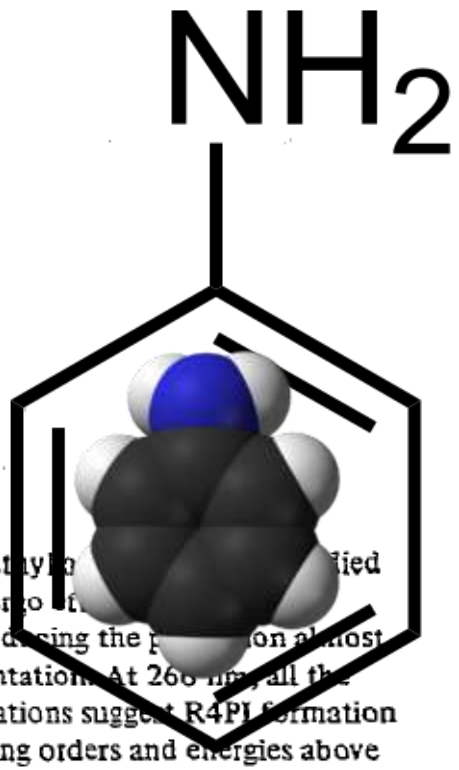

RESONANCE ENHANCED LASER IONISATION MASS SPECTROMETRY OF FOUR AROMATIC MOLECULES

Charles T. RETTNER * and John H. BROPHY **
Massachusetts Institute of Technology, Cambridge, Massachusetts 02139, USA

Received 12 September 1980

Multiphoton ionisation and fragmentation of aniline, benzene, N,N-dimethyl and 2,4-dimeth[illegible]lied by laser ionisation mass spectrometry under collision free conditions. All four molecules under[illegible] enhanced two-photon ionisation (R2PI) with relatively low laser intensities at λ = 266 nm produ[illegible]cing the p[illegible]on almost exclusively. At higher intensities, higher order processes compete producing extensive fragmentation. At 266 nm all the major fragment ions are produced by R3PI. For aniline excited at 294 nm, energetic considerations suggest R4PI formation of fragments with differences in fragmentation between 266 and 294 nm reflecting the differing orders and energies above threshold of the competing processes. Comparison of R2PI efficiencies in aniline and benzene shows that the cross sections for ionisation of the resonant intermediate $^1B_2$ excited state in both molecules are approximately equal and independent of wavelength in the range 250–300 nm.

High-Speed Photography of Excimer Laser Ablation of the Cornea

Carmen A. Puliafito, MD; David Stern, MS; Ronald R. Krueger, MD; Eric R. Mandel, MD

Arch Ophthalmol—Vol 105, Sept 1987

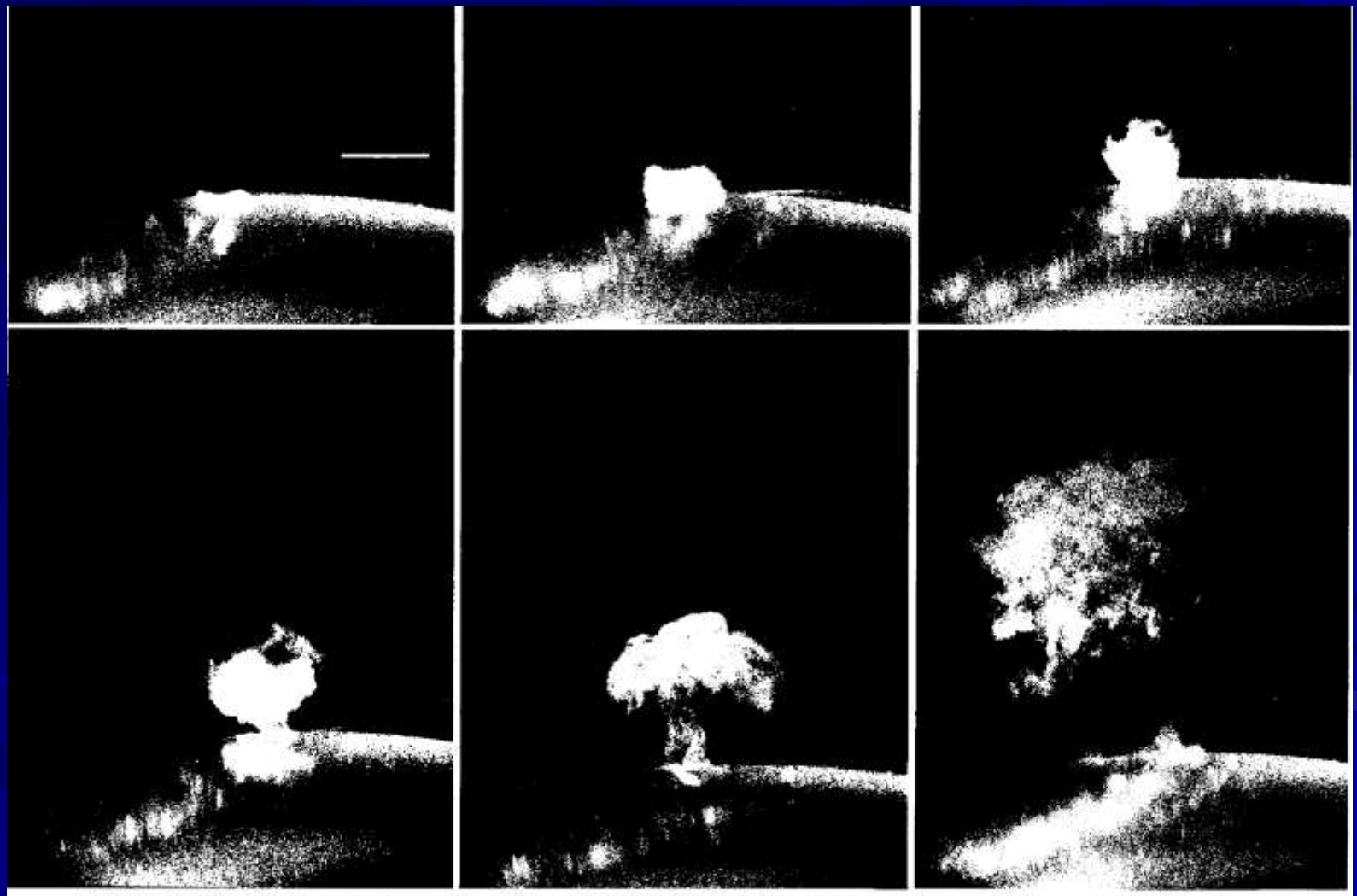

Fig 2.—Photographs of ablation plume at 193 nm and 900 mJ/cm^2. Top left, 0.5 μs. Top center, 1.5 μs. Top right, 5 μs. Bottom left, 15 μs. Bottom center, 50 μs. Bottom right, 150 μs. Excimer beam comes from top of photograph and strikes cornea near point indicated by arrow (top left). Bar indicates 1 mm (top left) (original magnification ×4.5).

Fig. 3 Schematic impact of laser pulse on polymer surface. (After R. Srinivasan and Bodil, 1988)

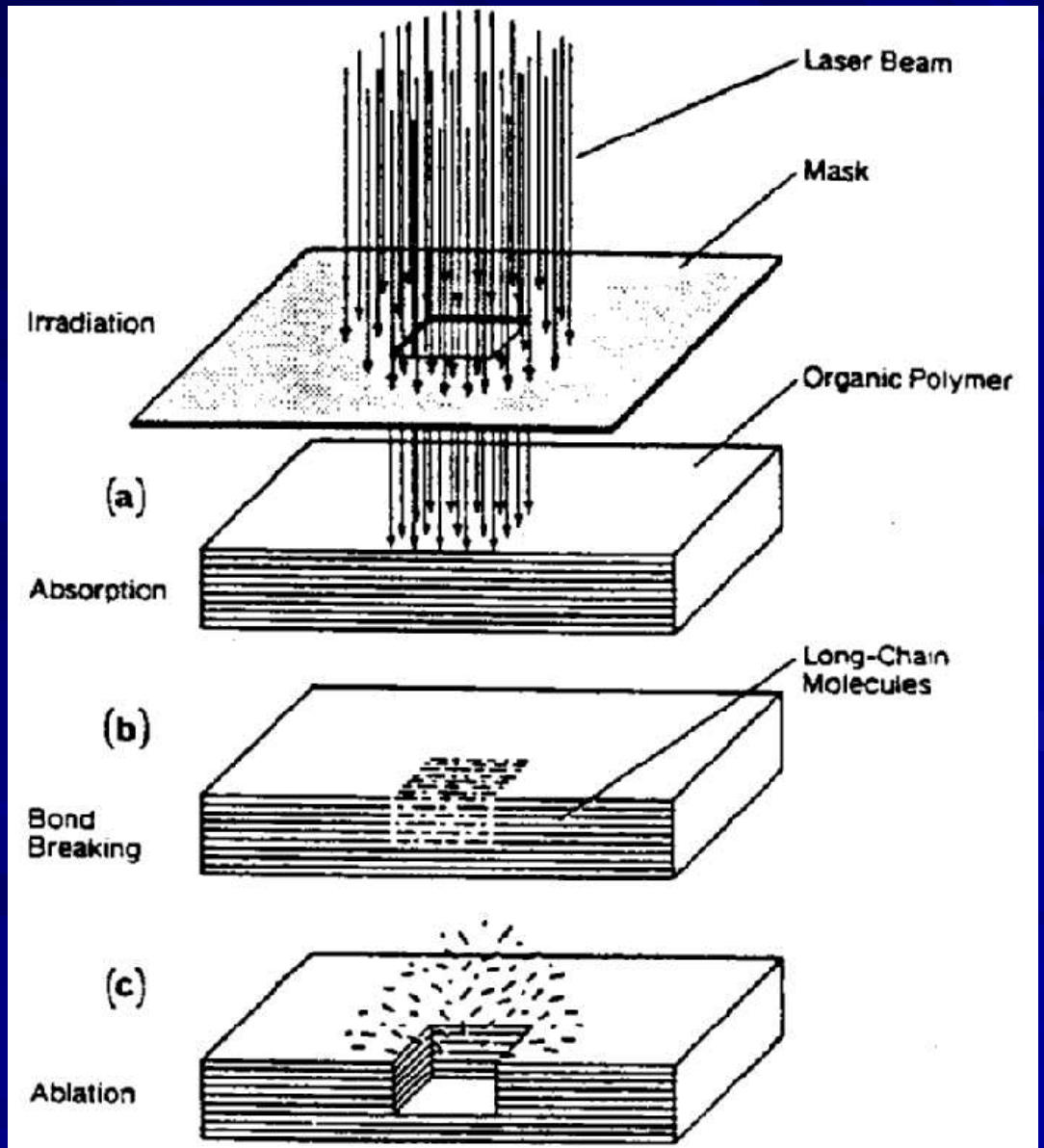

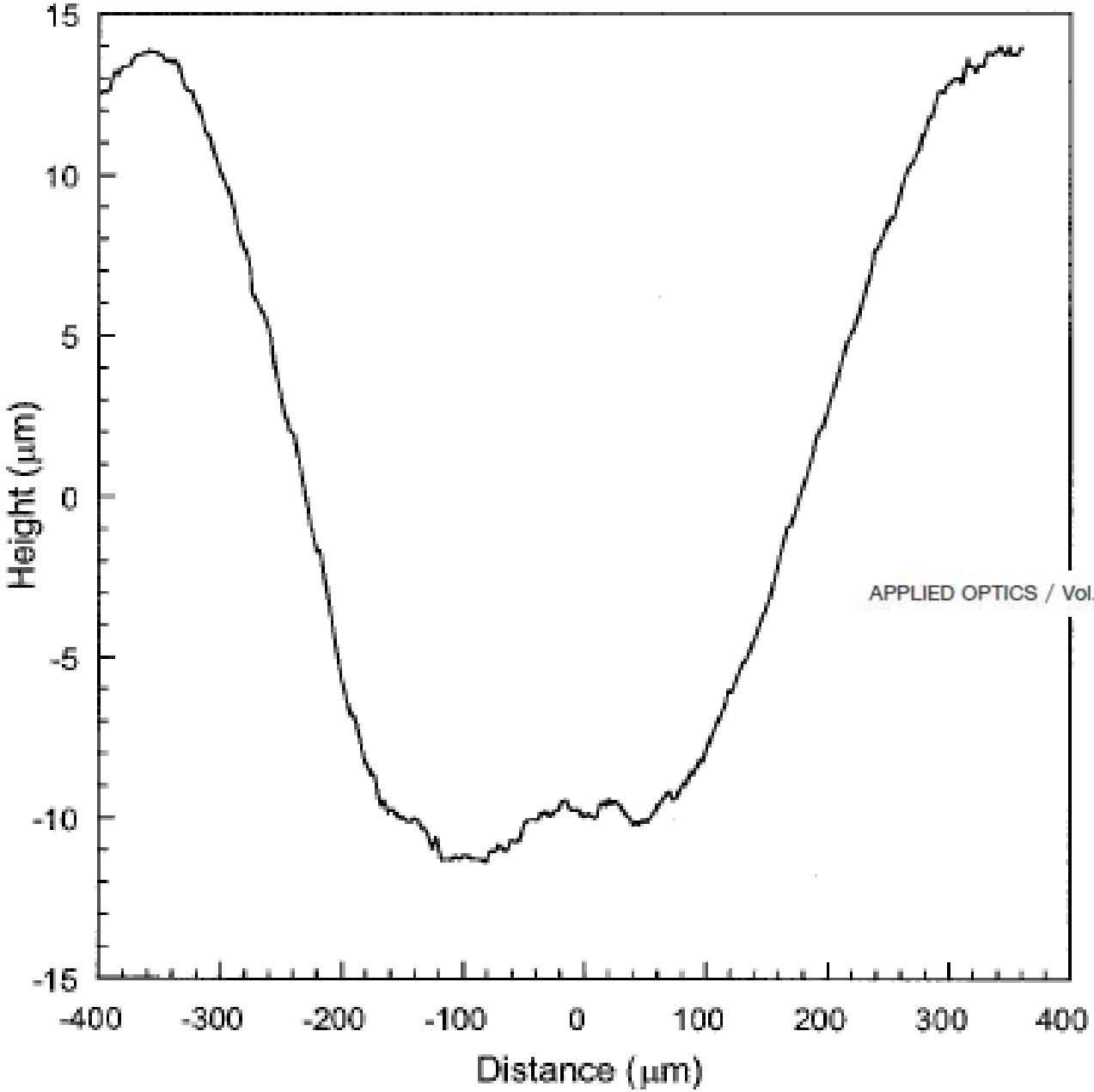

APPLIED OPTICS / Vol. 43, No. 29 / 10 October 2004

Fig. 4. Ablation crater showing ablation profile of the ArF excimer laser beam. The crater was recorded in bovine corneal tissue.

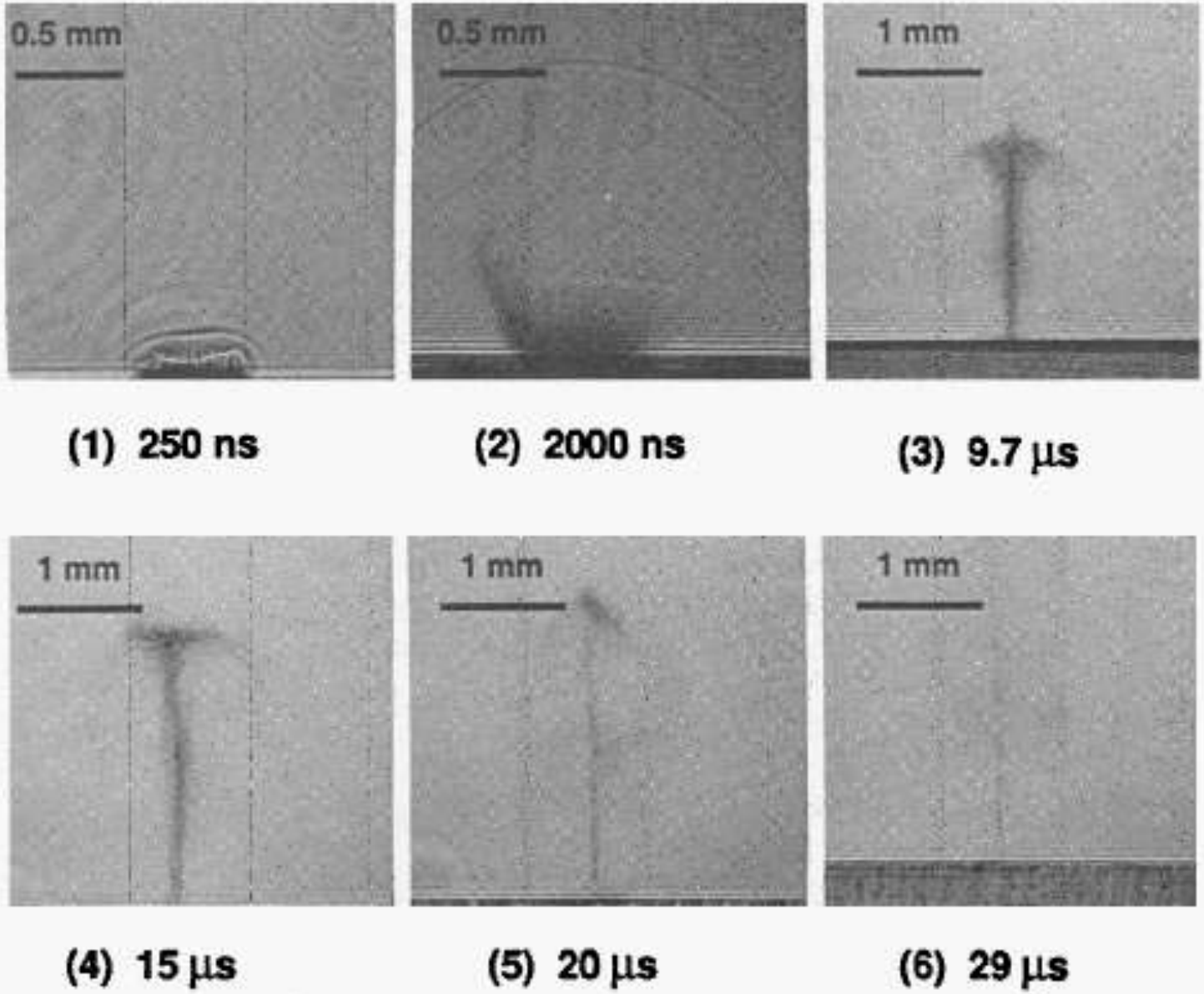

Fig. 4. Photographs of plume from ablation of PMMA with 248nm, 2.1 J/cm^2 pulses. The edge of the polymer sample which is seen in profile lies parallel to the bottom of each frame. Note change in the scale from the top row to the bottom row. The width of the ultraviolet beam is 600 μm.

The excimer “cuts” the carbon bonds in plastic

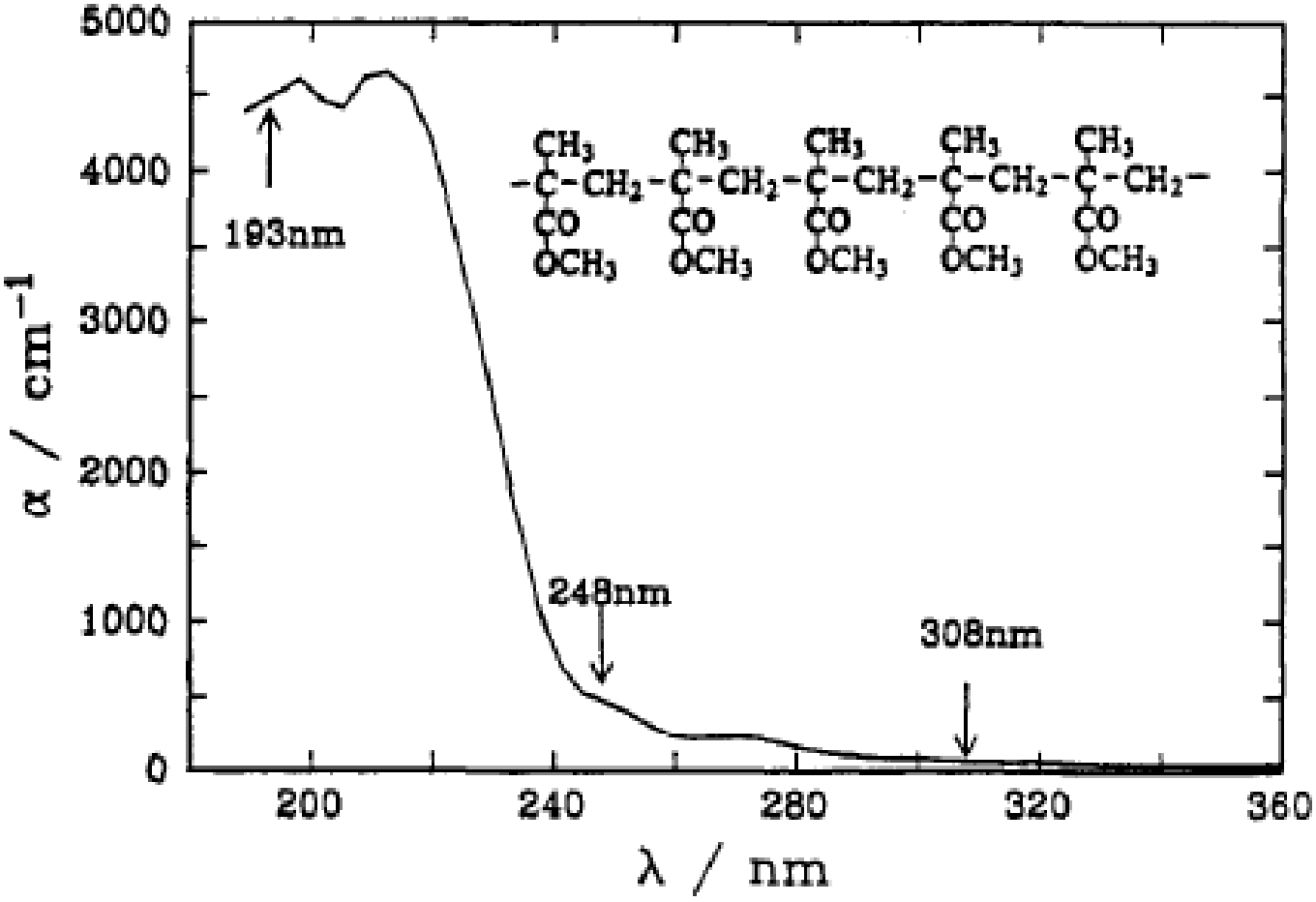

Fig. 1. Ultraviolet absorption spectrum of PMMA. The arrows point to the wavelengths of the strong emission lines from an excimer laser

Lasik debris from plastic: gas and polymer pieces

- At the laser wavelength of 248nm, the principal product of the ablation of PMMA (MW 10*6) is an oligomer of much lower molecular weight .
- The number average molecular weight of the product is 2500 and the weight average molecular weight, 4500.
- In addition there are gaseous products such as C2, CO, and C02 but very little of the monomer. The composition of the products is different when a laser wavelength of 193nm is used. In addition to the gases mentioned above, the monomer accounts for 18% of the polymer that is decomposed.
- **A** polymer of low *(cu.* 1000) weight is also formed.

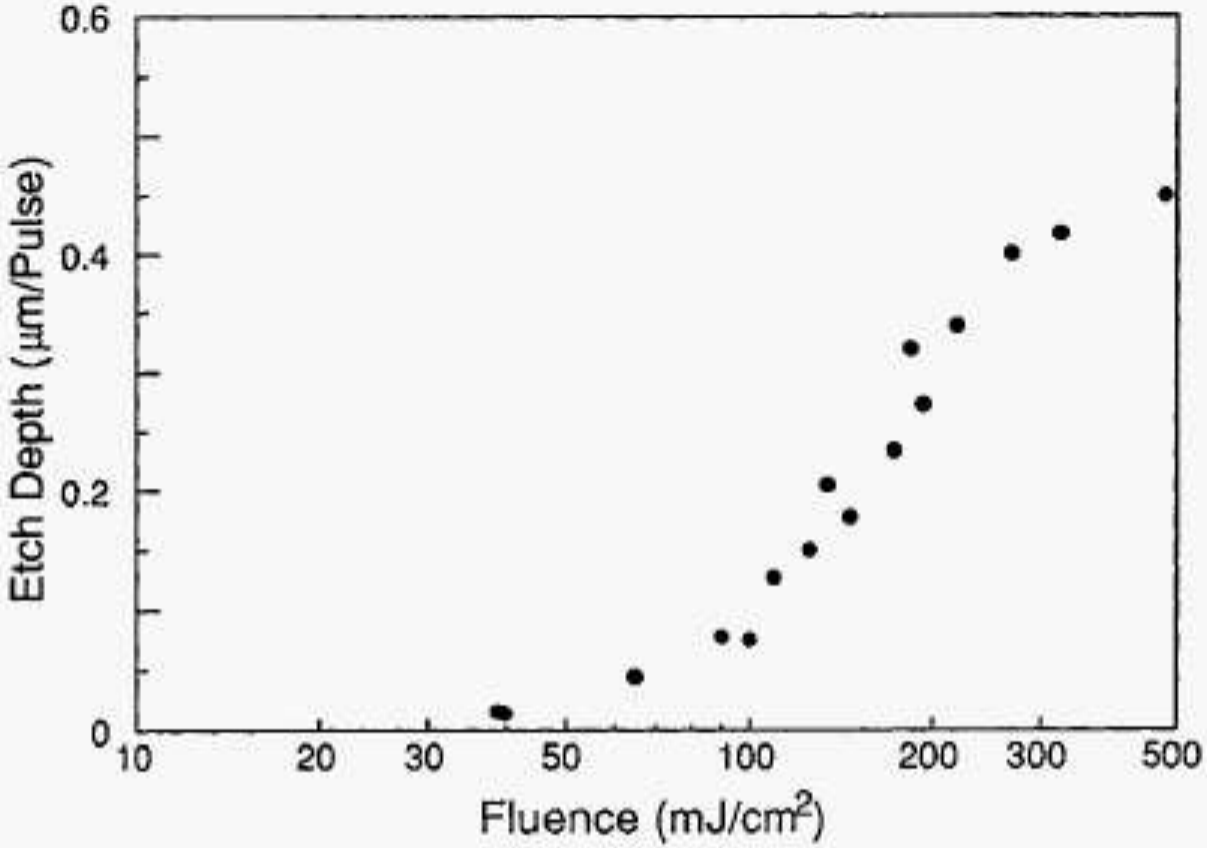

Fig. 2. Plot of etch depth vs log (fluence) in the laser ablation of PMMA at 193nm.

Fig. 3. Time synchronized laser and stress waveforms for laser-irradiated PMMA at 193nm. The larger amplitude signal is the laser pulse which varies slightly in shape due to different operating voltages being used.

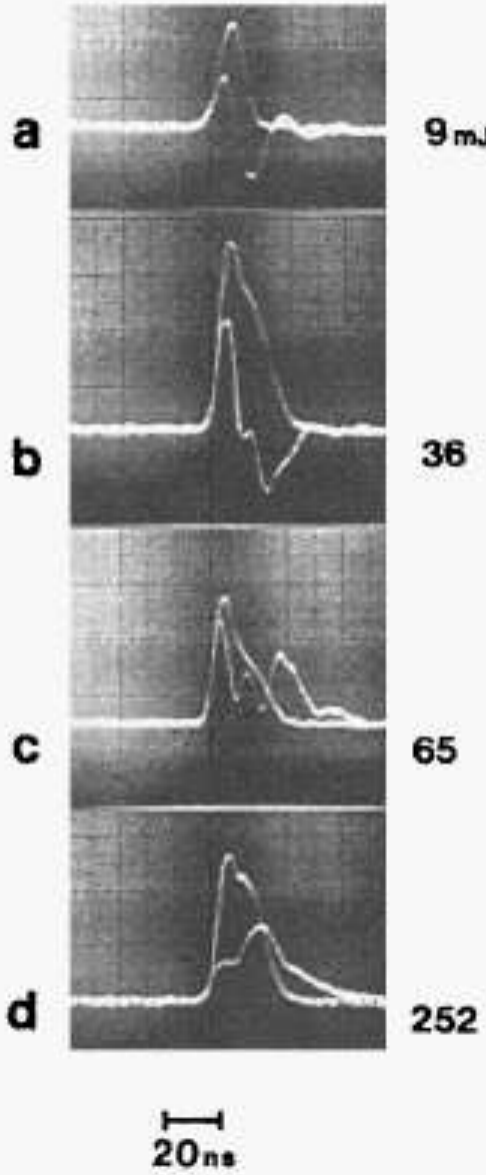

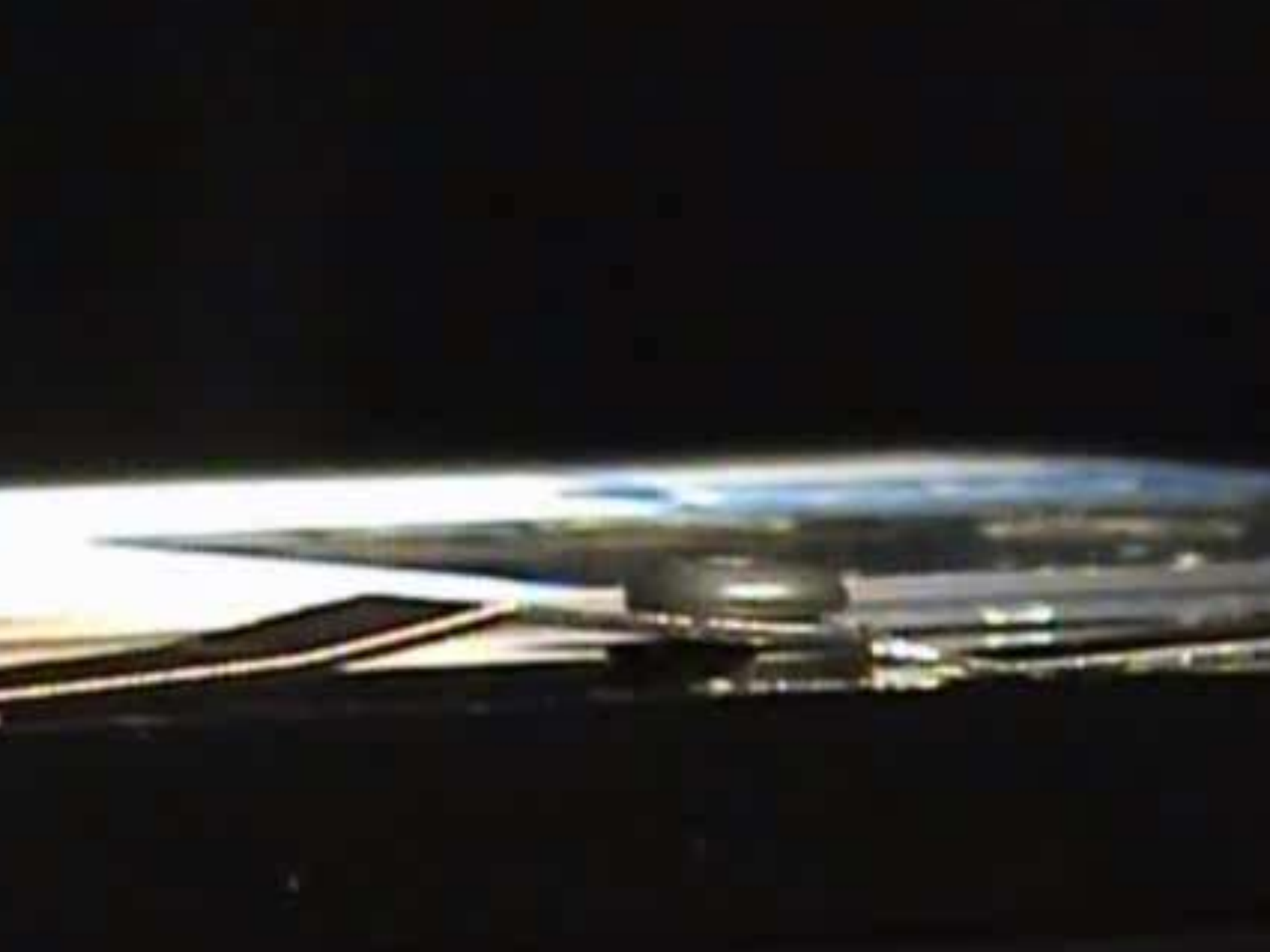


ADVANC
EDIC

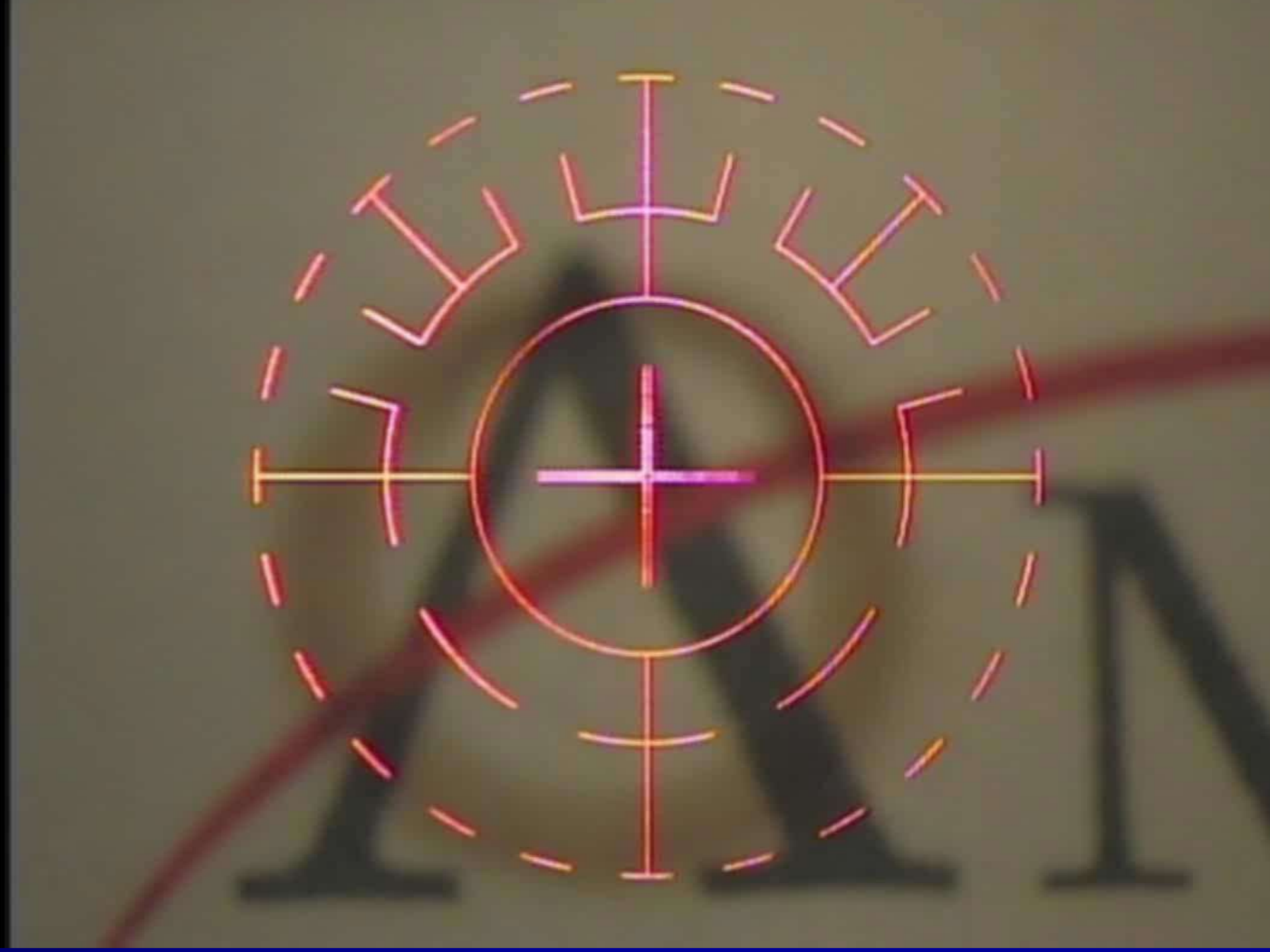

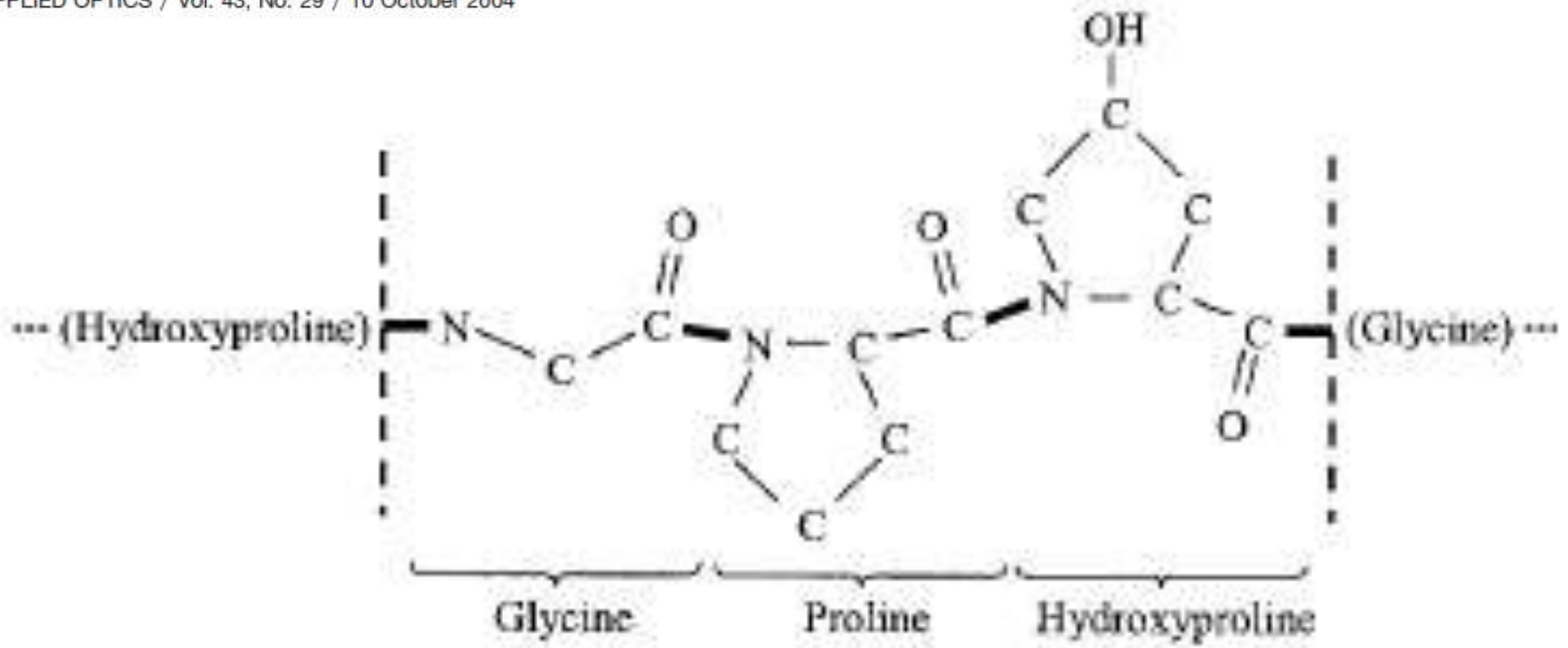

Fig. 1. Amino acid sequence constituting the primary structure of collagen ($C_{12}H_{17}N_3O_4$). Bold lines indicate peptide bonds (C–N) between adjoining amino acids.


Sphere
Cylinder
Visx High Myopia
with Blend
Spherical aberration
Sphere and
Spherical aberration

Cellular mechanism: Outflow

- Induced junction disassembly and increased permeability of Schlemm's canal cells.
  - Exposure to factors secreted by
    - lasered Schlemm canal cells
    - lasered trabecular meshwork cells
  - The application of prostaglandin analogs

Am J Ophthalmol. 2010 Aug;150(2):254-64

Micro-pulse Laser Trabeculoplasty

	MLT	SLT	ALT
Wavelength	532 nm, 577 nm	532 nm	488/514 nm, 532 nm
Mechanism	Thermally effects - not destroys - pigmented TM cells	Selective destruction of pigmented TM cells without thermal or collateral damage	Shrinkage of TM with adjacent stretching
Repeatable	Yes	Yes	No
Treatment Endpoint	No visible tissue reaction	Small bubbles	Blanching (mild) to bubbles (intense)
Post op Inflammation	None	Yes	Yes
Spot Size	300 µm Smaller spot to access narrow angles	400 um	50 um
	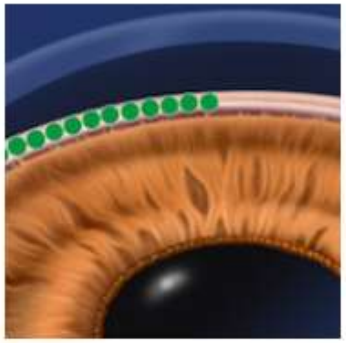	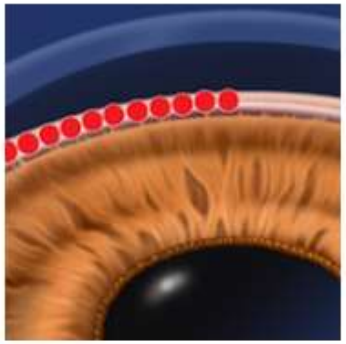	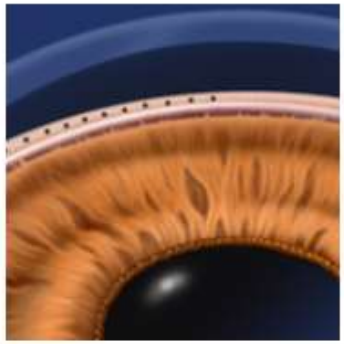

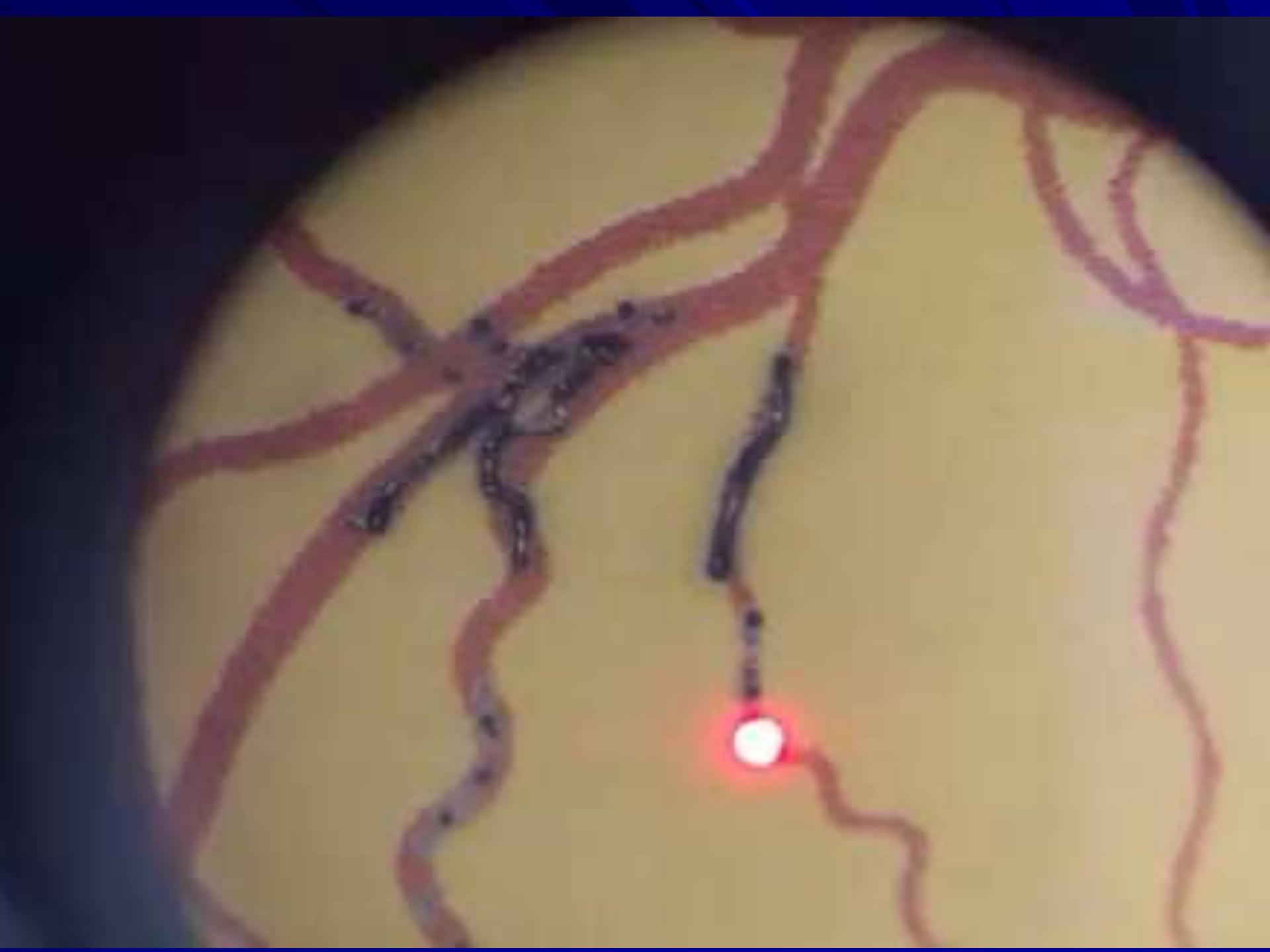

Average IOP reduction using 532-nm MLT at various powers.
Subjects achieved a 30% IOP reduction with 1,000 mW at 4 months.

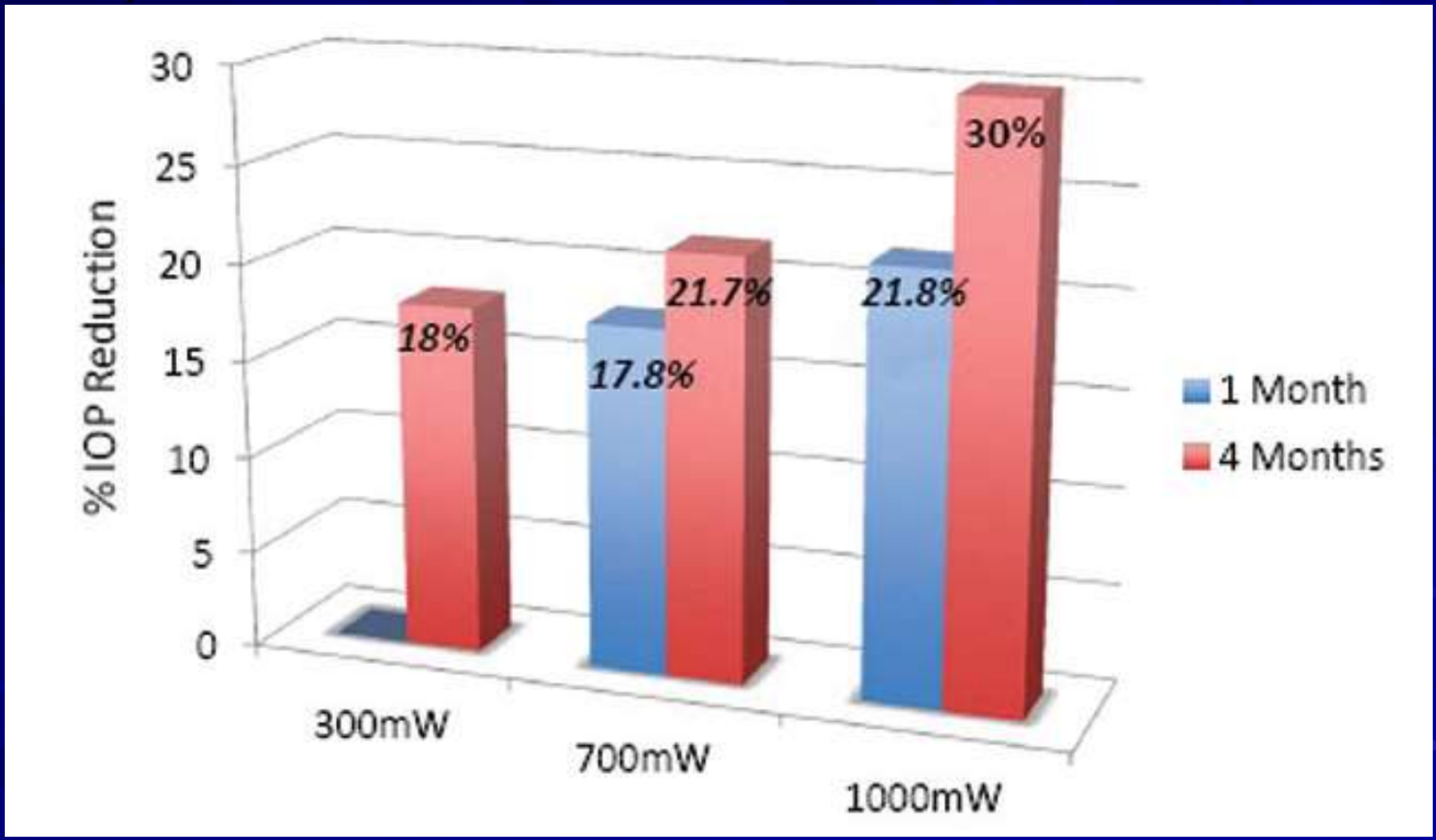

Typical power at NLEA 1500 to 2000 mW

Apoptosis

Programmed cell death

Early Wound Healing Response to Epithelial Scrape Injury in the Human Cornea

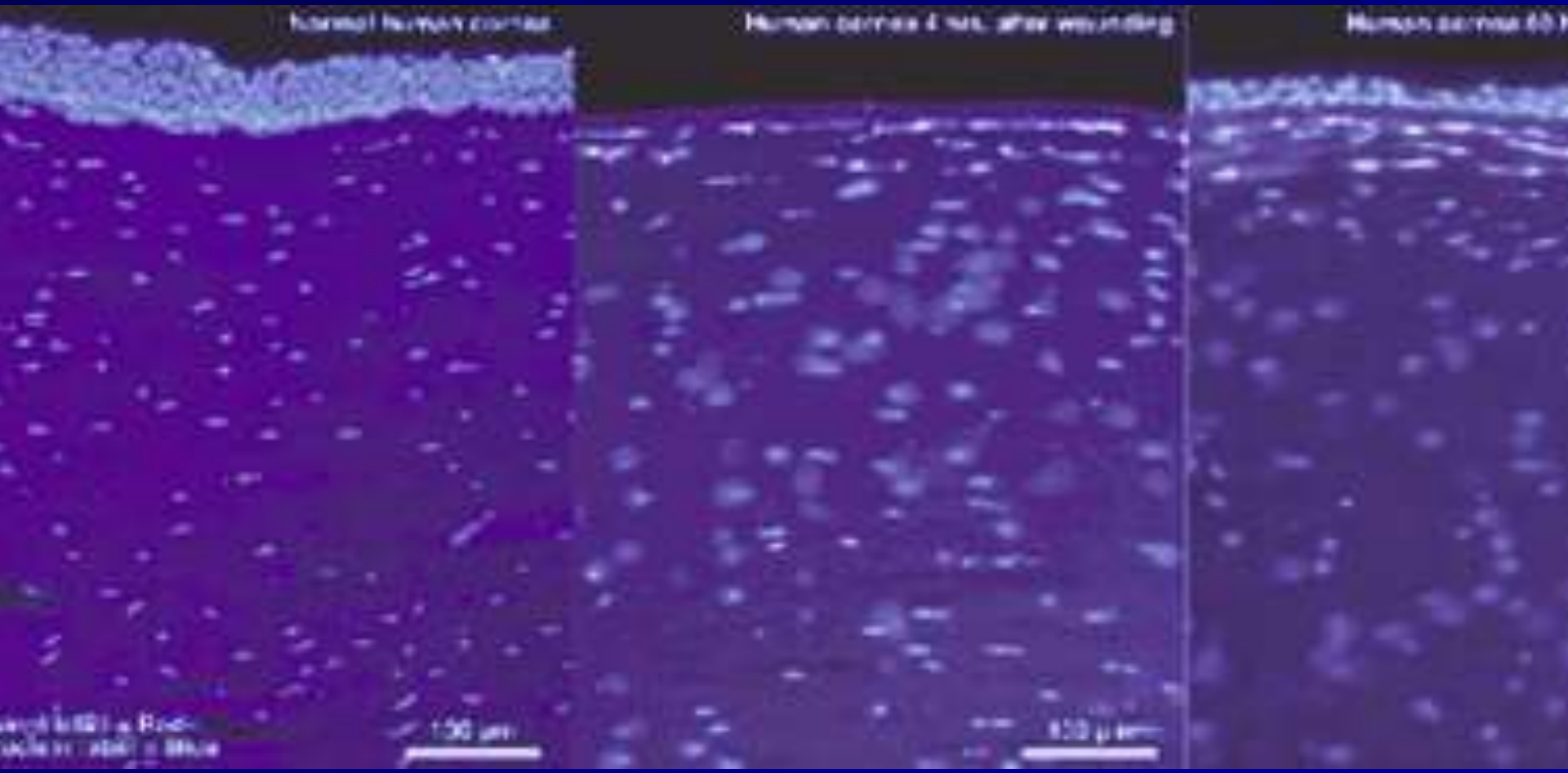

Invest Ophthalmol Vis Sci 2002;43: E-Abstract 4206.

Unraveling the Mysteries of Corneal Scarring

Post PRK Haze

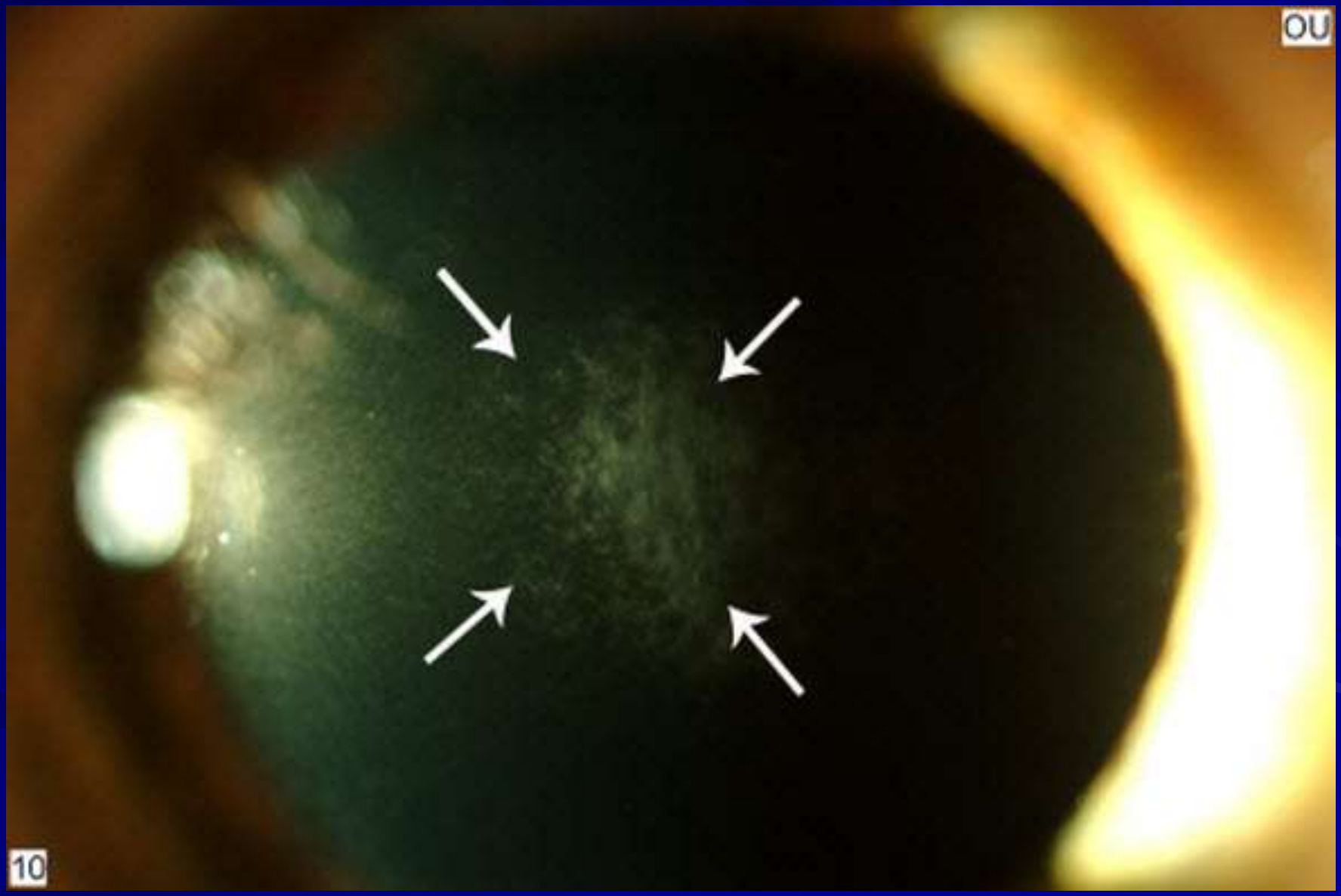

Fibrosis at the edge of the Lasik Flap

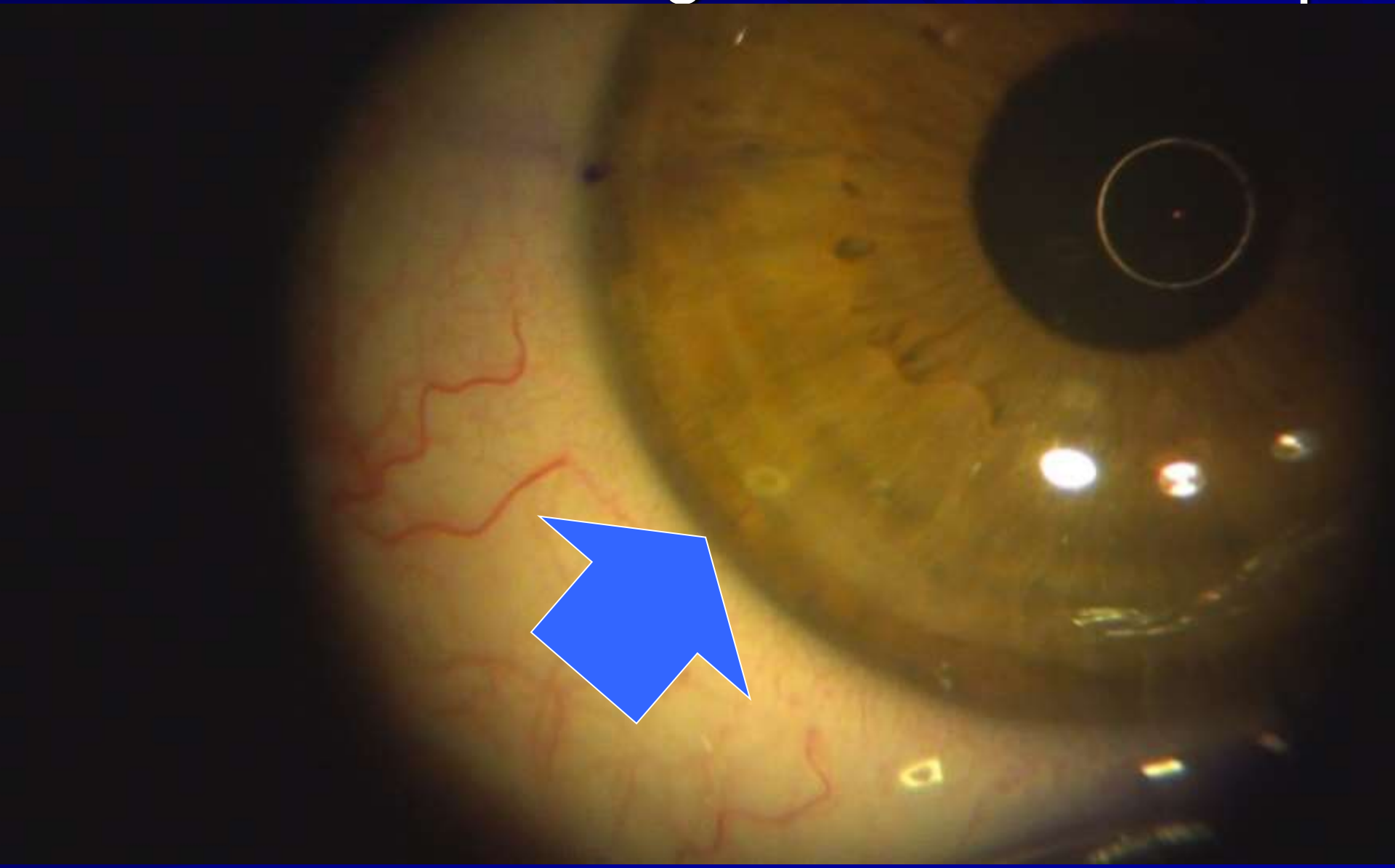

Peripheral scar noted with enhancement

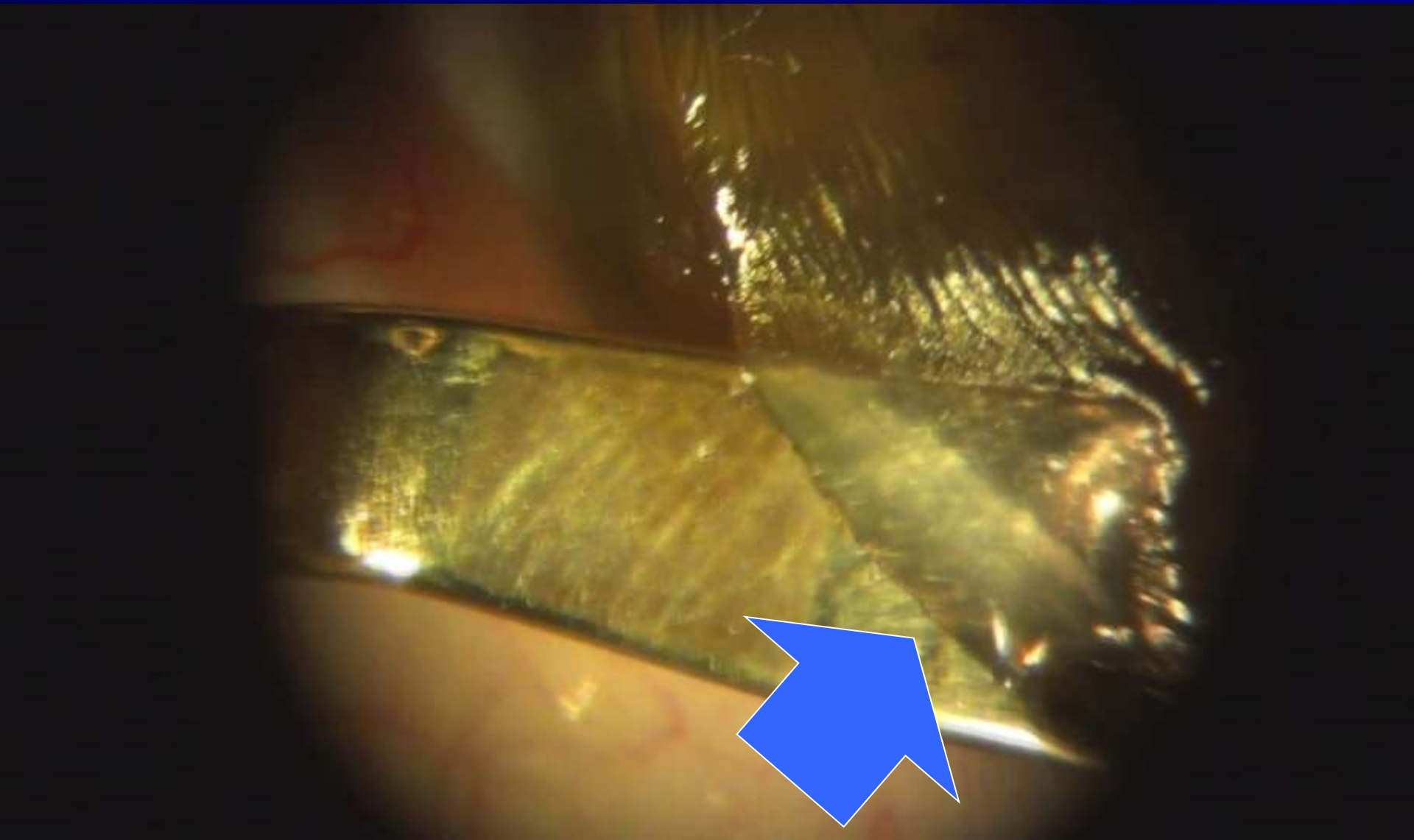

Scar at the edge of the bed

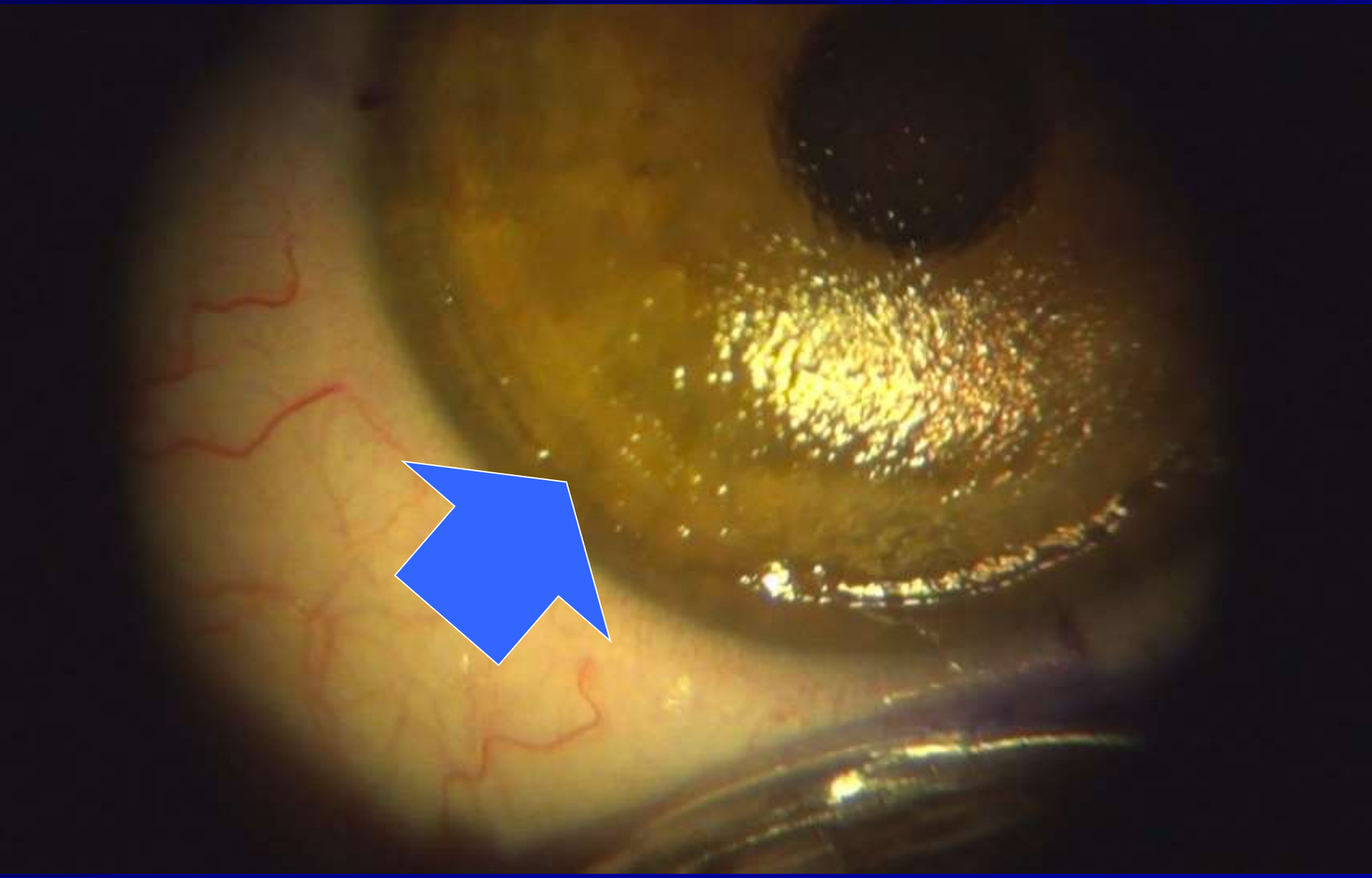

IntraLase: enhancement

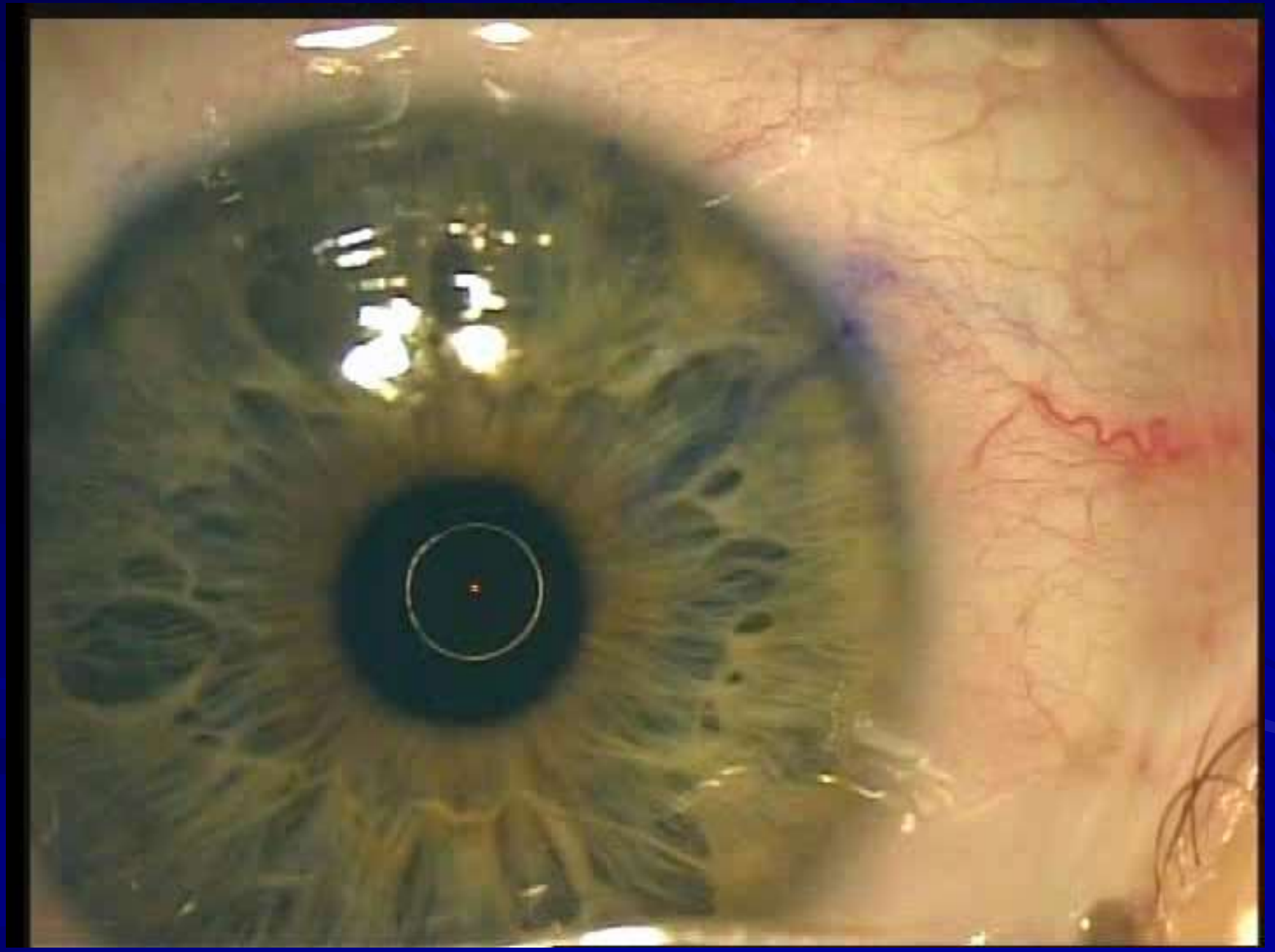

Percent +/- .0.50 D after enhancement

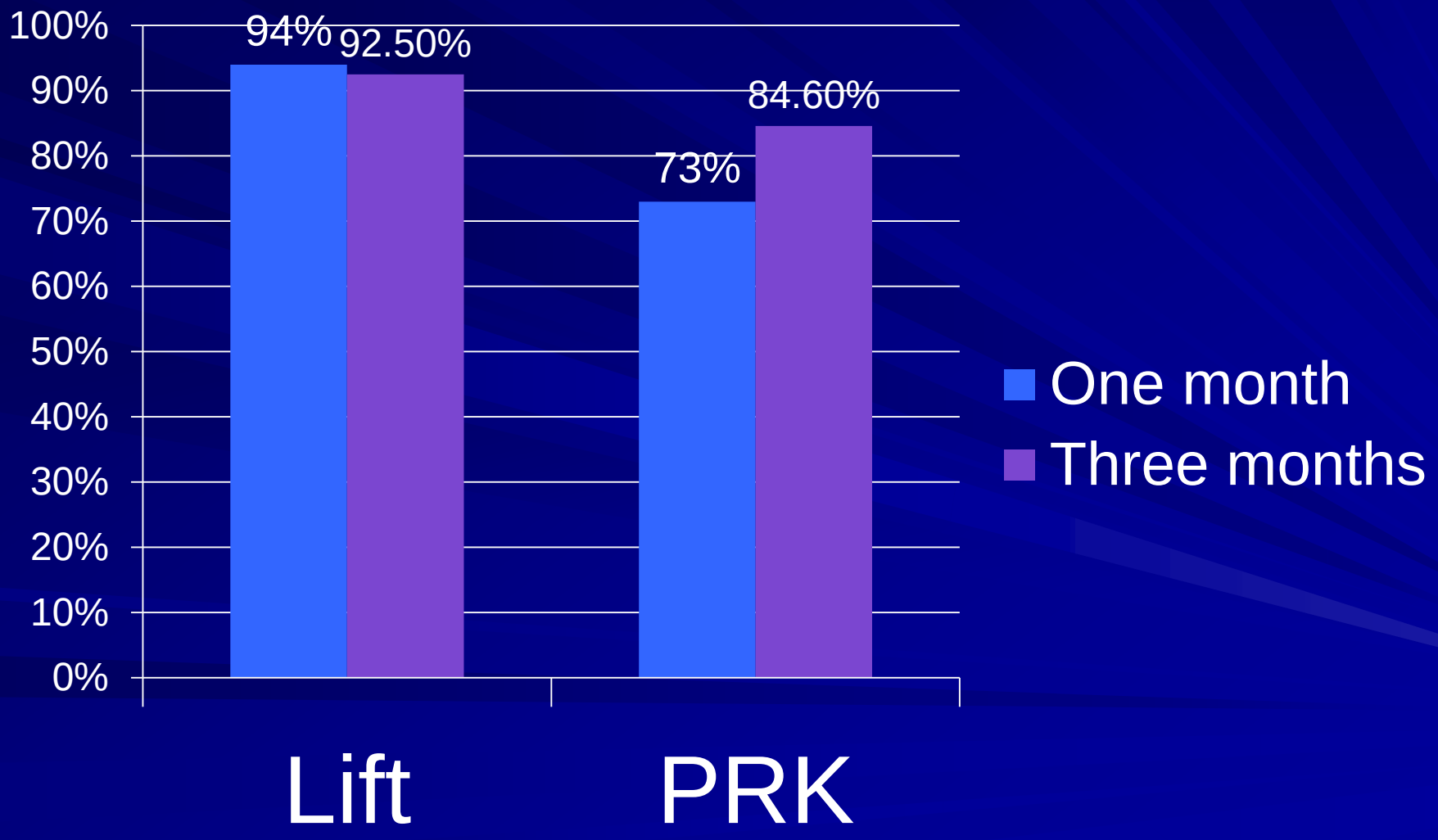

Stromal cell loss with crosslinking

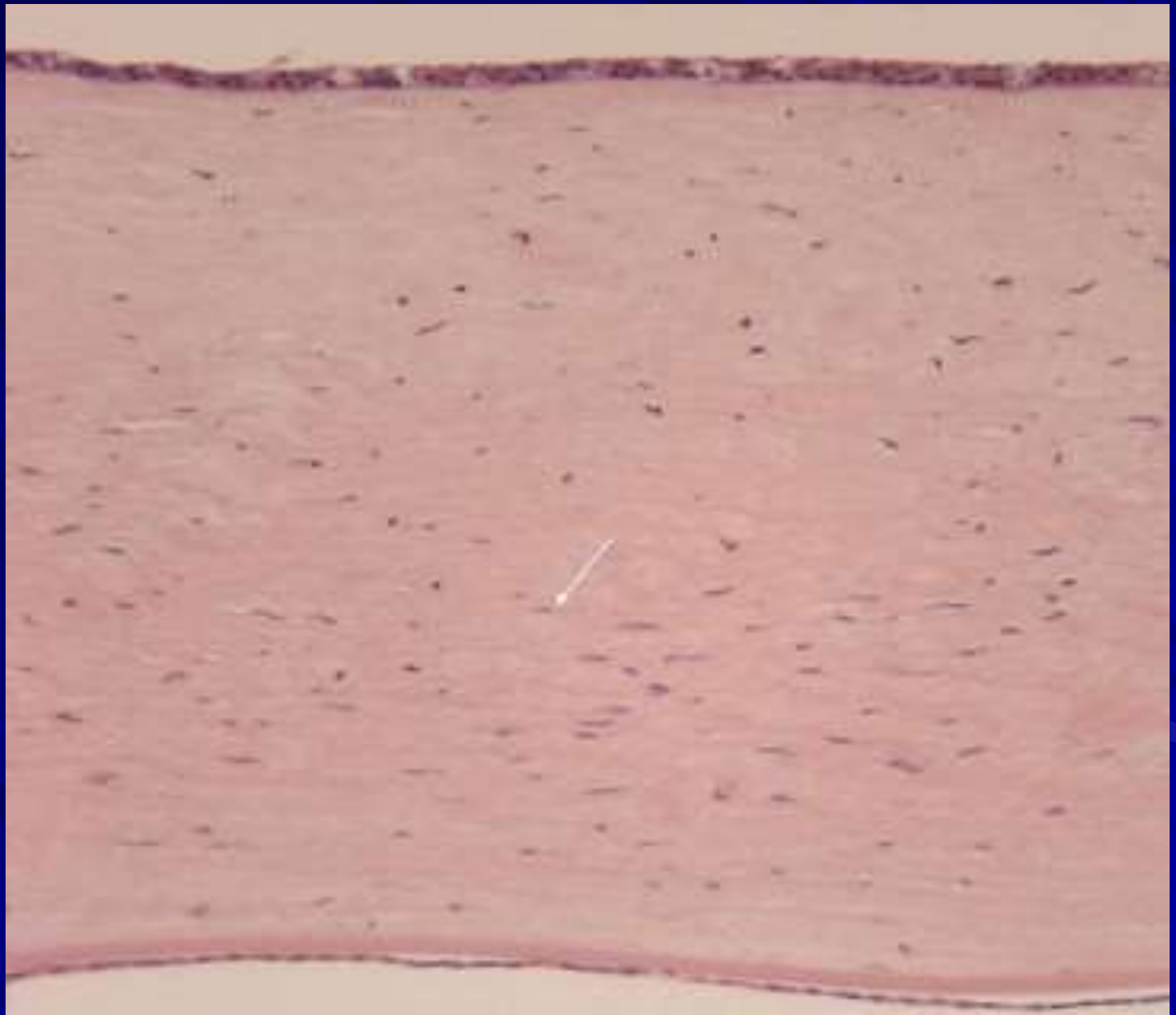

Refractive Outcomes 2015

Visx wide blend -0.14 ± 0.20

Wavelight -0.15± 0.28 D

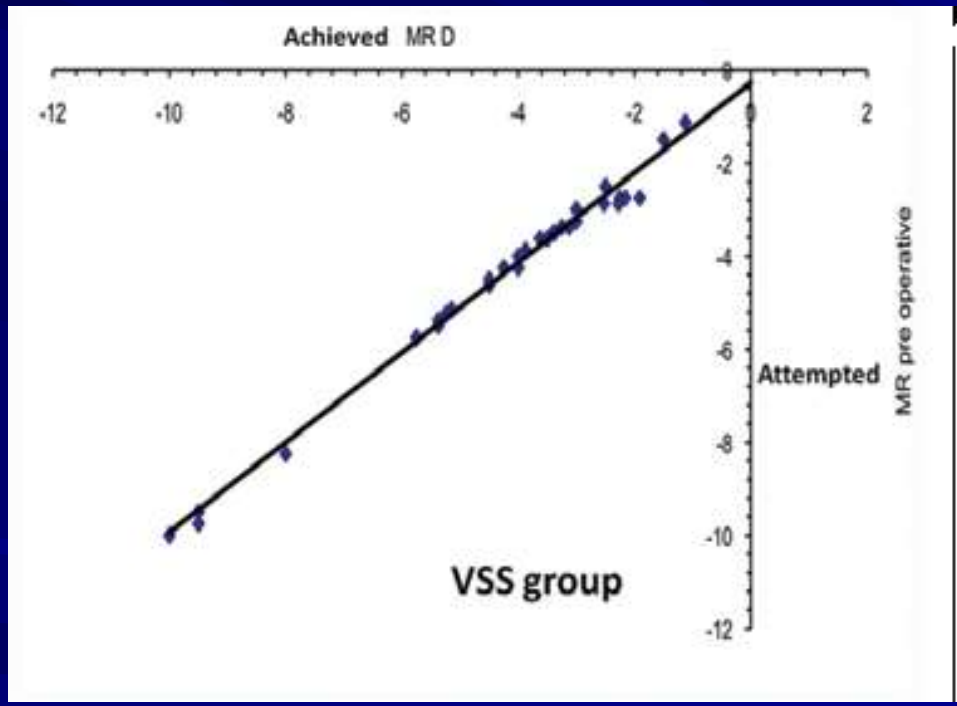

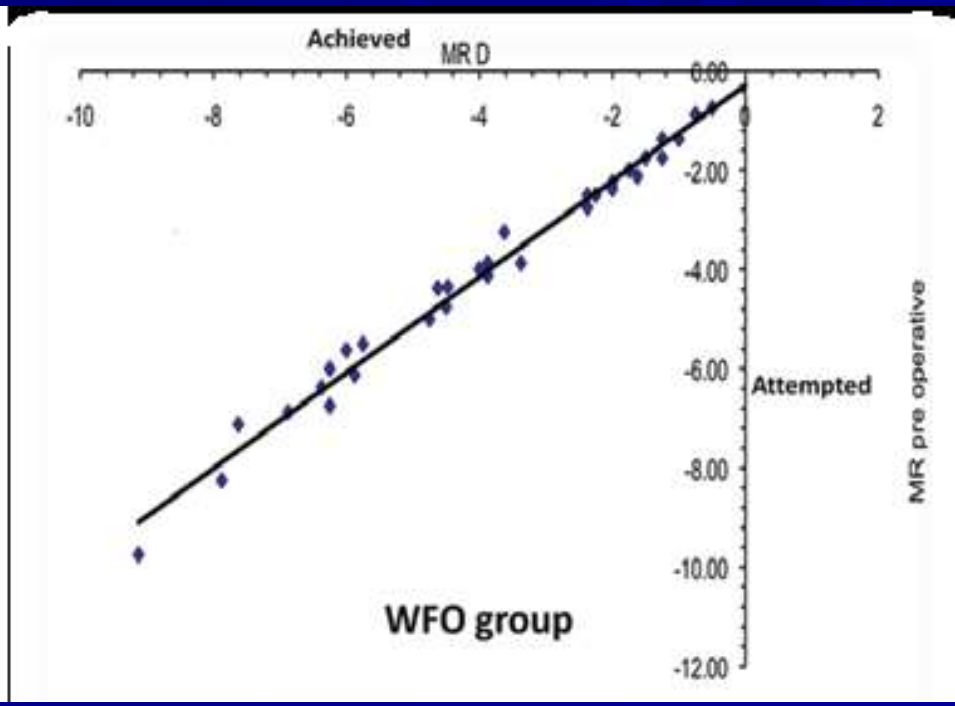

NLEA Fall 2014

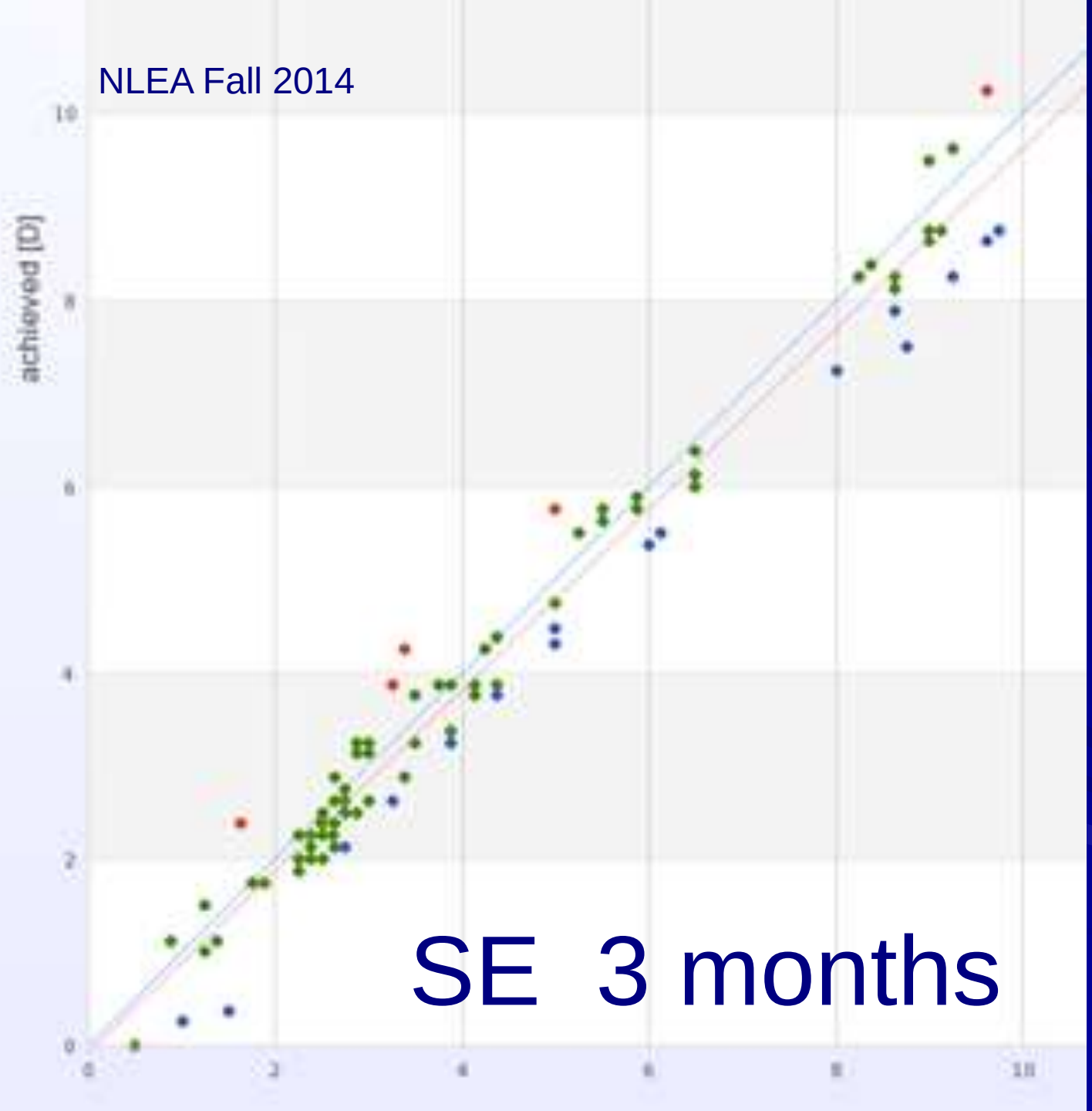

SE 3 months

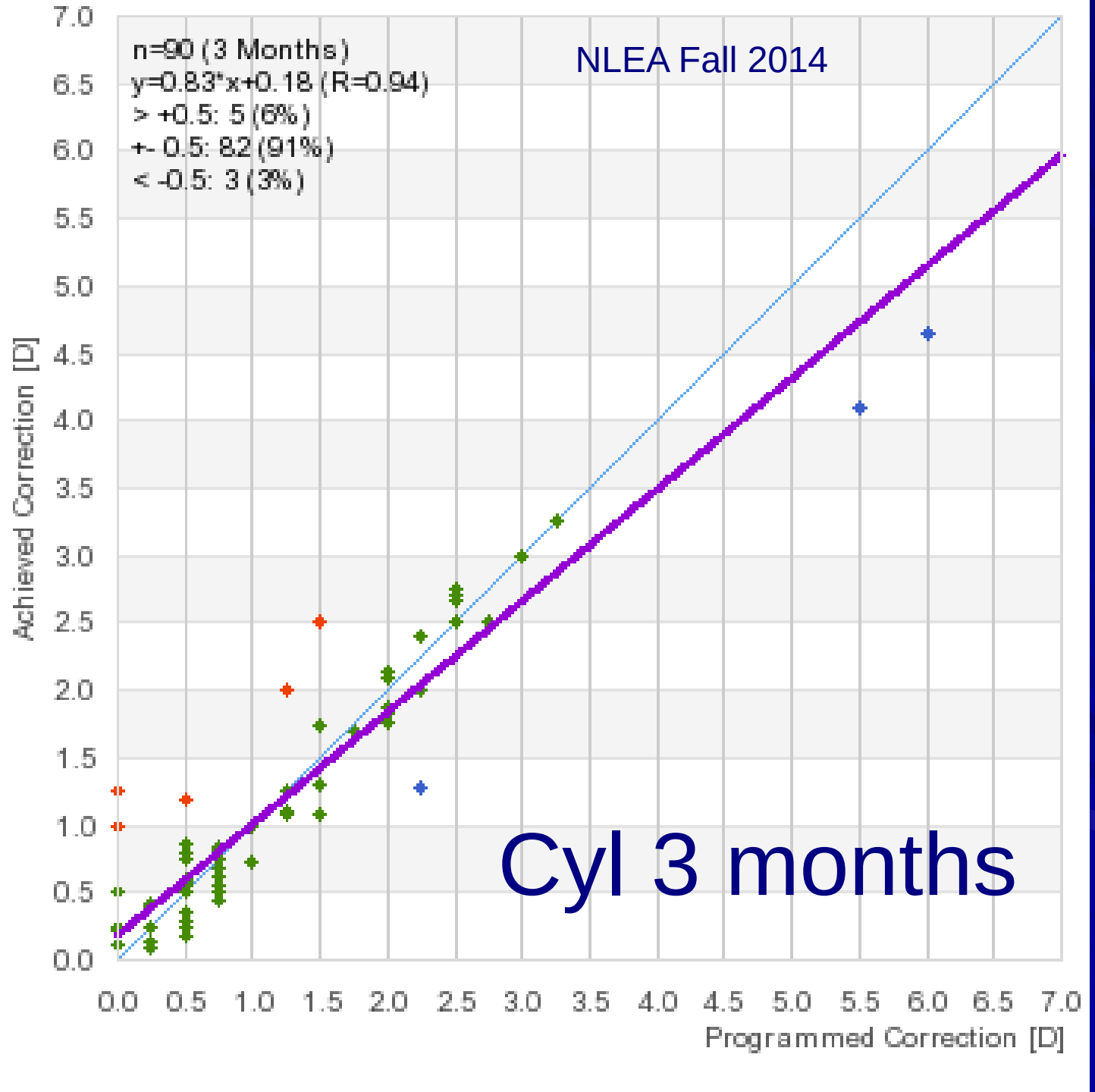
n=90 (3 Months)
y=0.83*x+0.18 (R=0.94)
> +0.5: 5 (6%)
+- 0.5: 82 (91%)
< -0.5: 3 (3%)
NLEA Fall 2014
Cyl 3 months
Achieved Correction [D]
Programmed Correction [D]
0.0
0.5
1.0
1.5
2.0
2.5
3.0
3.5
4.0
4.5
5.0
5.5
6.0
6.5
7.0

SE 1 month / 3 months

-0.10 +/- 0.48 -0.16 +/- 0.35

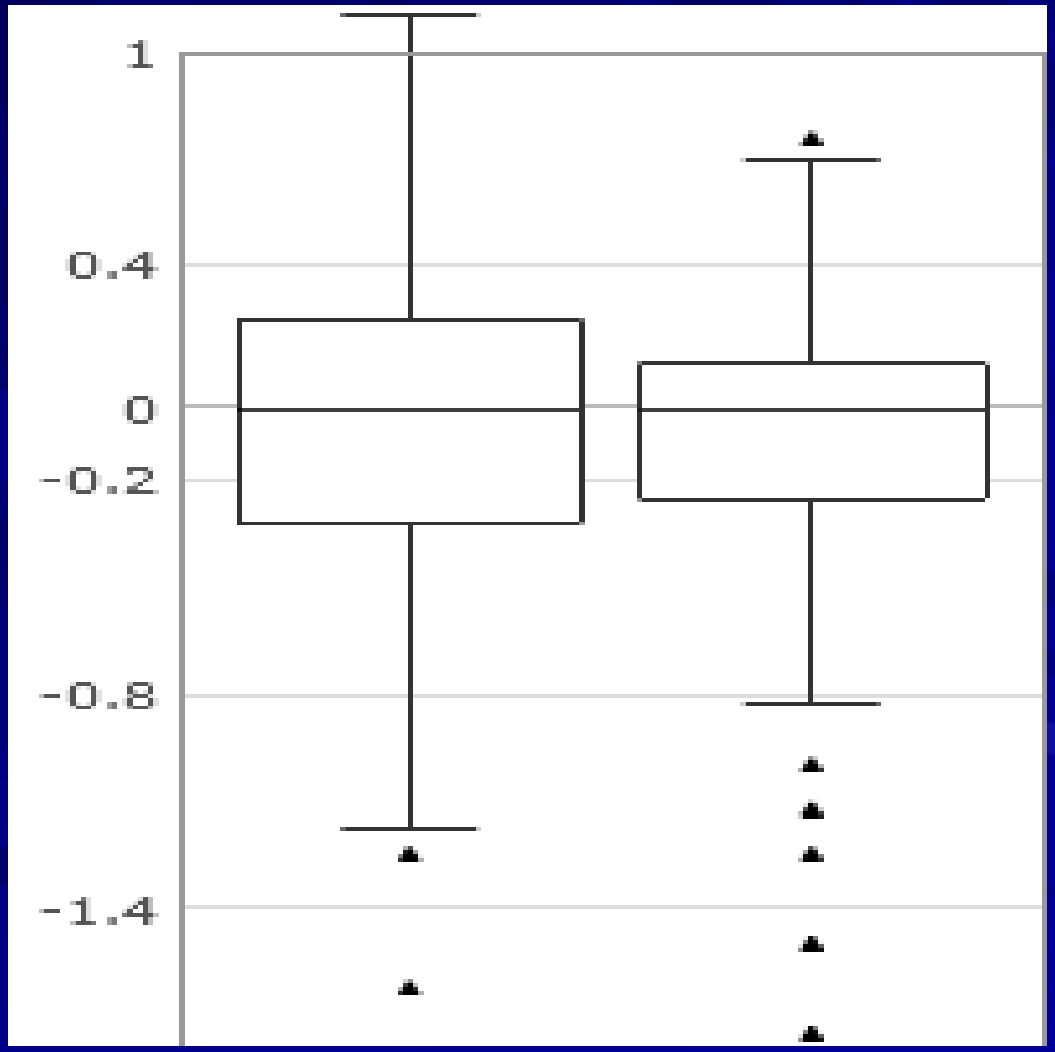

Cylinder 1 month / 3 months

-0.29 +/- 0.5 -0.29 +/- 0.11

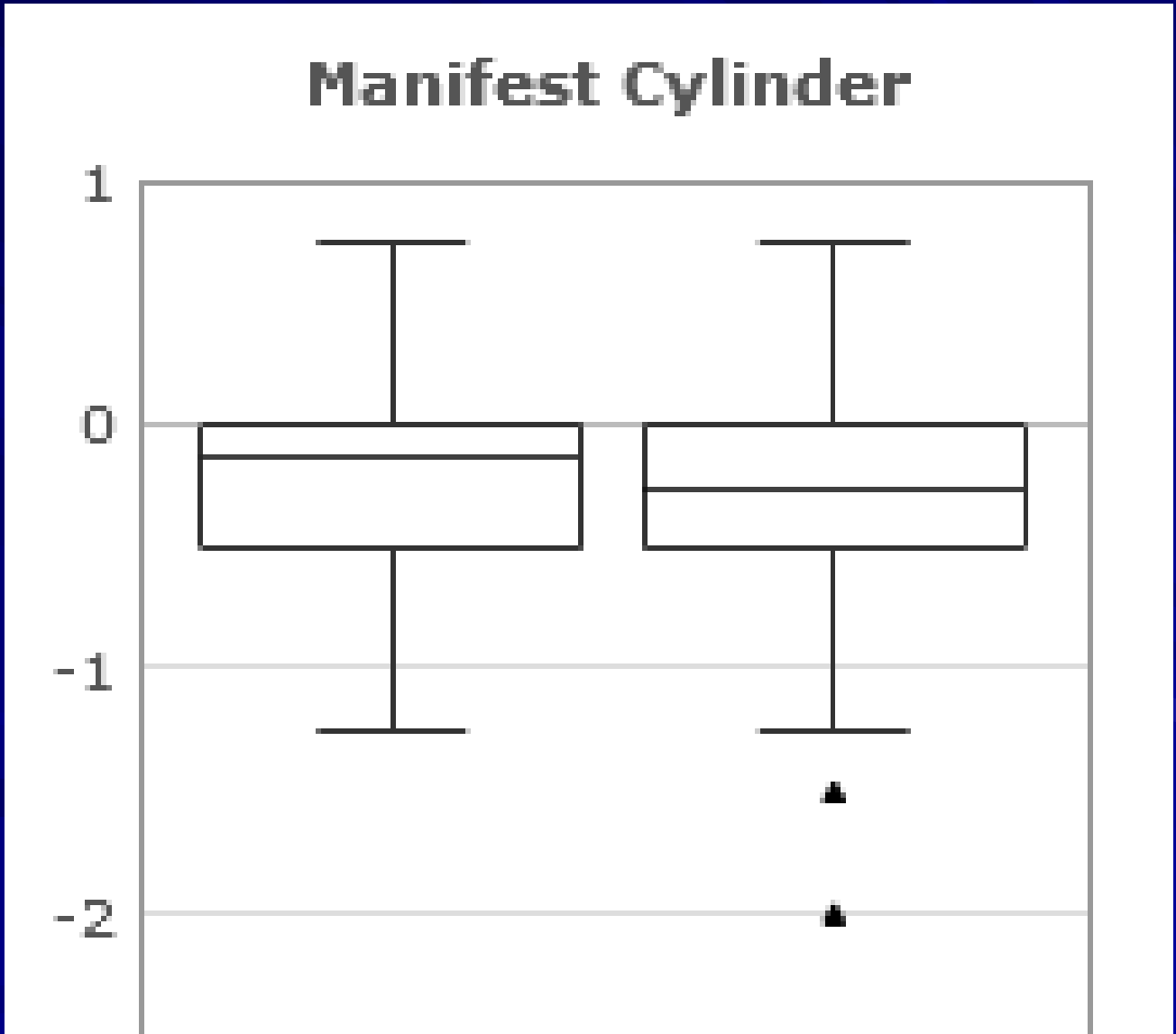

High Cylinder (Over 1.50) is associated with a much higher enhancement rate

Astigmatism (D)		UCDVA 3 m		
Pre	3 m	≥ 6/6	≥ 6/9	< 6/12
-0.35	-0.24	82.46 %	94.74 %	5.26 %
-1.81	-0.35	64.52 %	80.65 %	19.35 %

Average pre-enh: Sphere -4.50,Cyl -1.25

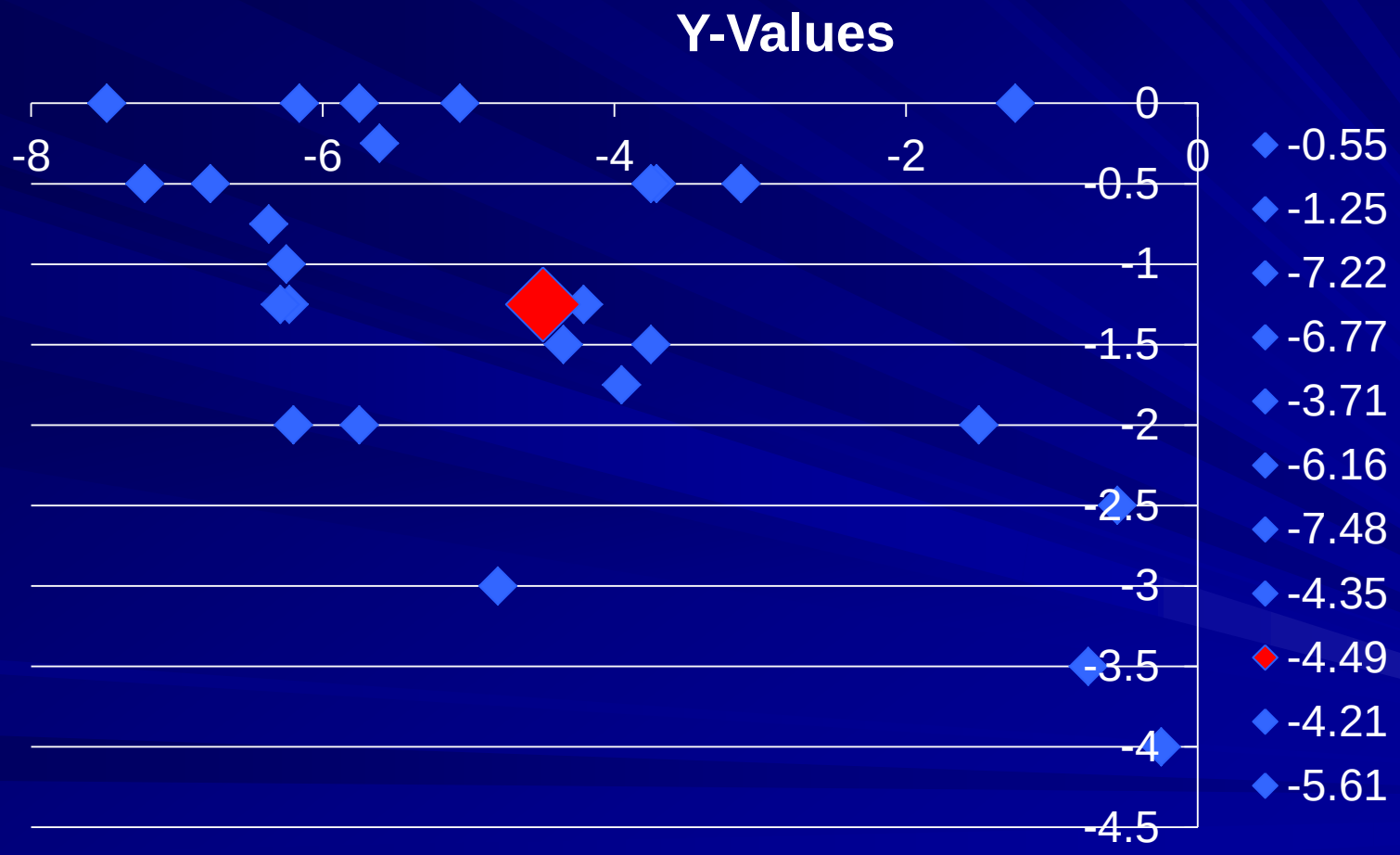

Pre-op Sphere-Cyl enhancement

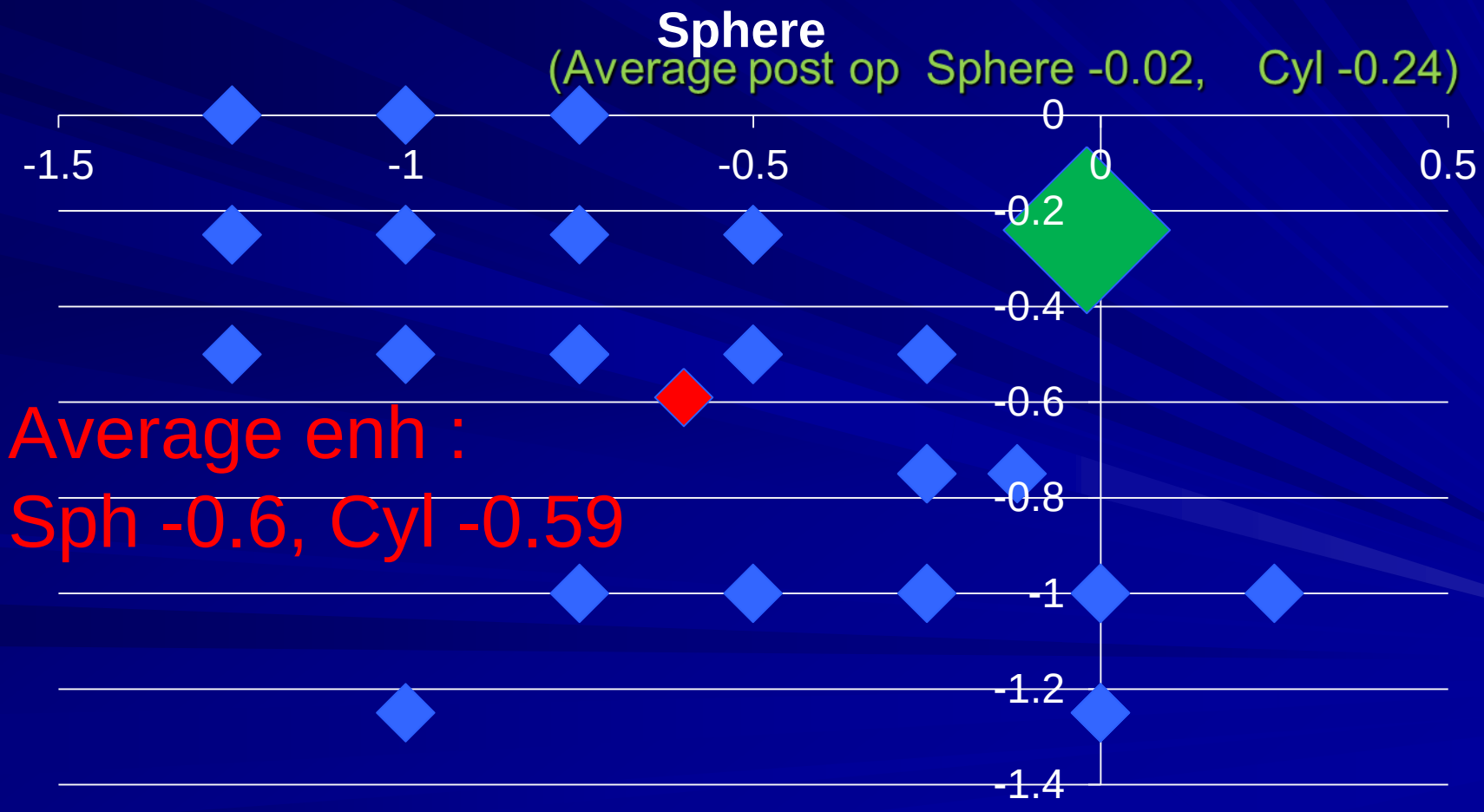

Enhancement Cyl and Axis
No set pattern

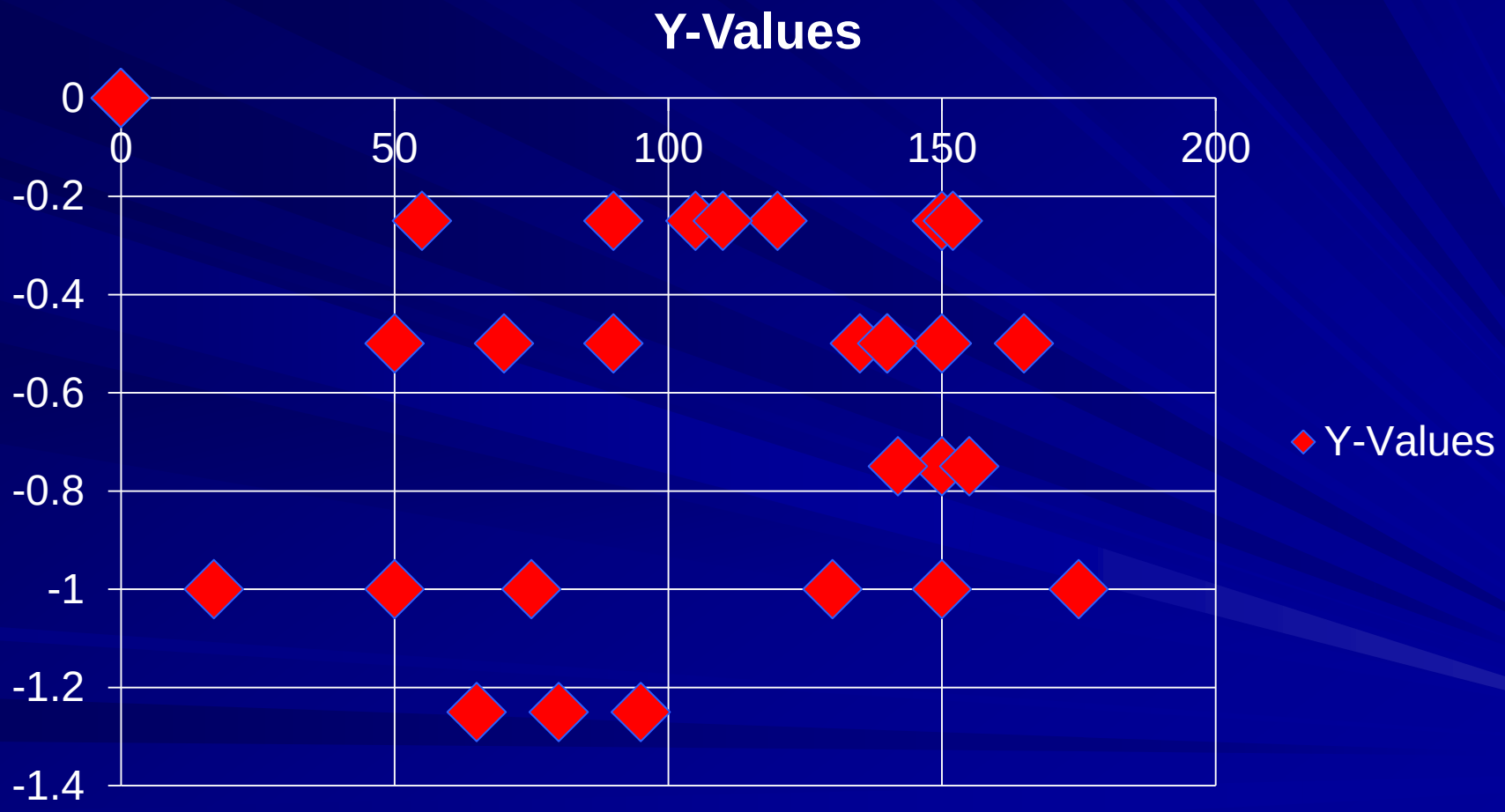

Intraocular lens calculation after refractive surgery for myopia: Haigis-L formula , uses K's, AL and ACD

Wolfgang Haigis, MS, PhD Journal of Cataract & Refractive Surgery Volume 34, Issue 10, Pages 1658-1663 (October 2008) DOI:

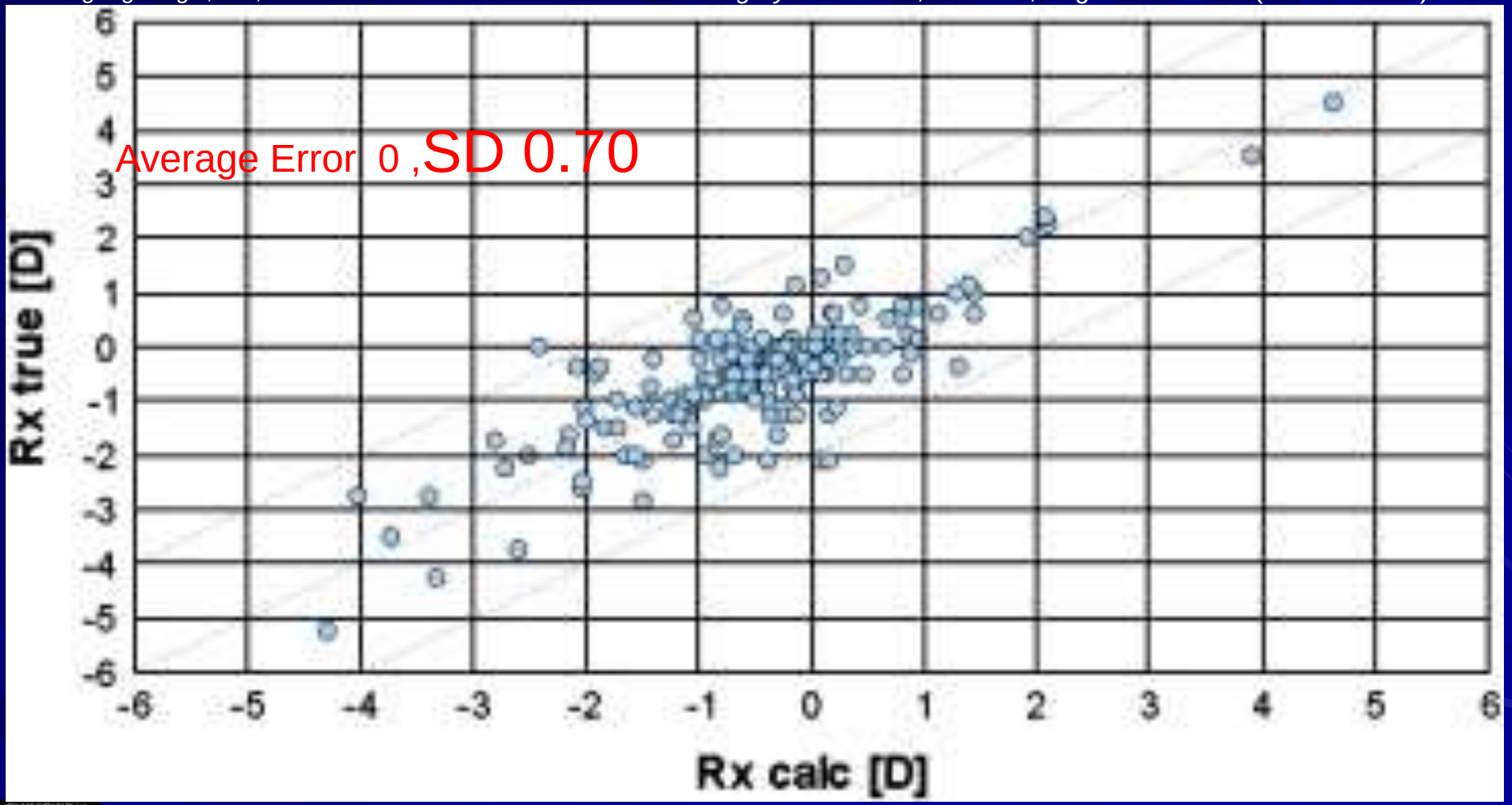

Anterior and posterior curvatures measured to calculate total corneal power for IOL selection

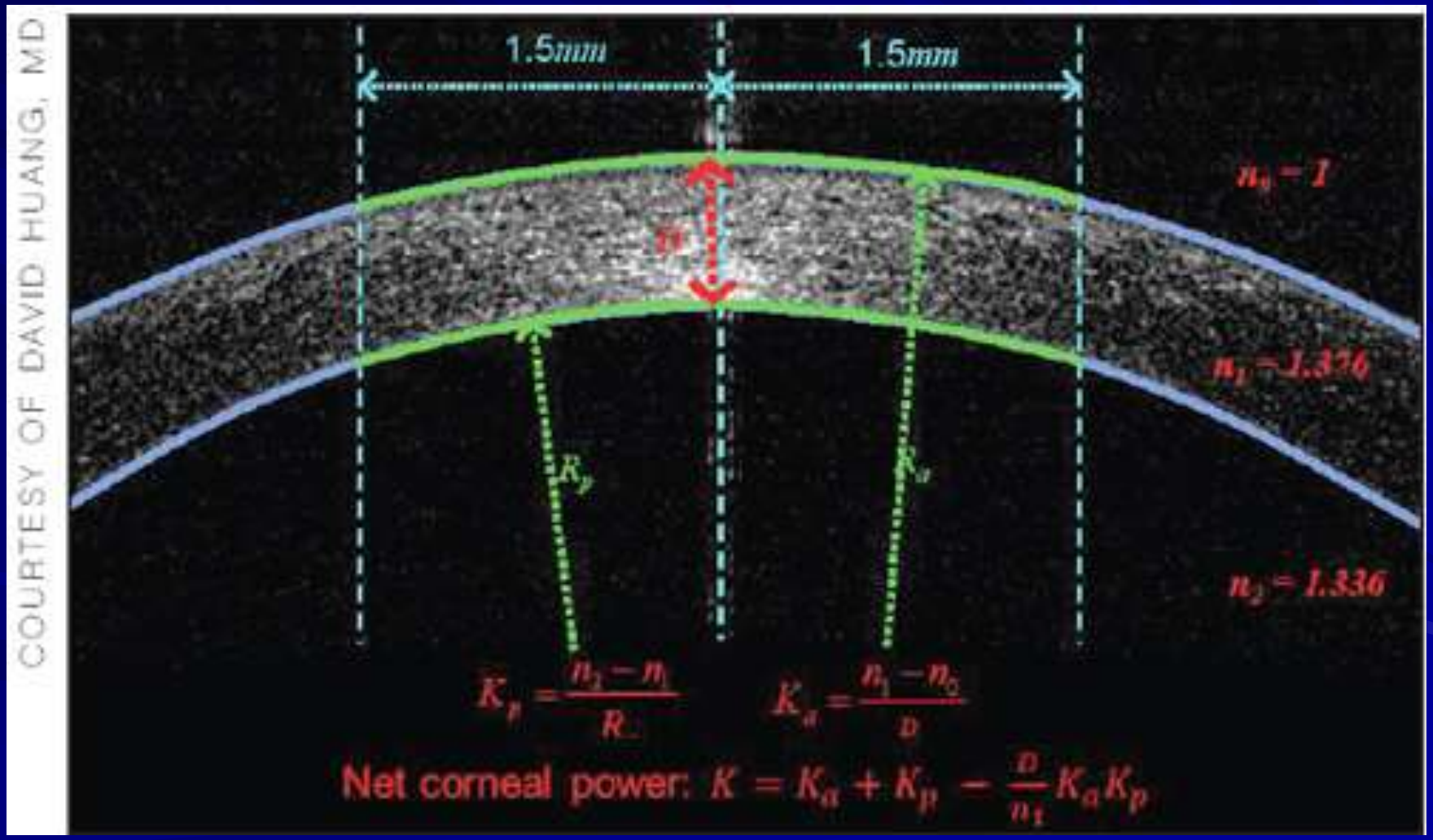

NLEA Average outcome SE -0.34 D, SD 0.63 D

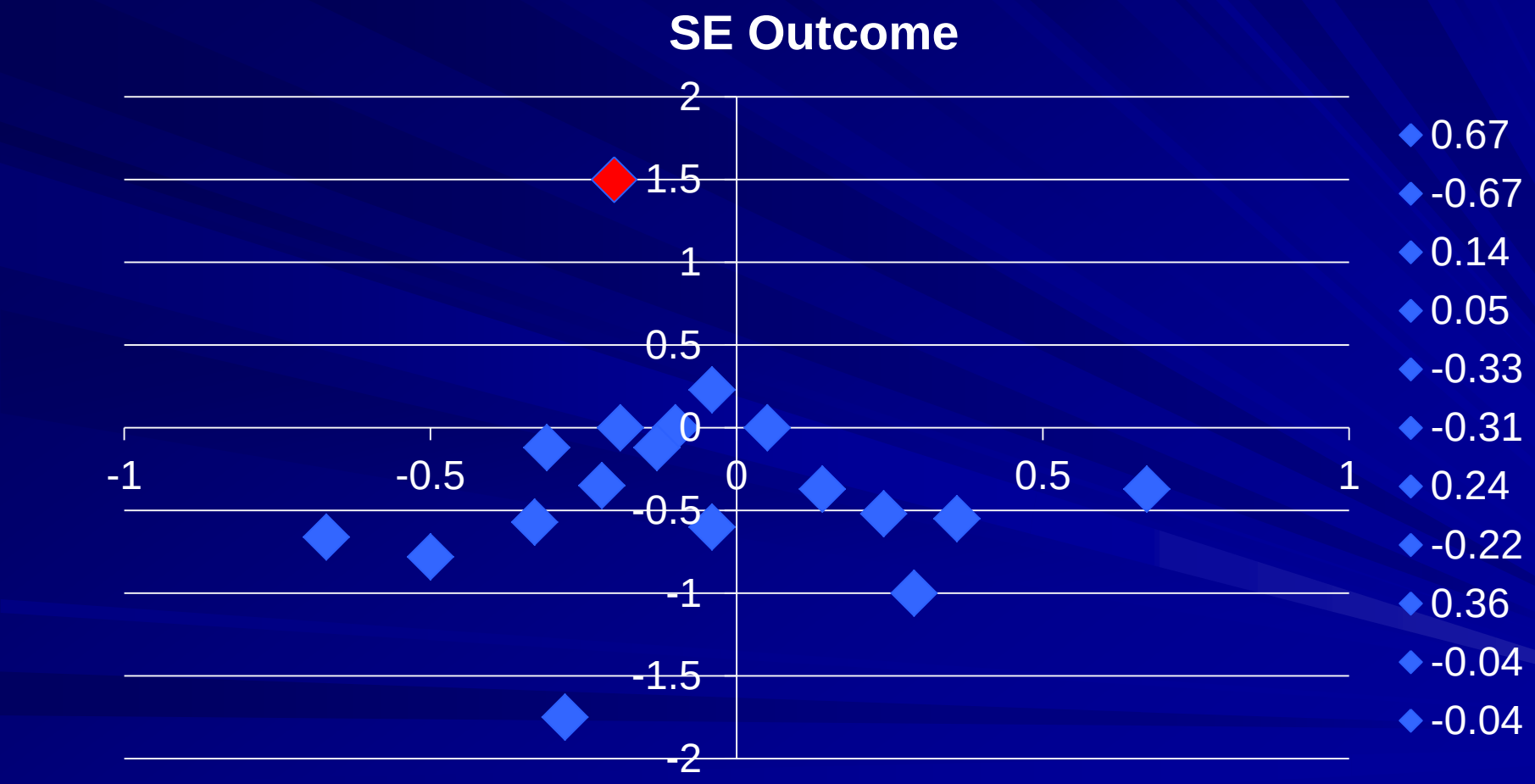

Average error from calculated SE -0.27 D,SD 0.70 D

Trackers

Angle Kappa

Line of sight is close to light reflex

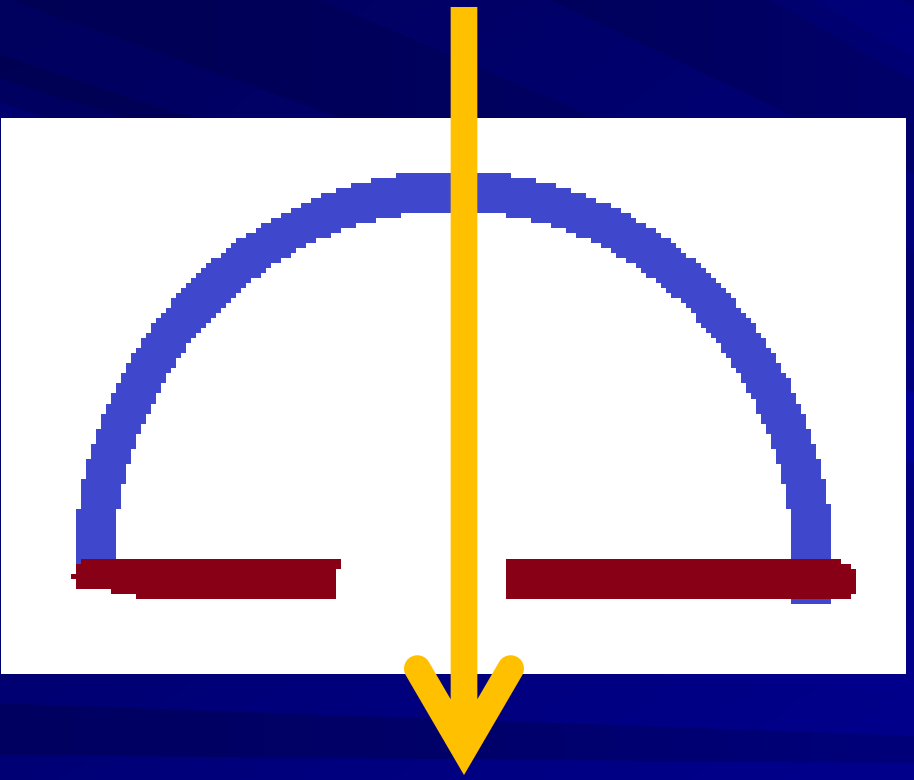

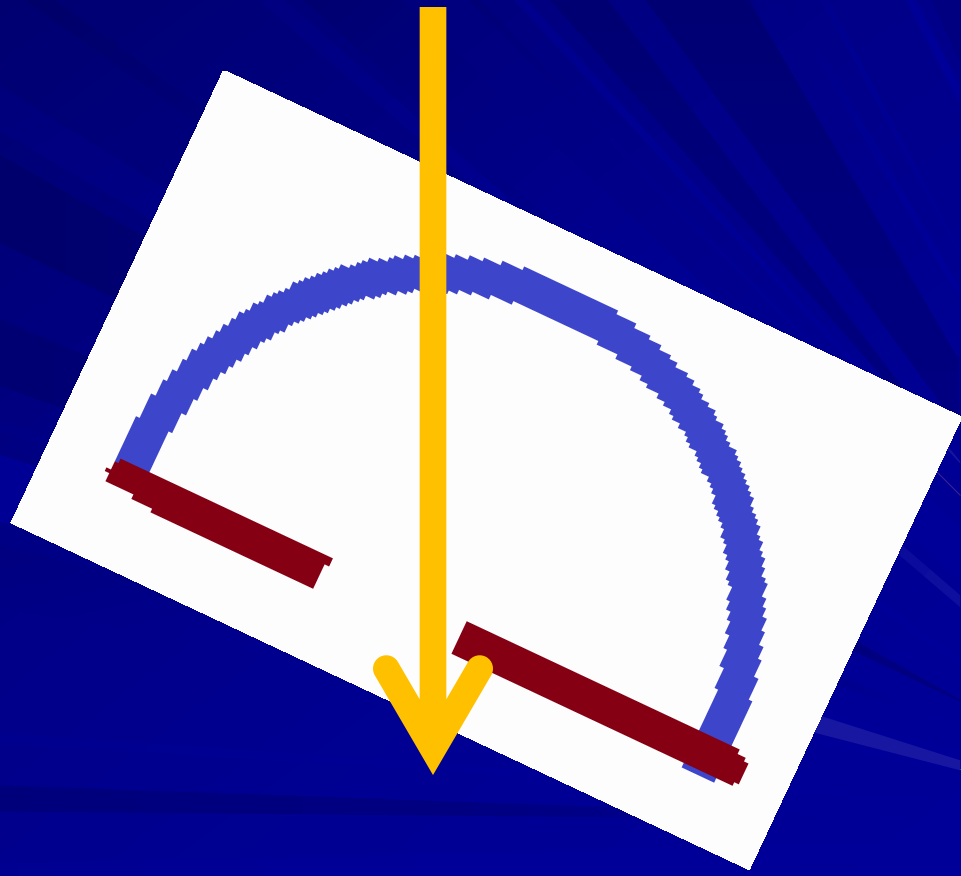

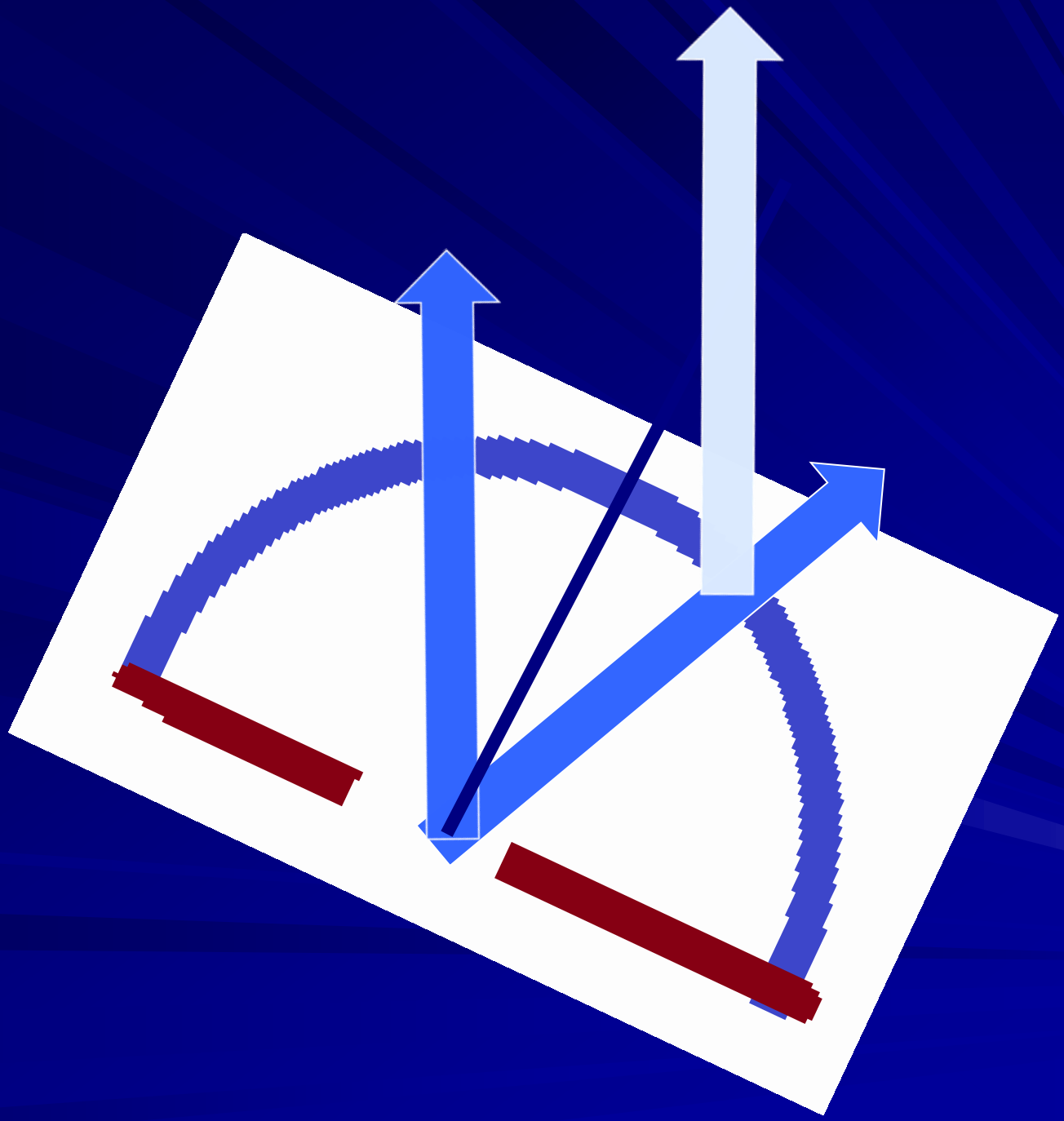

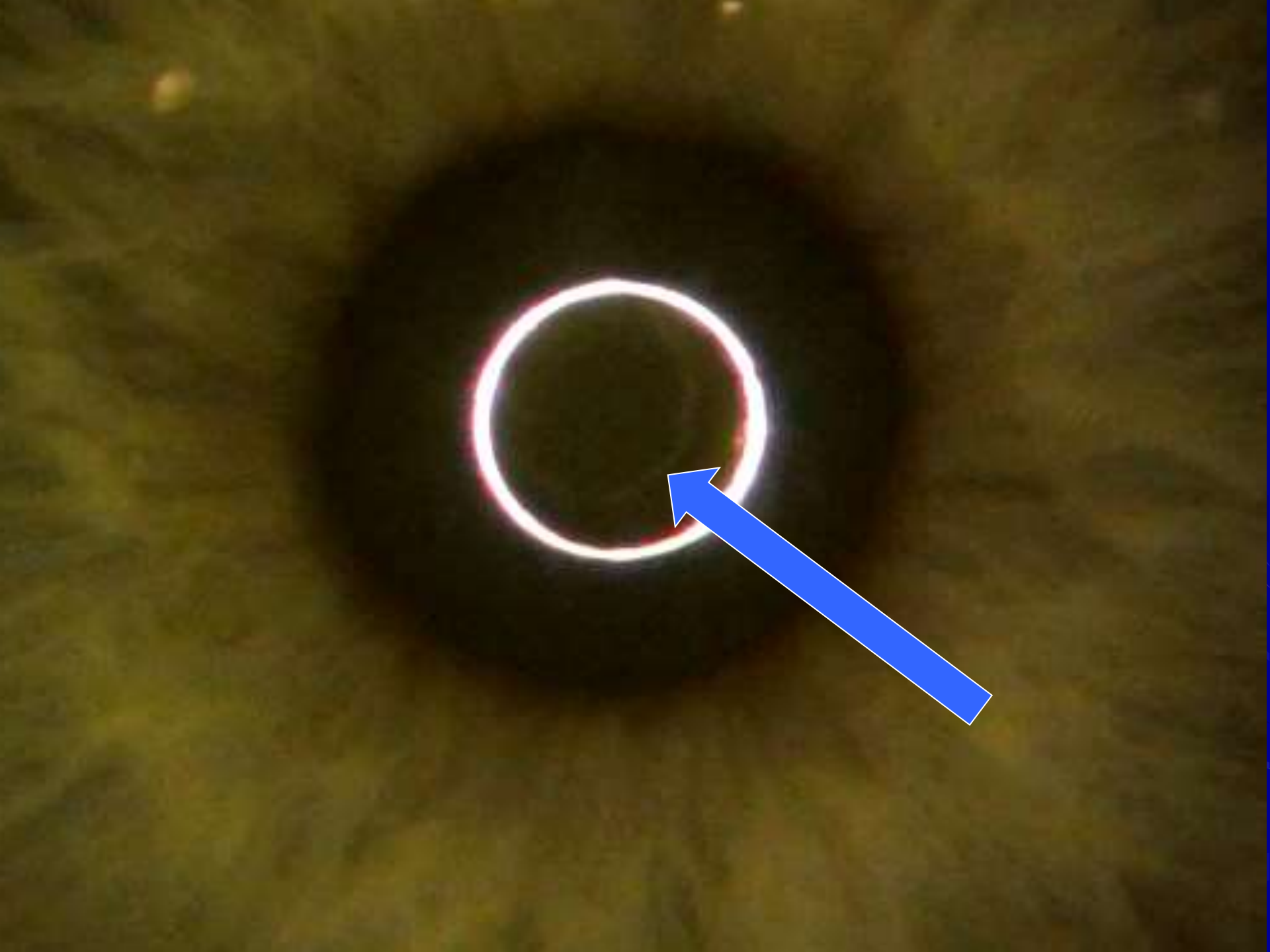

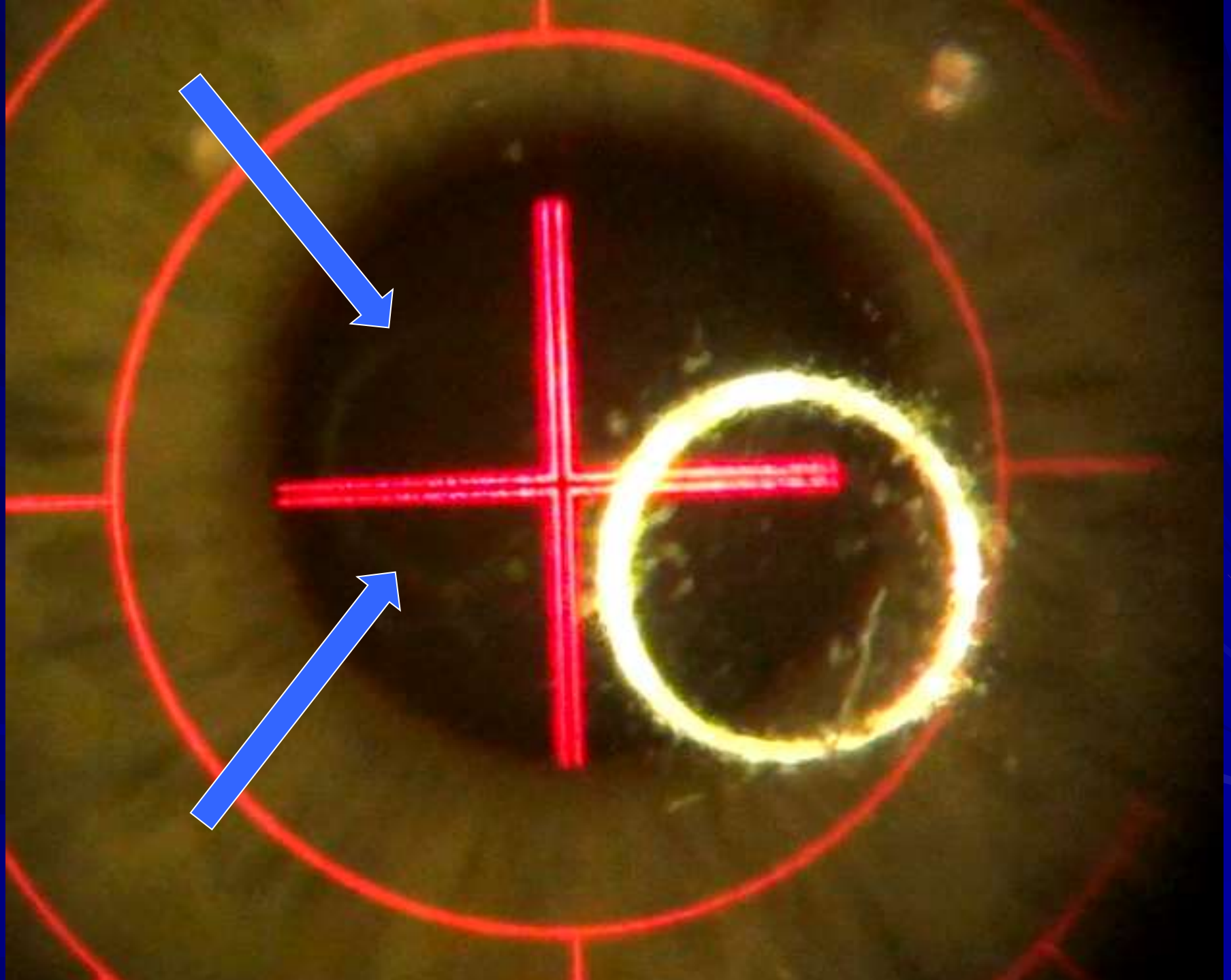

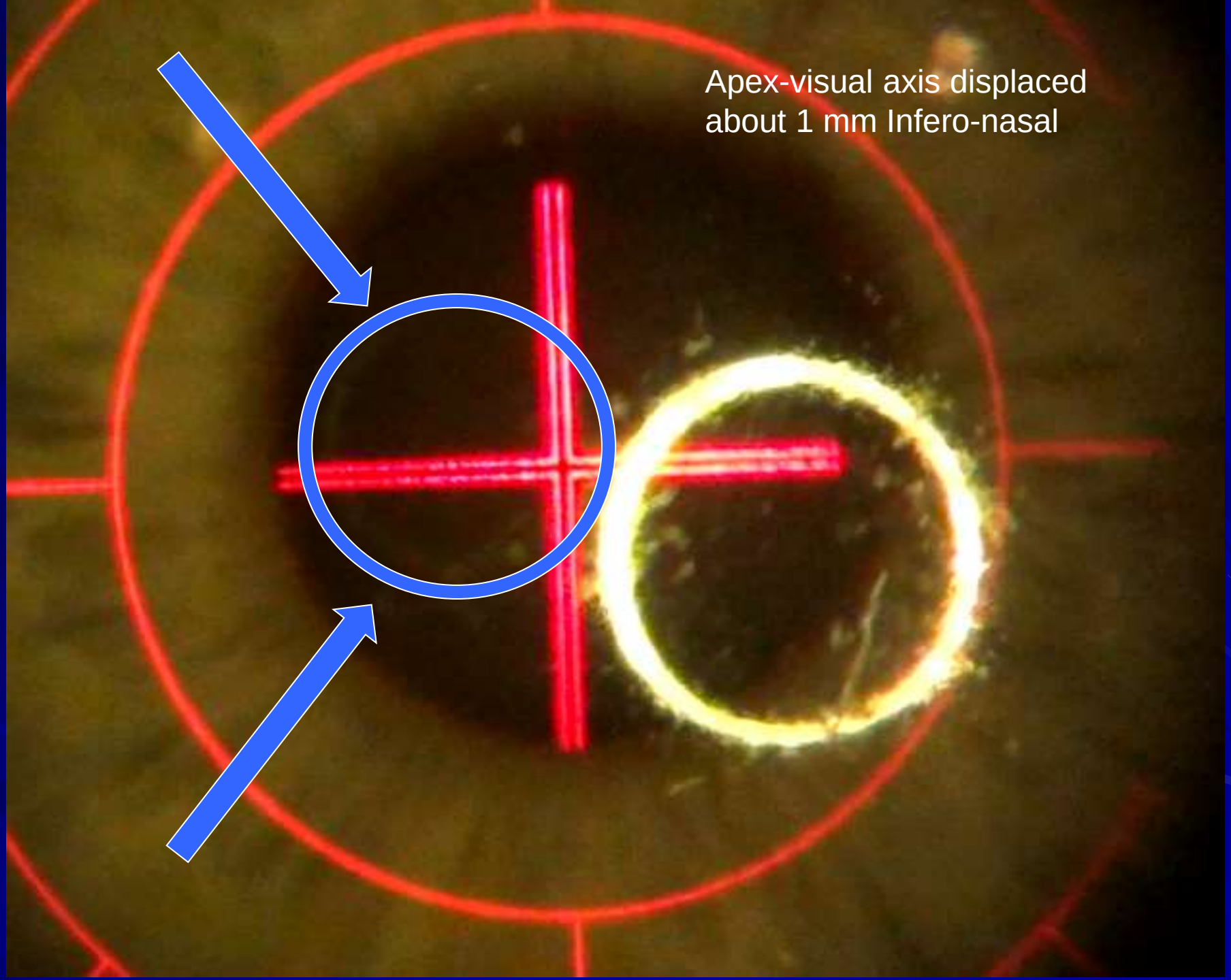
Apex-visual axis displaced
about 1 mm Infero-nasal

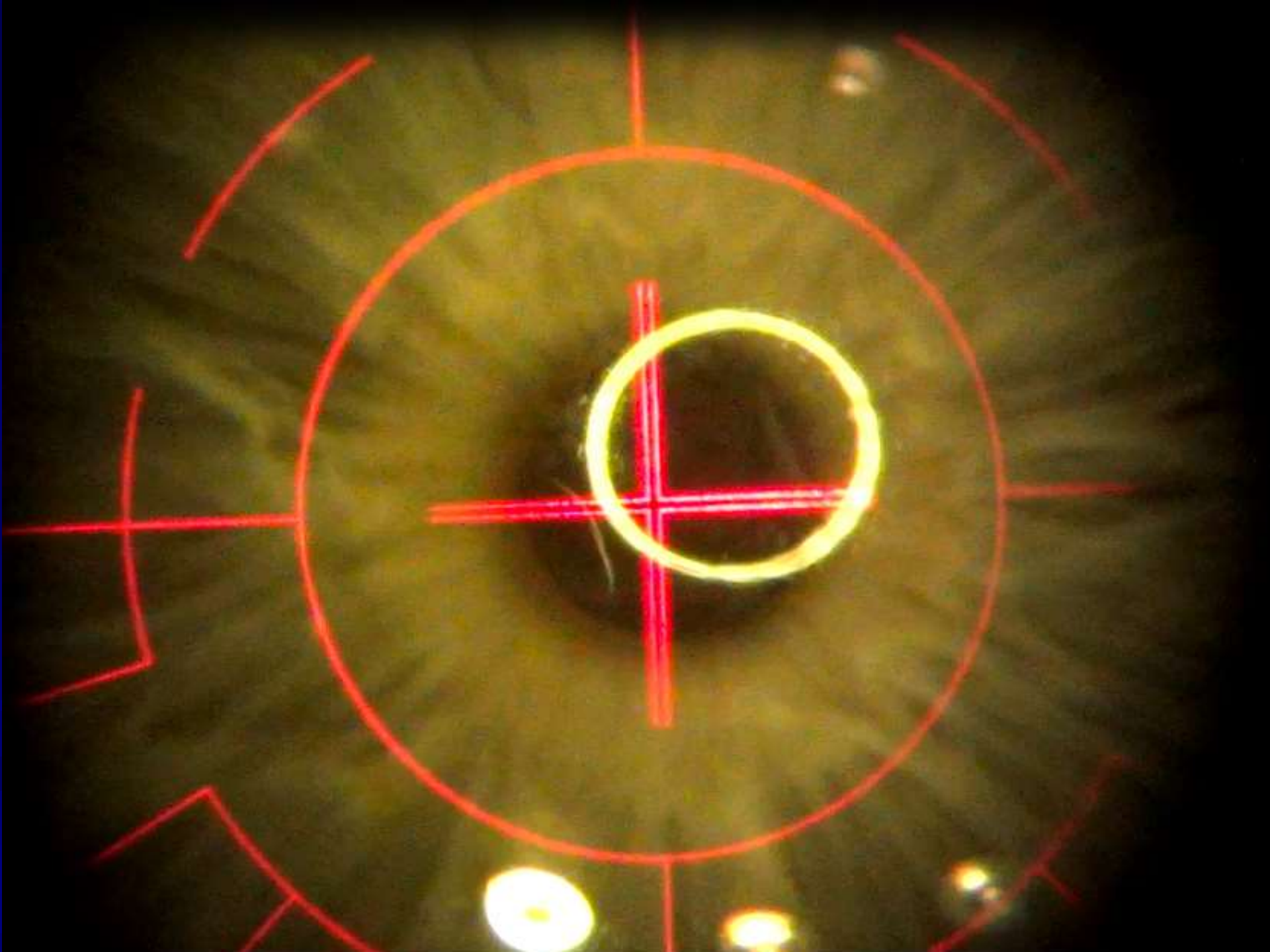

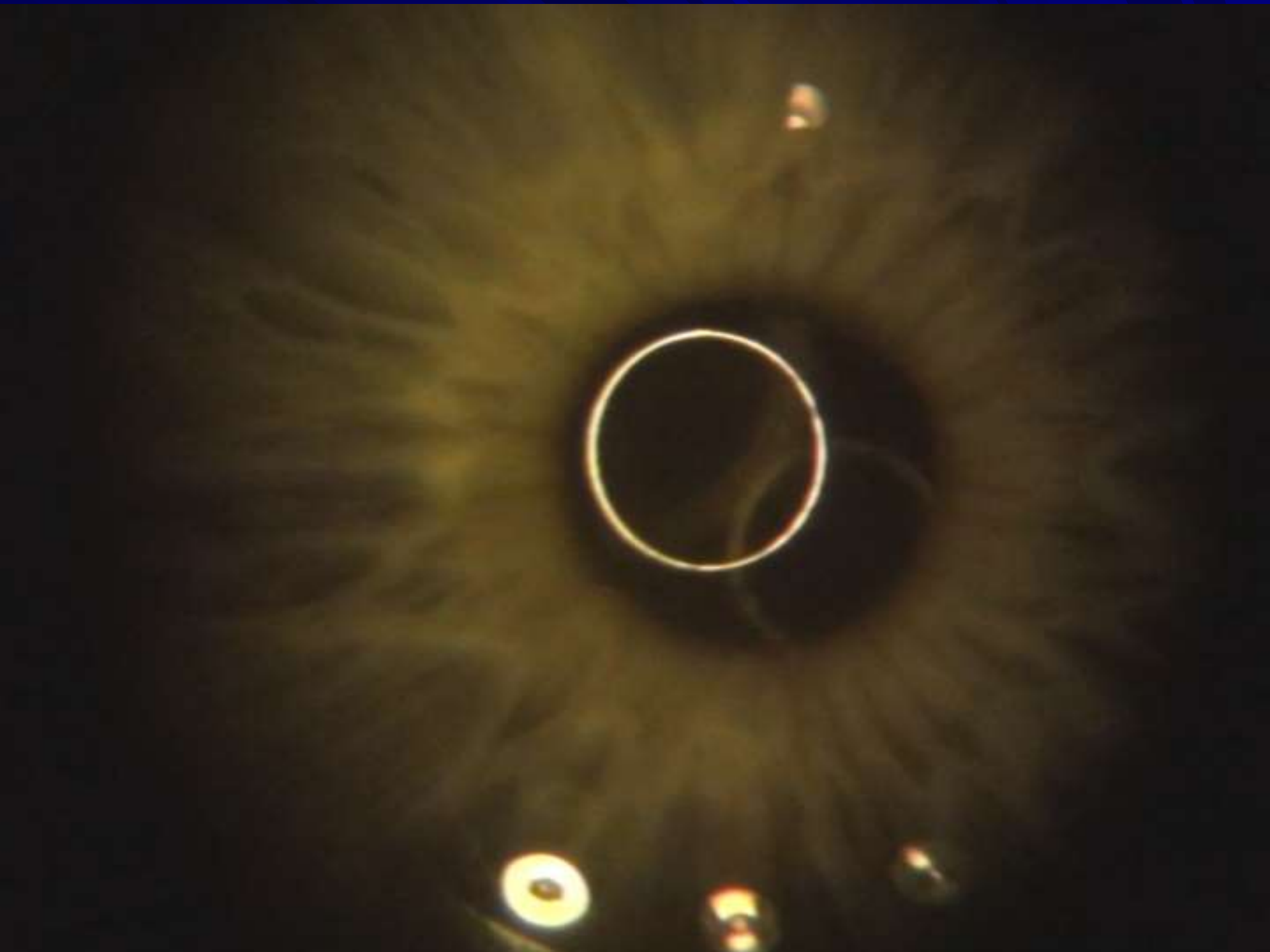

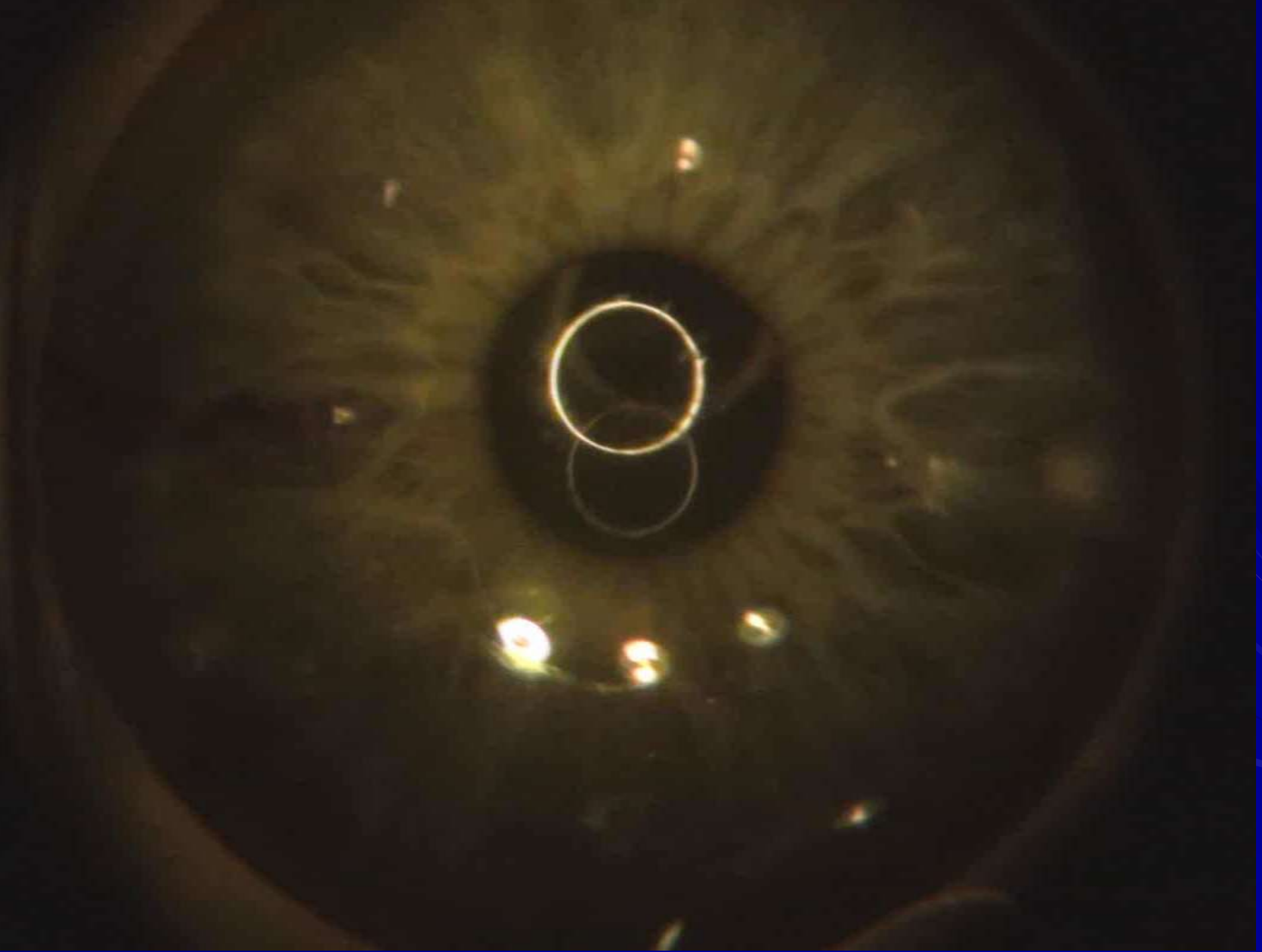

Can estimate the true location of the fish by triangulation with view 90 degrees apart

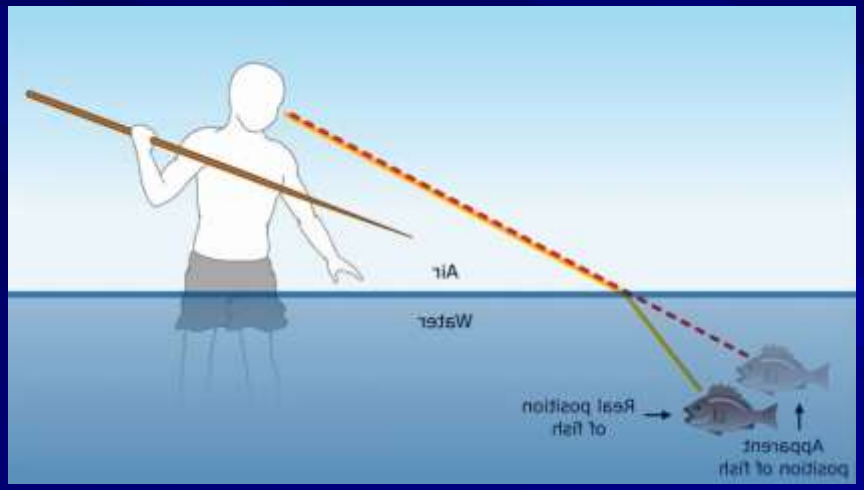

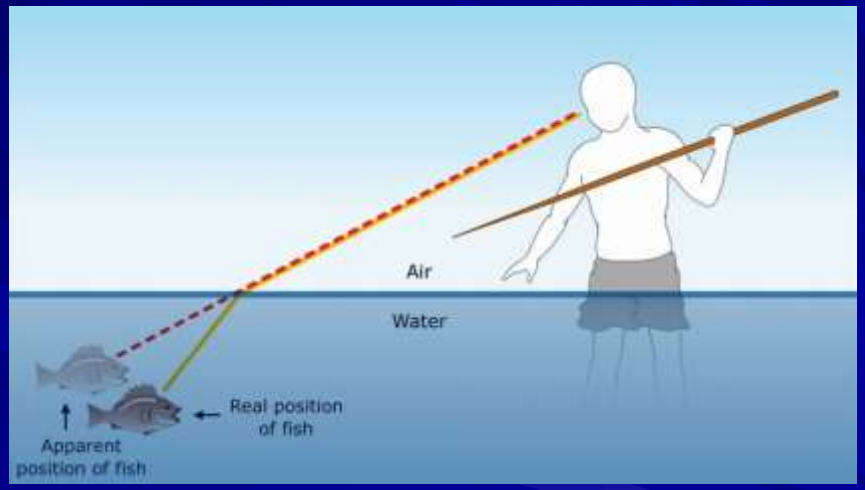

STAR S3™ Tracking Mechanism

- Surgeon controlled
- Tracks entire pupil
  - Tracks on pupil edge not on pupil center
  - Tracker stops laser from firing with eye movement of 1.5mm or more
  - Treatment resumes when eye is repositioned

A Visx Standard 6.5 mm optical zone with 8.0 mm blend zone was used.

The reticle is used to estimate the offset,

limited to 0.35mm by the laser

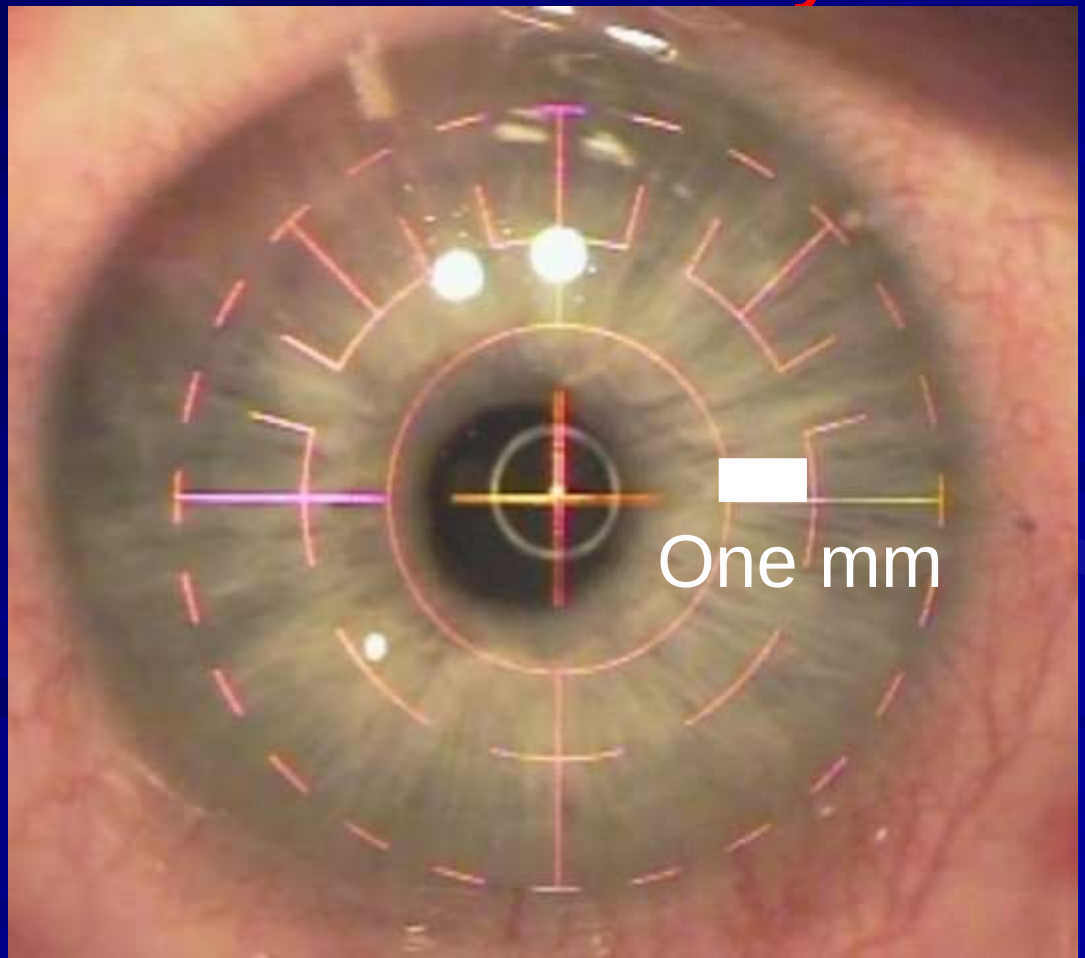

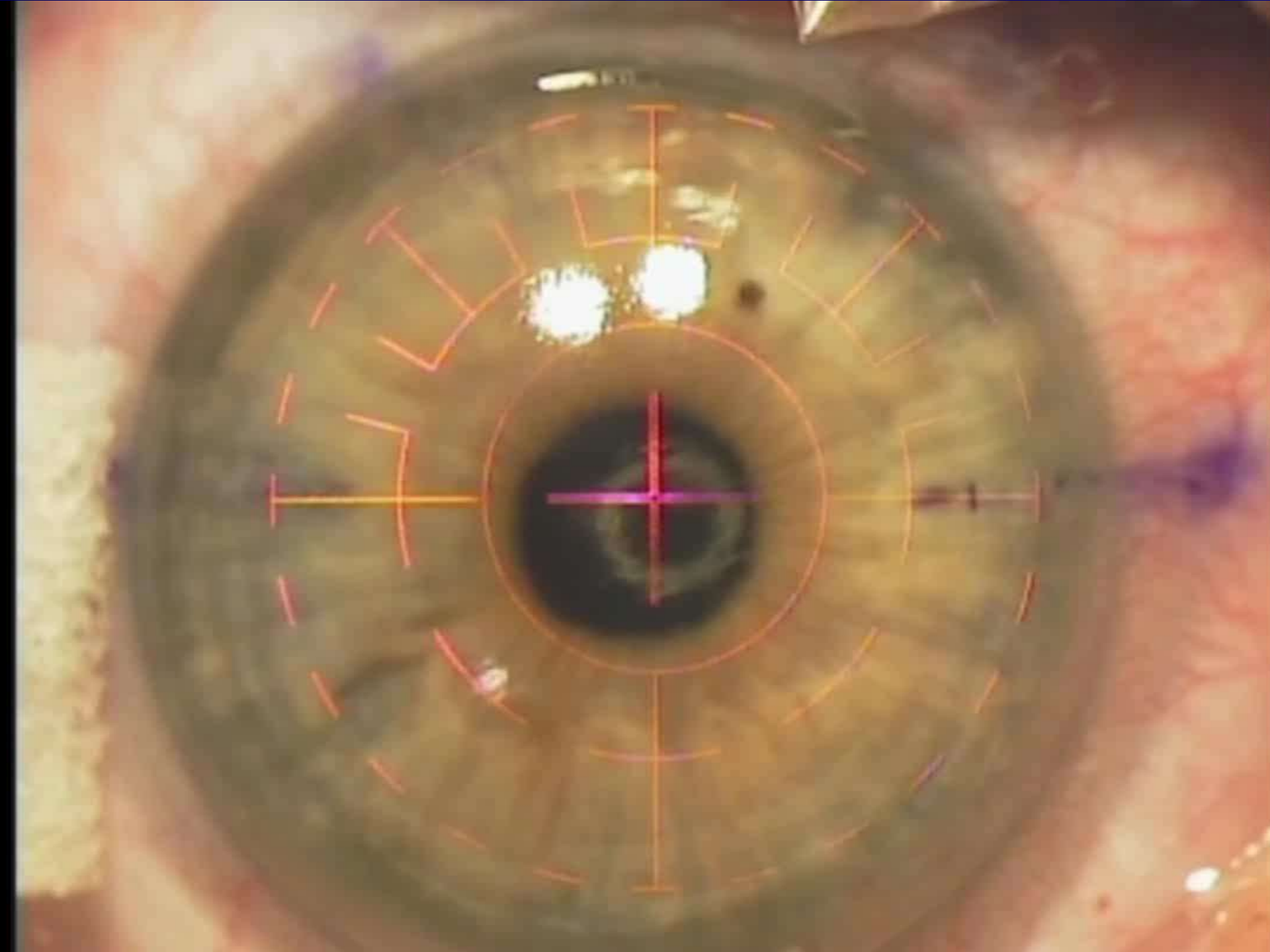

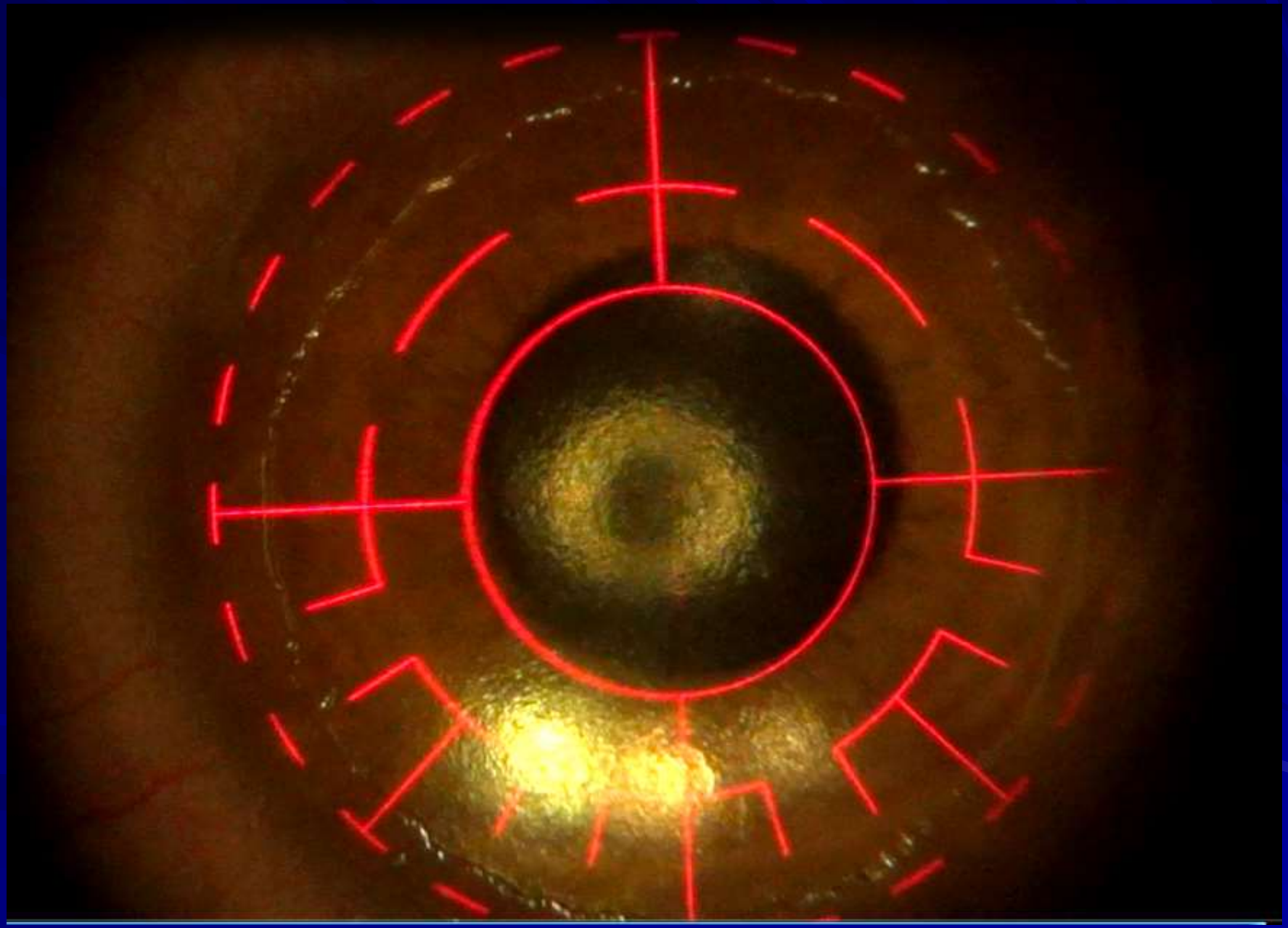

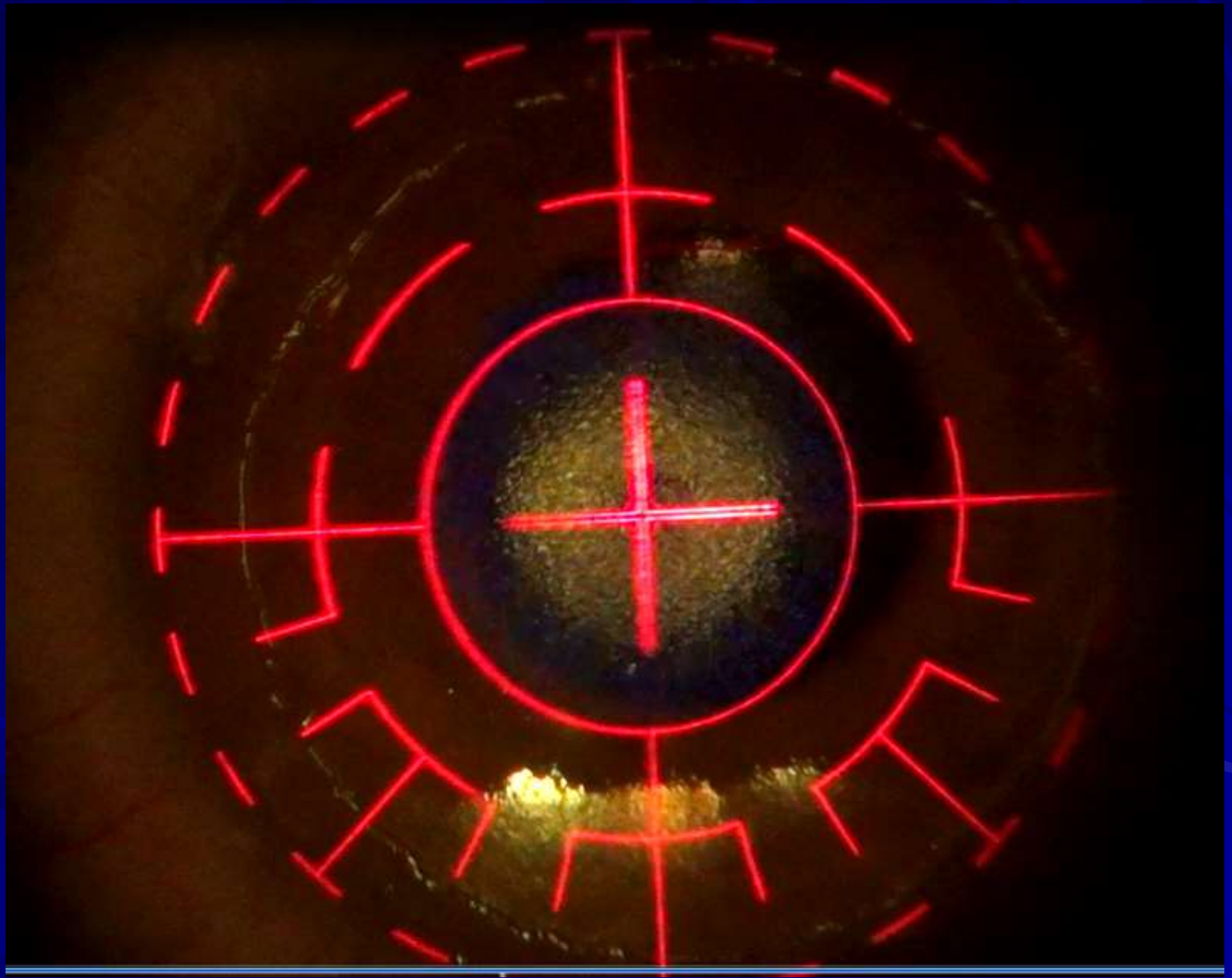

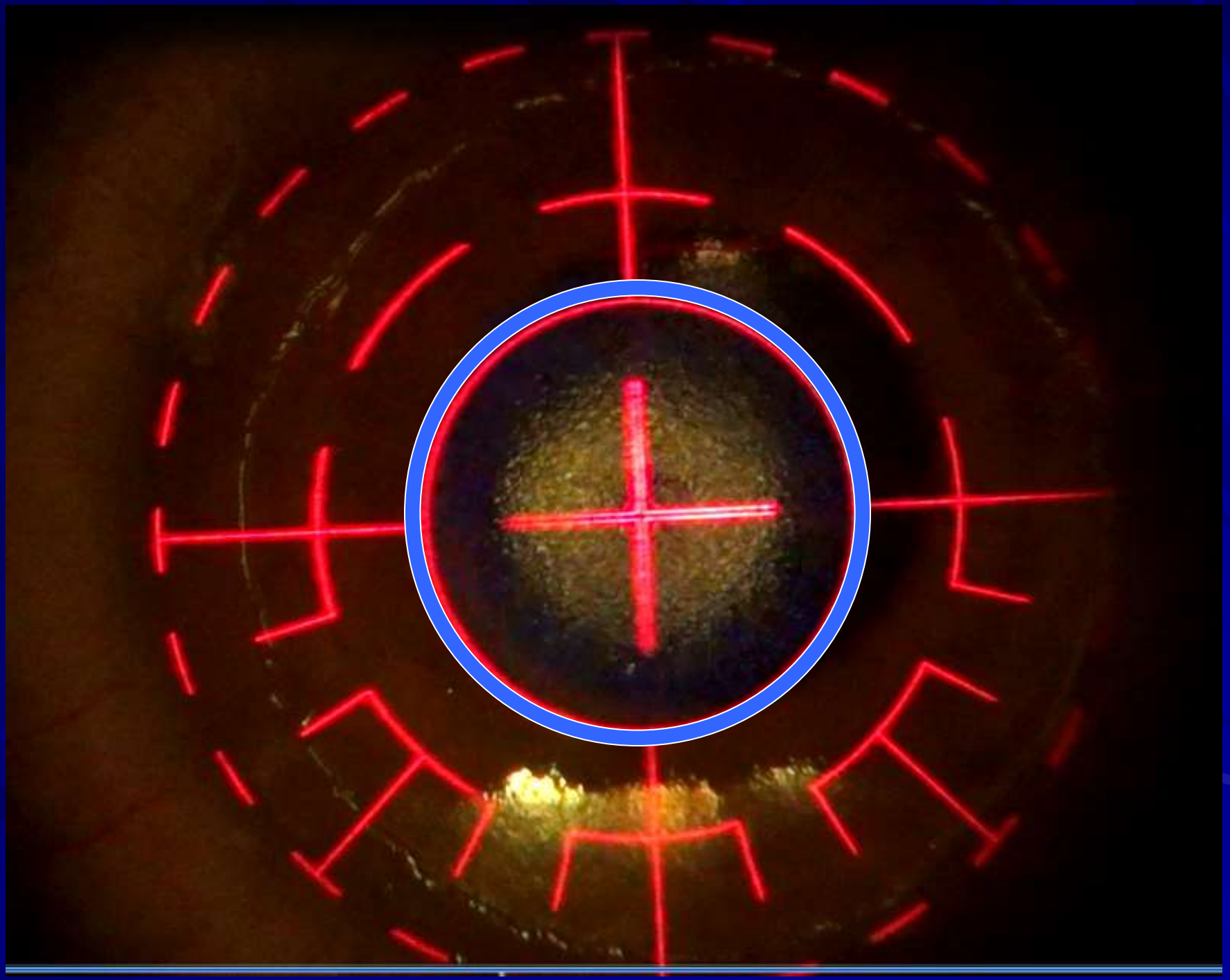

Centroid Shift: Constricted pupil typically moves Superior Temporal

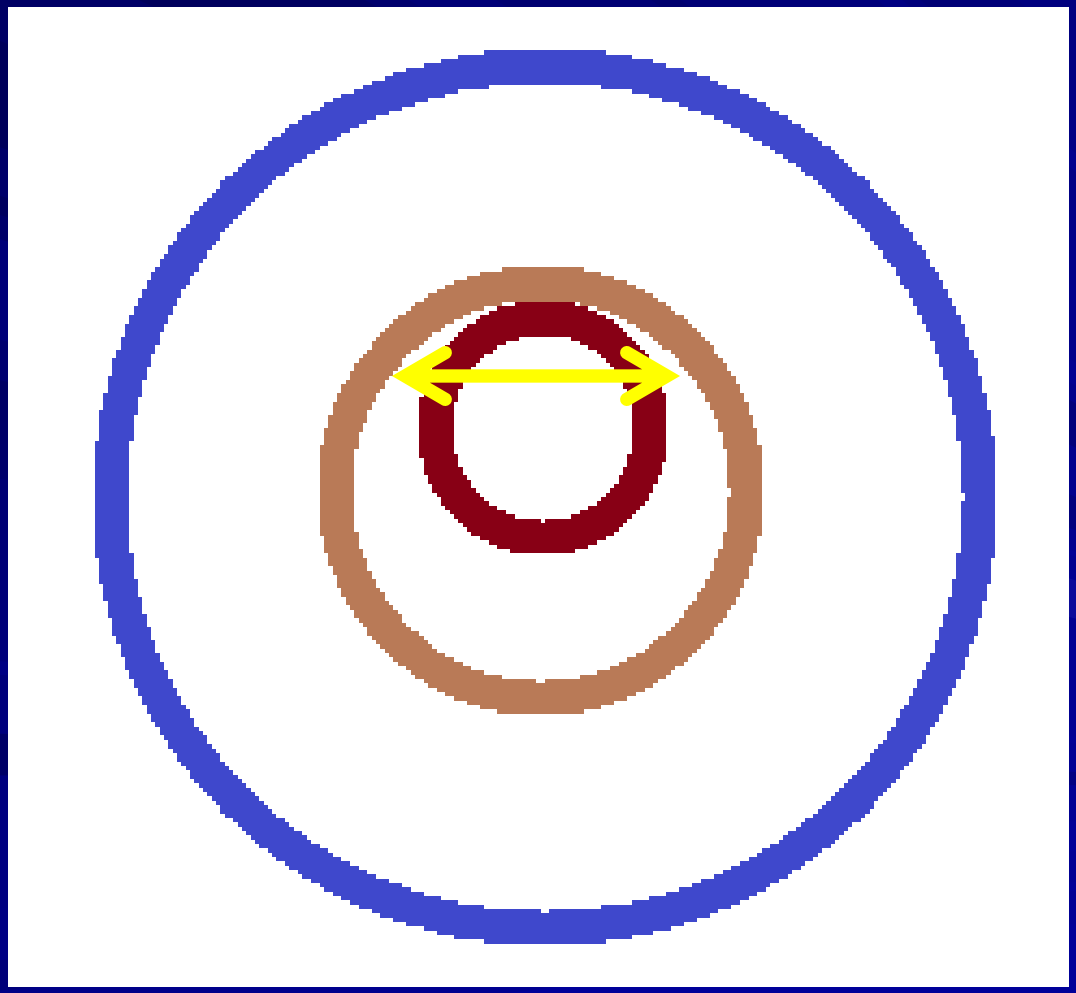


Tracker offset laser more than 0.35 mm
One mm

Pupil has constricted and shifted up, relative to the visual axis.
Why is the tracker not moving the ablation up and out as well ?

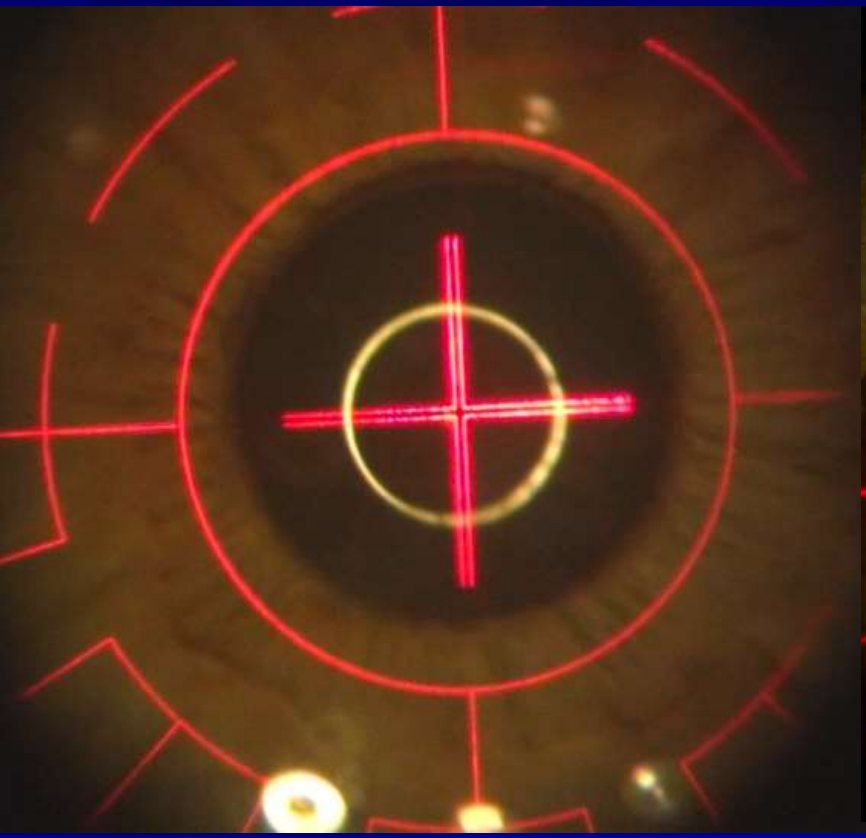

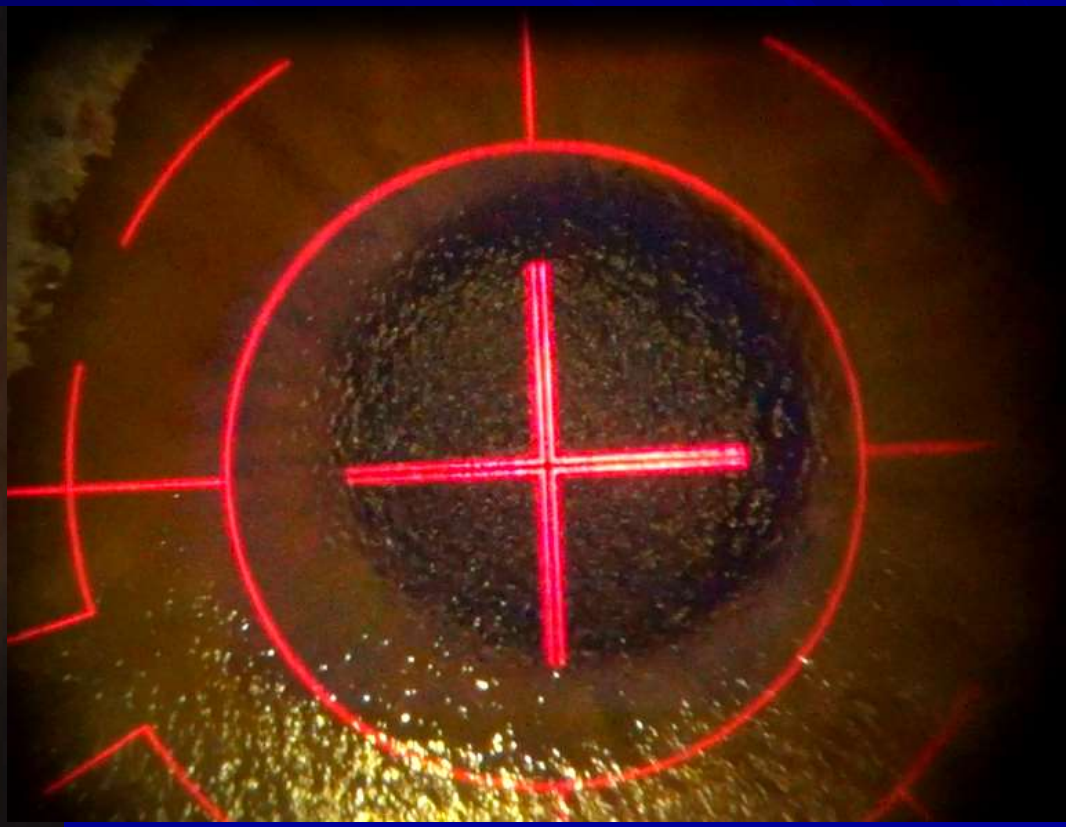

Thickness Map
Post minus Pre equals Difference

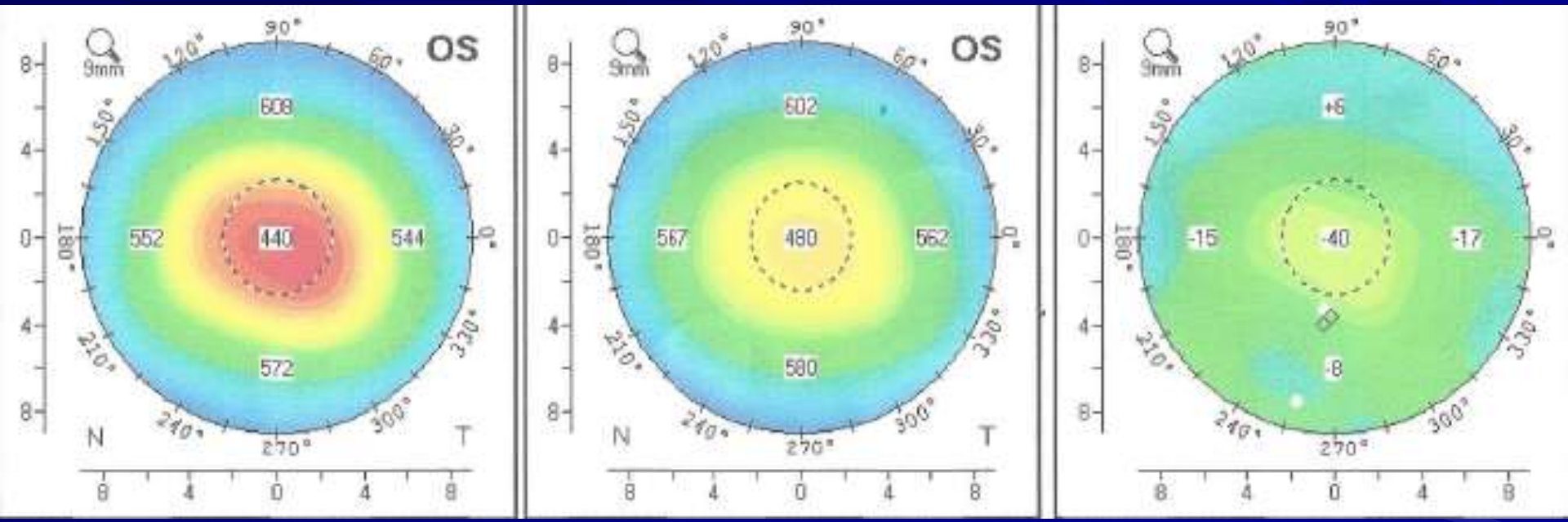

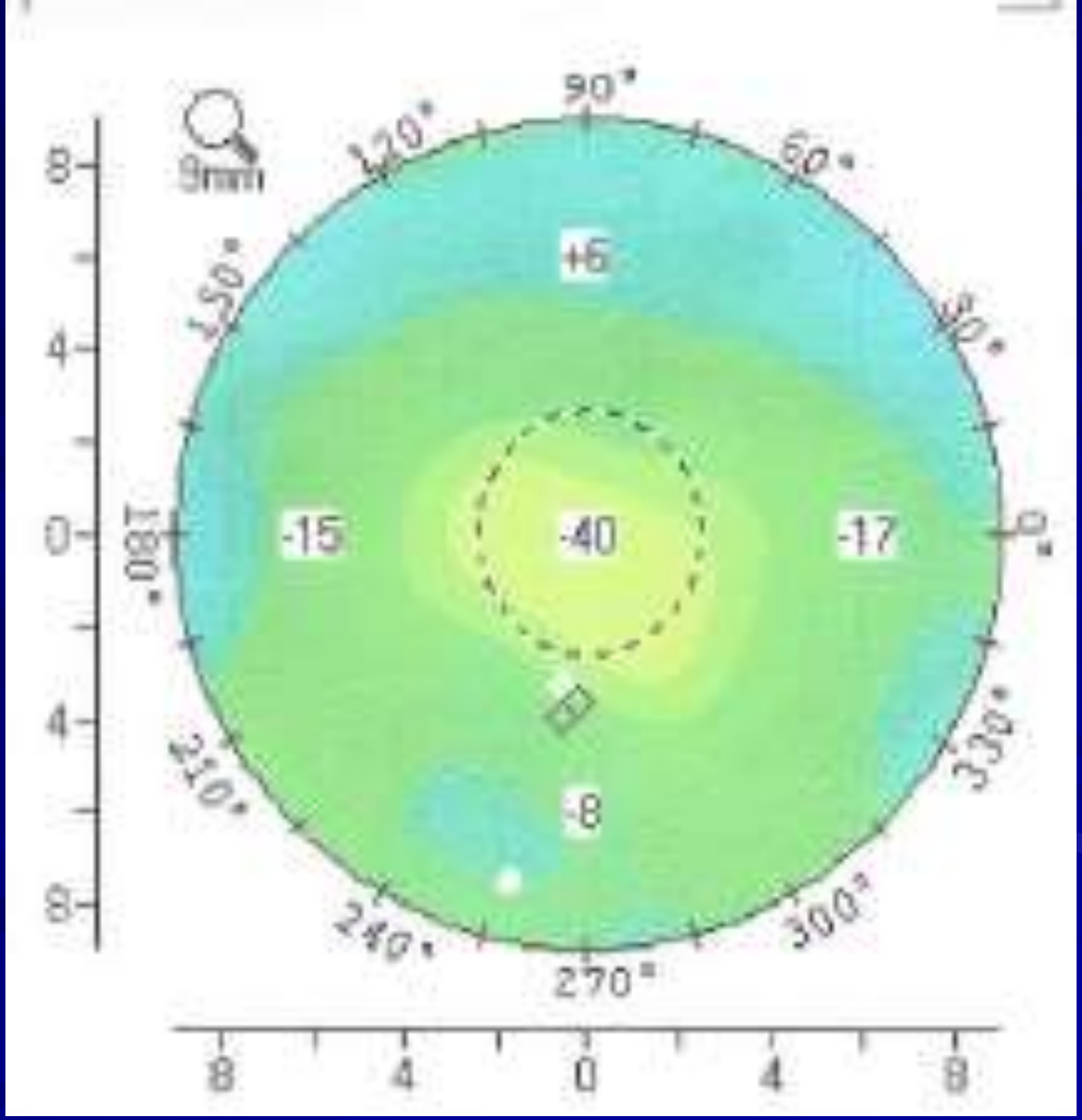
90°
120°
60°
150°
30°
180°
0°
210°
330°
240°
300°
270°
+6
-15
-40
-17
-8
8
4
0
4
8

Anterior Elevation Map

Post minus Pre equals Difference

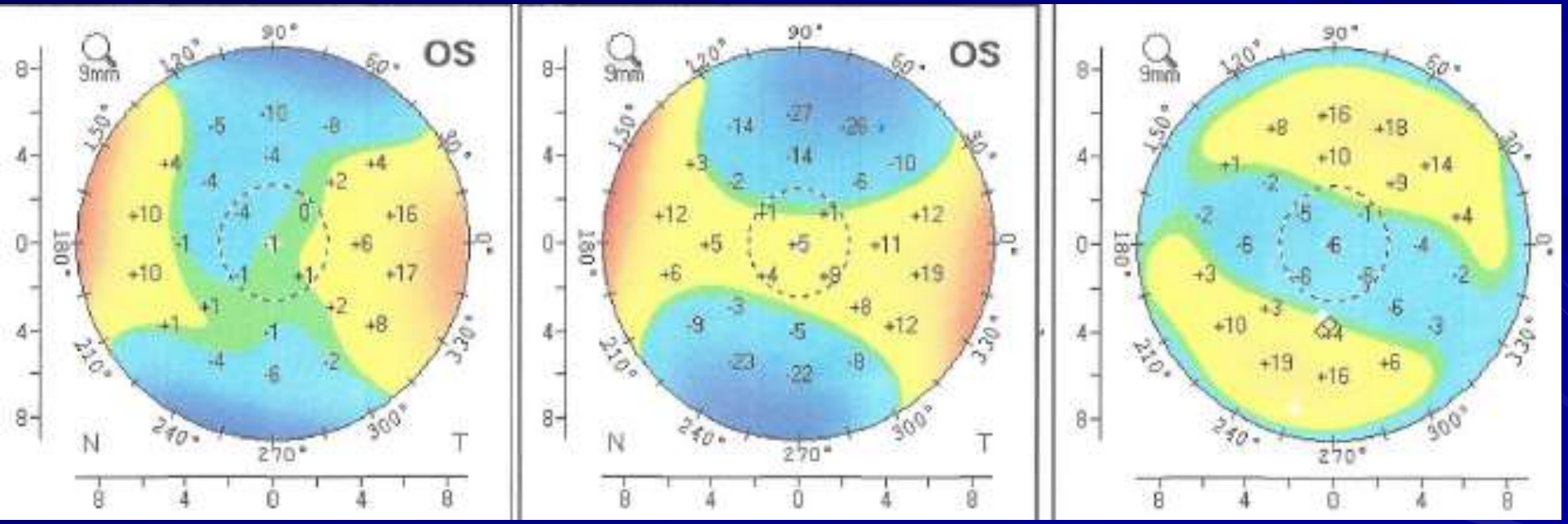

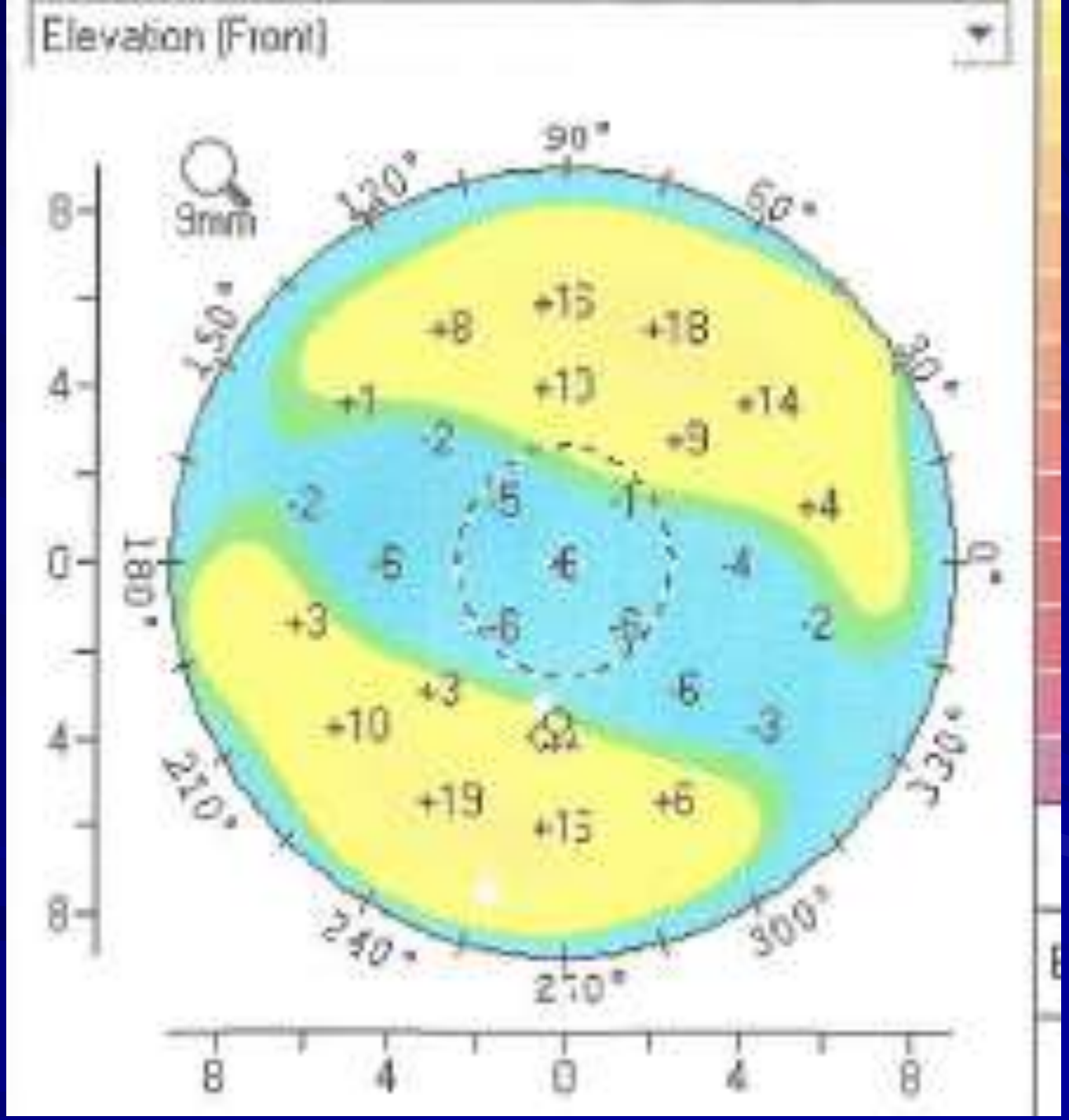
Elevation (Front)
9mm
90°
120°
60°
150°
30°
180°
0°
210°
330°
240°
300°
270°
8
4
0
4
8
+8
+15
+18
+1
+13
+14
-2
+9
-2
-5
-1
+4
-6
-4
-4
+3
-6
-2
+3
+10
+19
+15
+6
-3

Curvature Map

Post minus Pre equals Difference

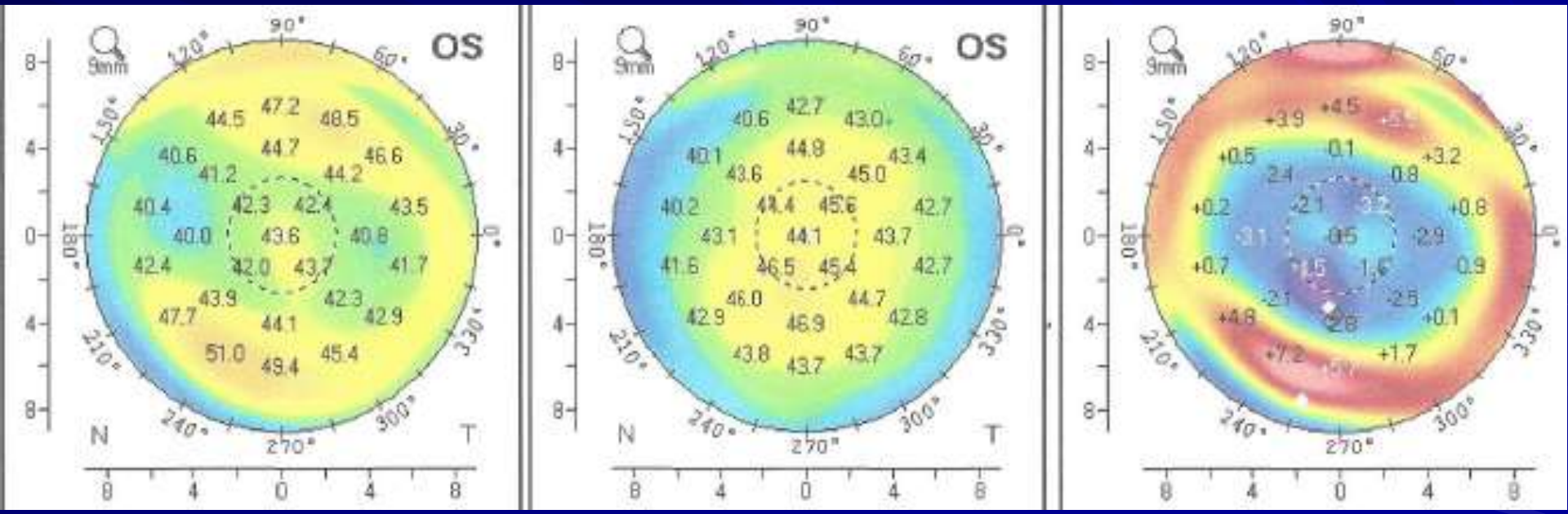

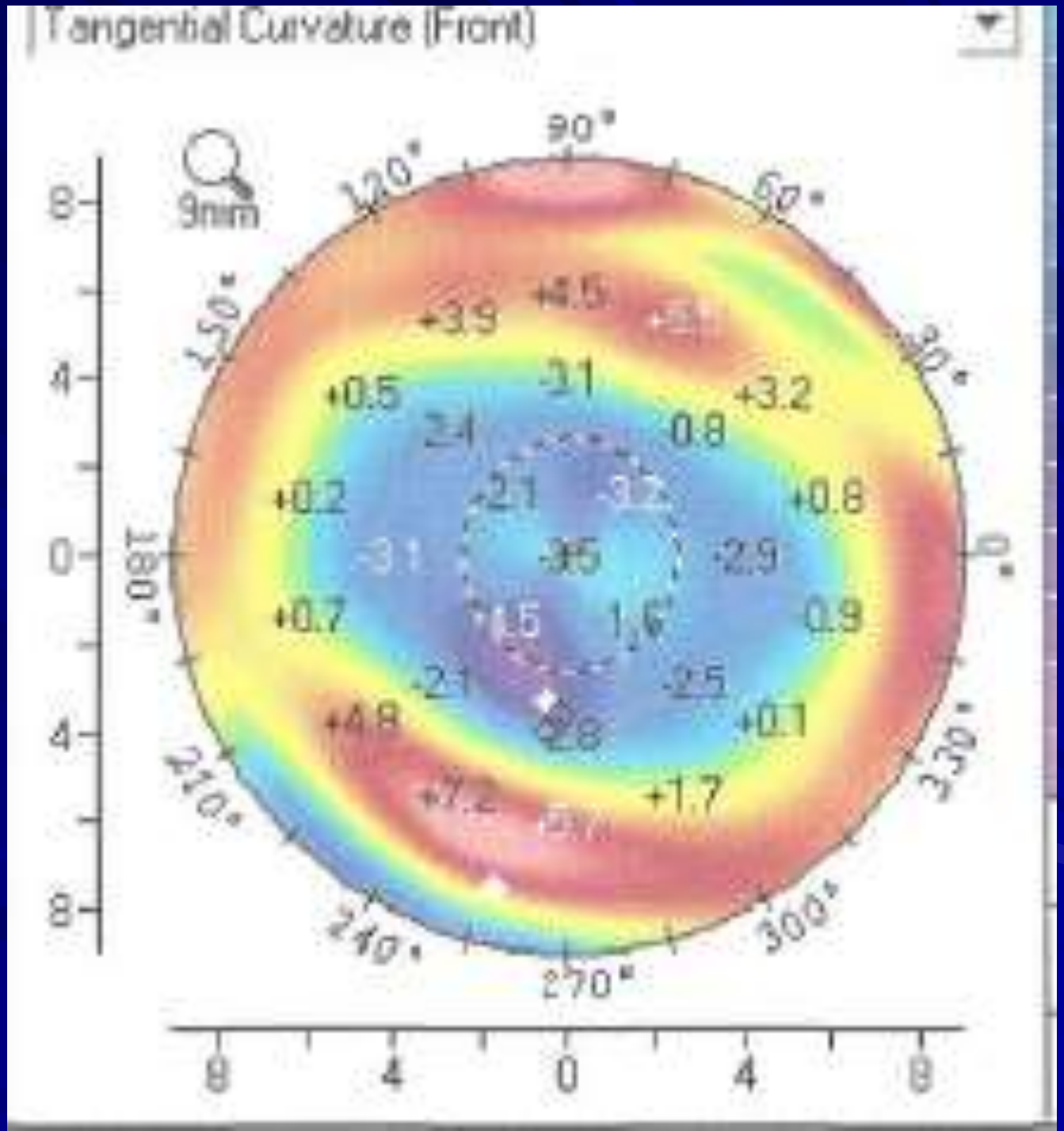
Tangential Curvature (Front)
9mm
90°
120°
60°
150°
30°
180°
0°
210°
330°
240°
300°
270°
+3.9
+0.5
-3.1
+3.2
2.4
0.8
+0.2
-2.1
-3.2
+0.8
-3.1
-3.5
+2.9
+0.7
1.6
0.9
-2.1
-2.5
+4.8
+0.1
+7.2
+1.7
8
4
0
4
8
8
4
0
4
8

Calculated position of virtual pupil
With off axis appears up to 0.4 mm closer

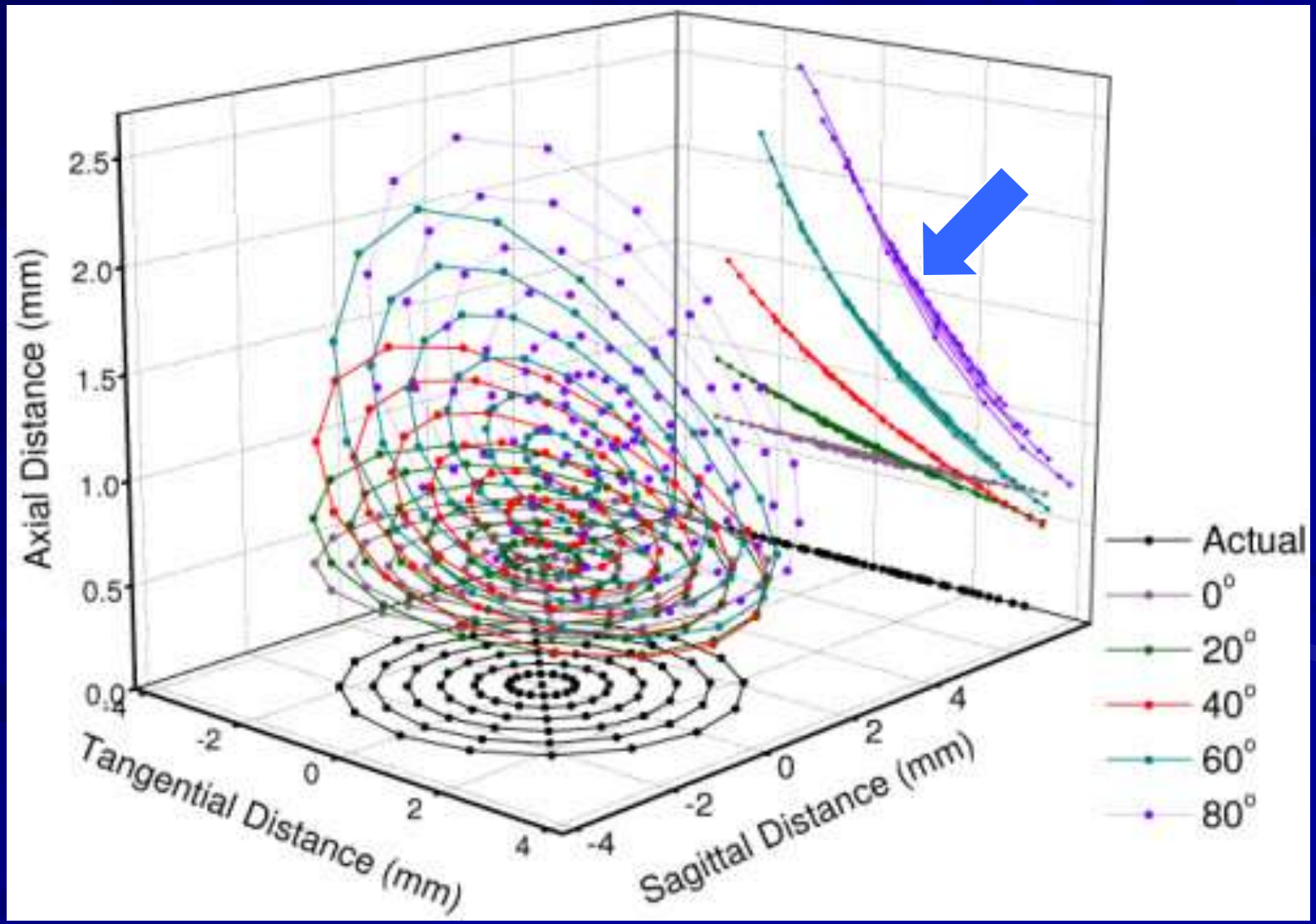

Pupil shifts when viewed off axis

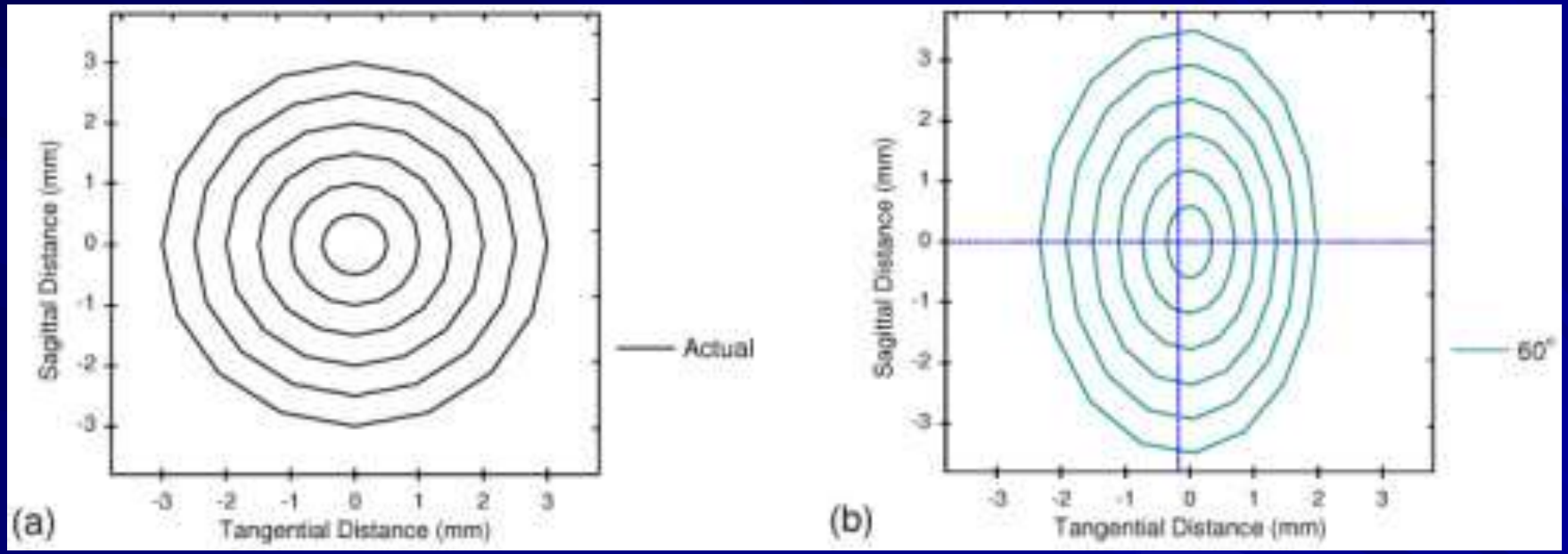

http://www.opticsinfobase.org/oe/fulltext.cfm?uri=oe-18-21-22364#&slider2=1

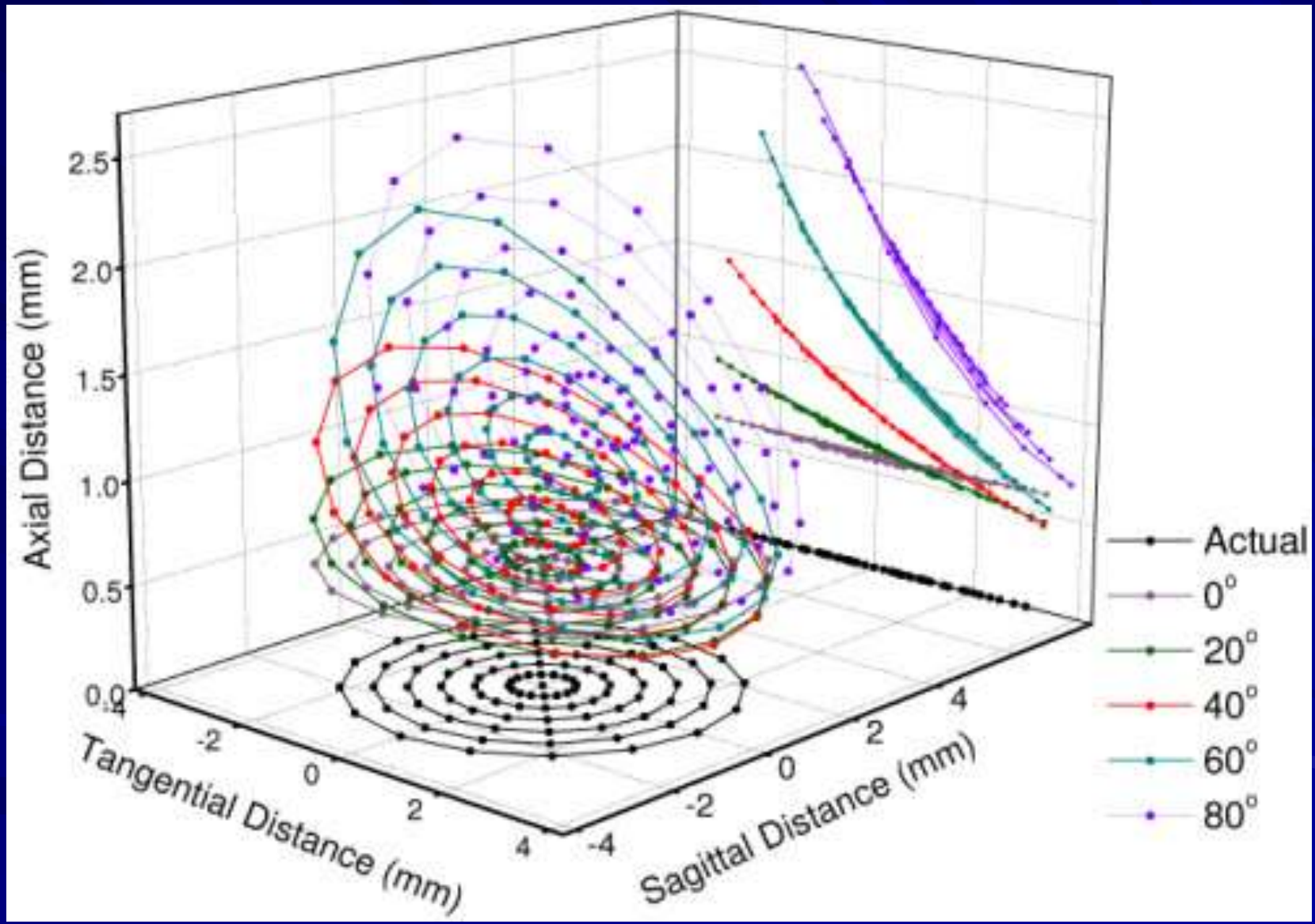
Axial Distance (mm)
2.5
2.0
1.5
1.0
0.5
0.0
Tangential Distance (mm)
-4
-2
0
2
4
Sagittal Distance (mm)
-4
-2
0
2
4
Actual
0°
20°
40°
60°
80°

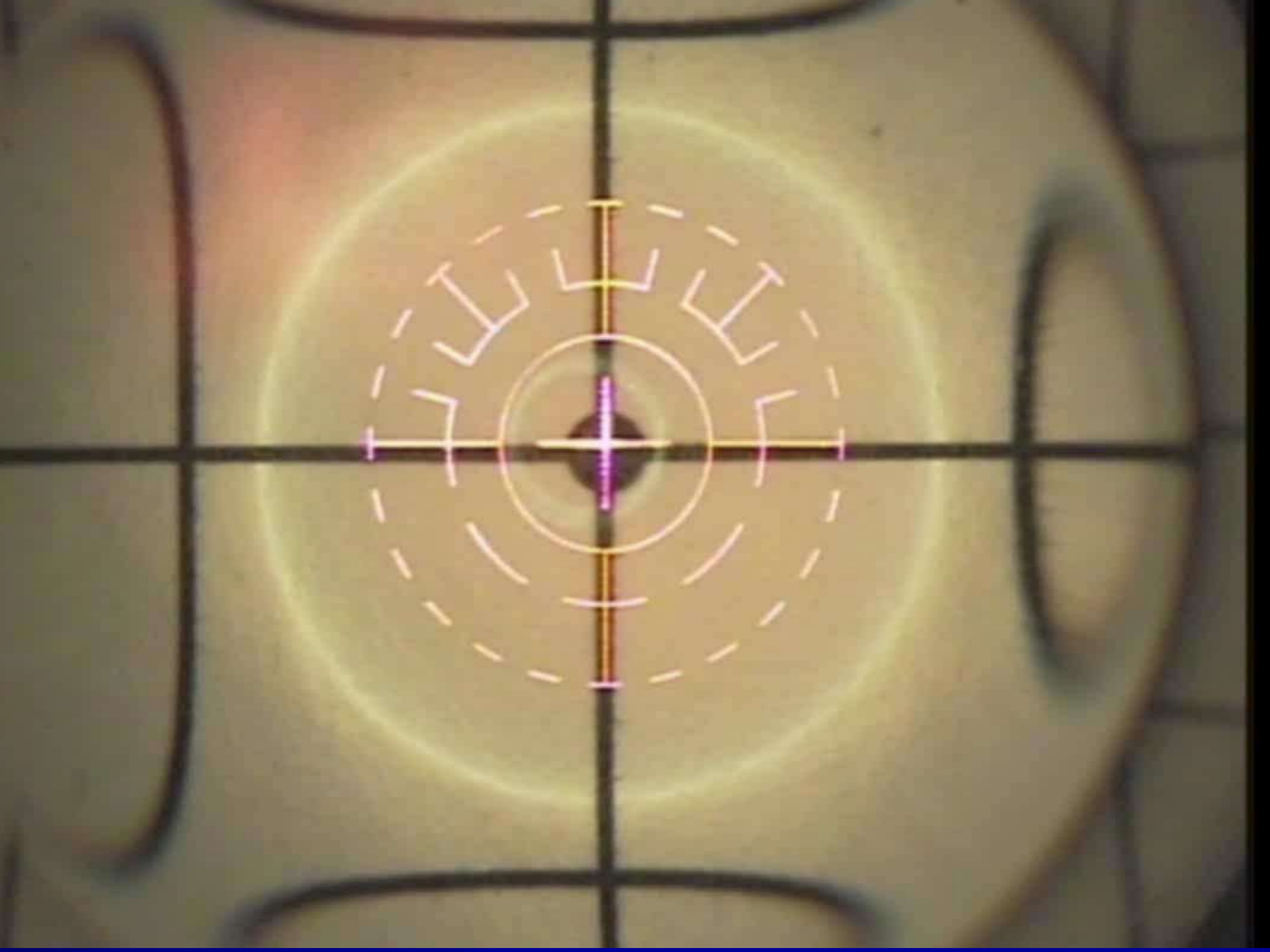

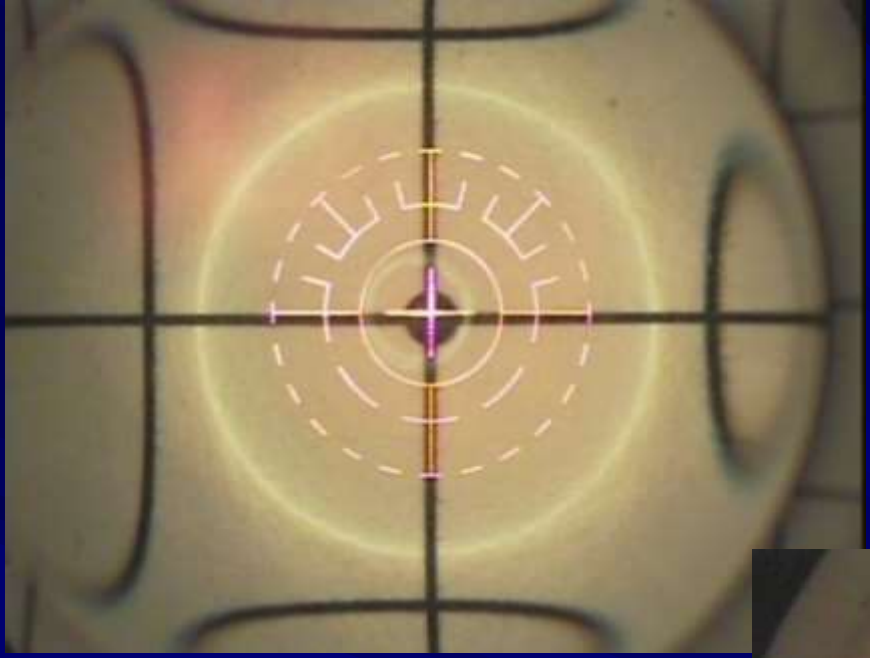

Pupil appears to move in the opposite direction from the apex

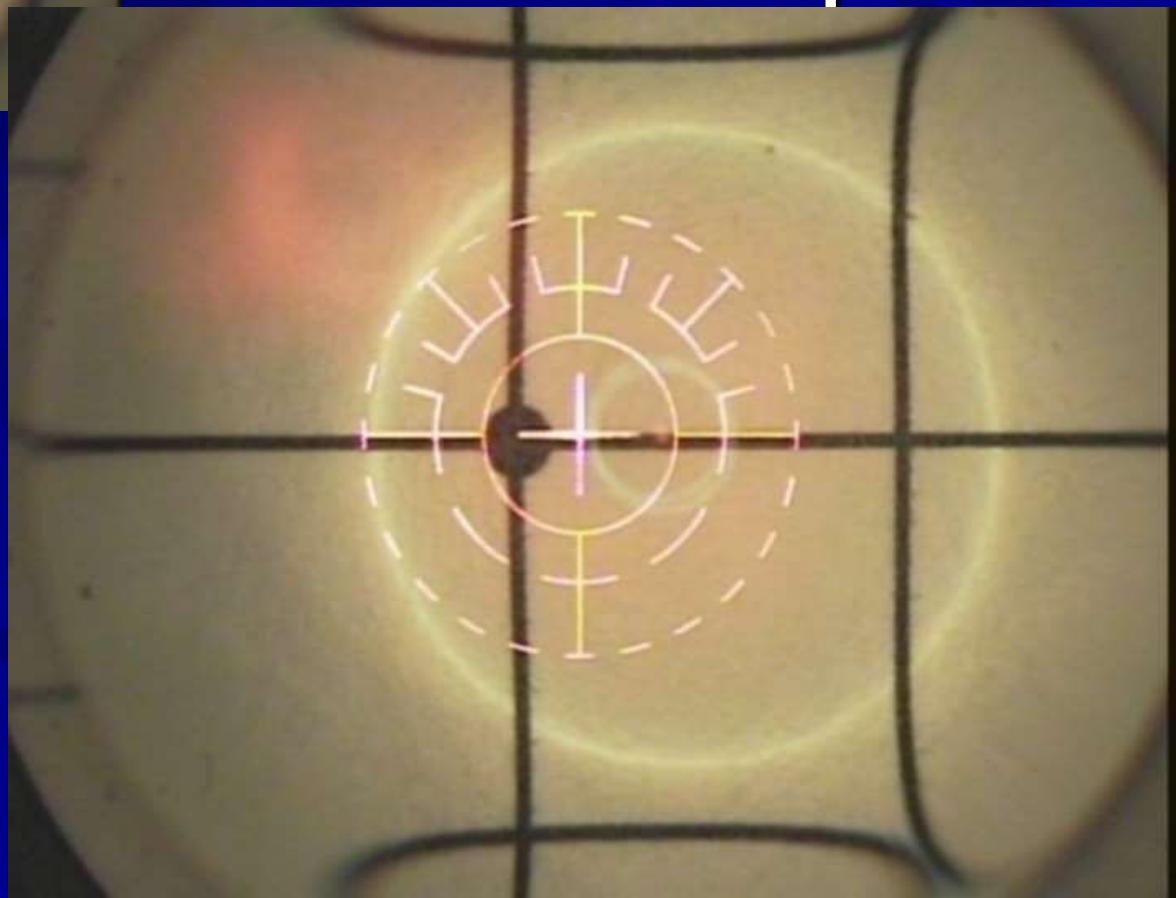

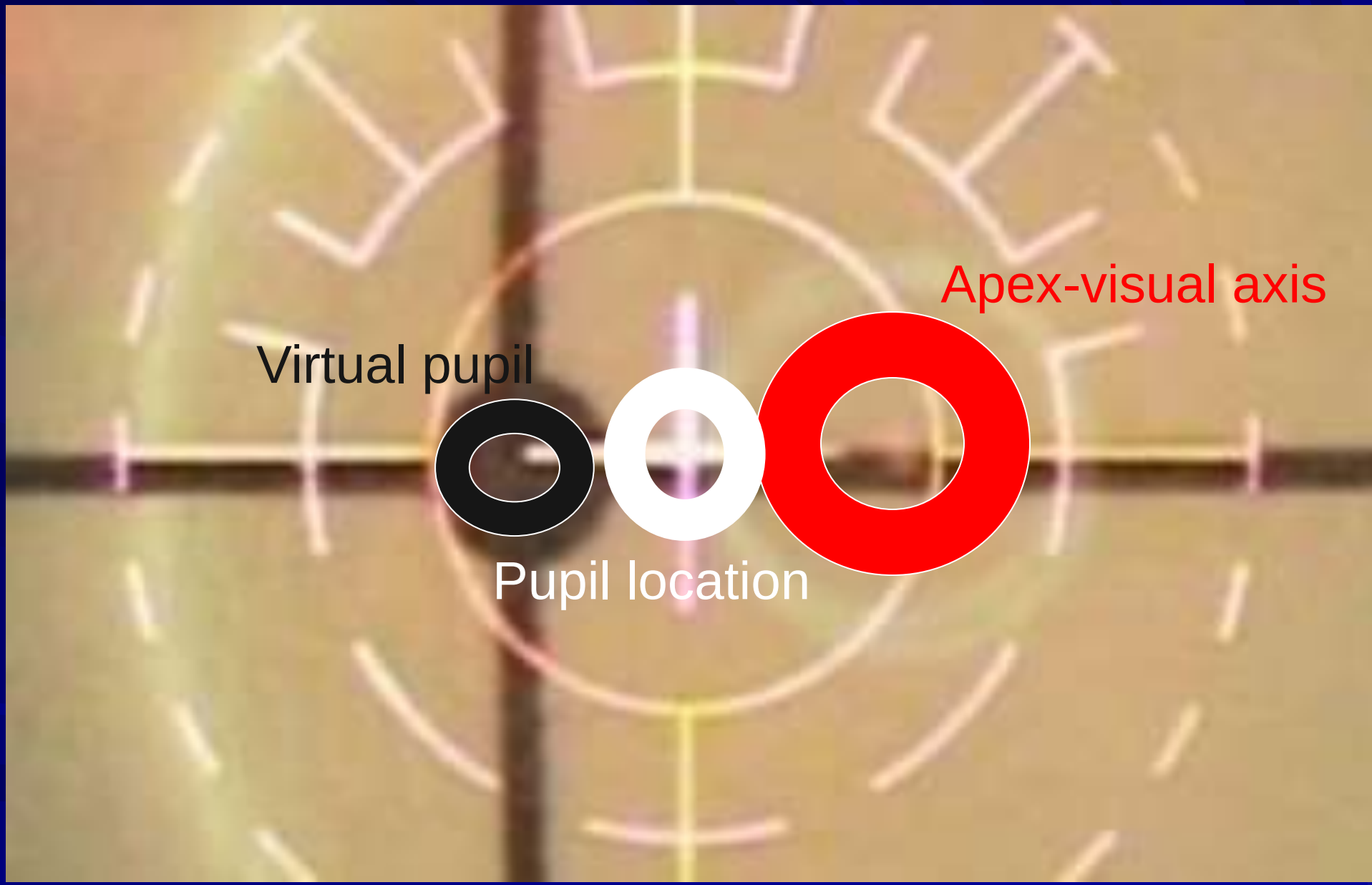
Apex-visual axis
Virtual pupil
Pupil location

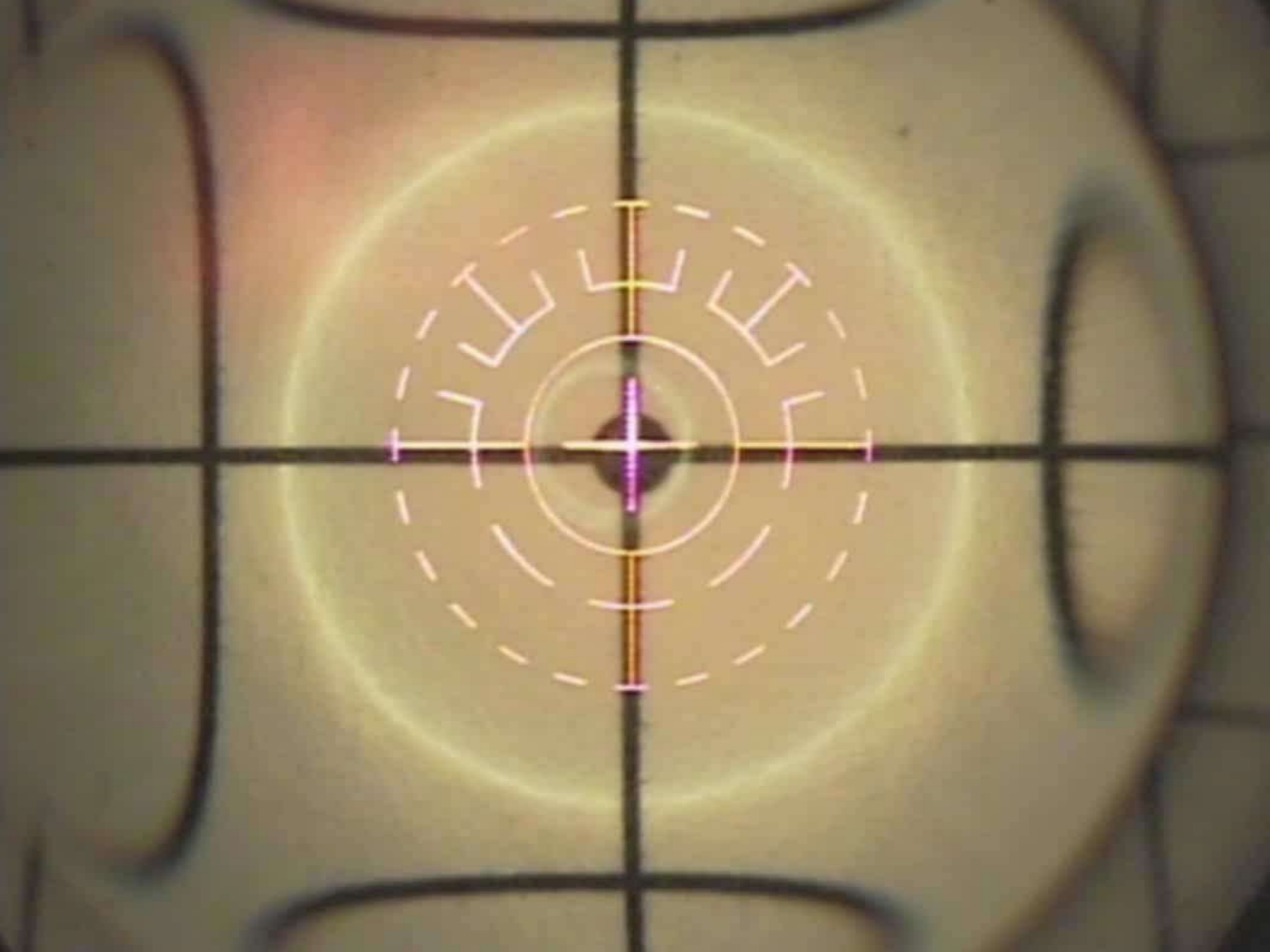

2015 Refractive Surgery

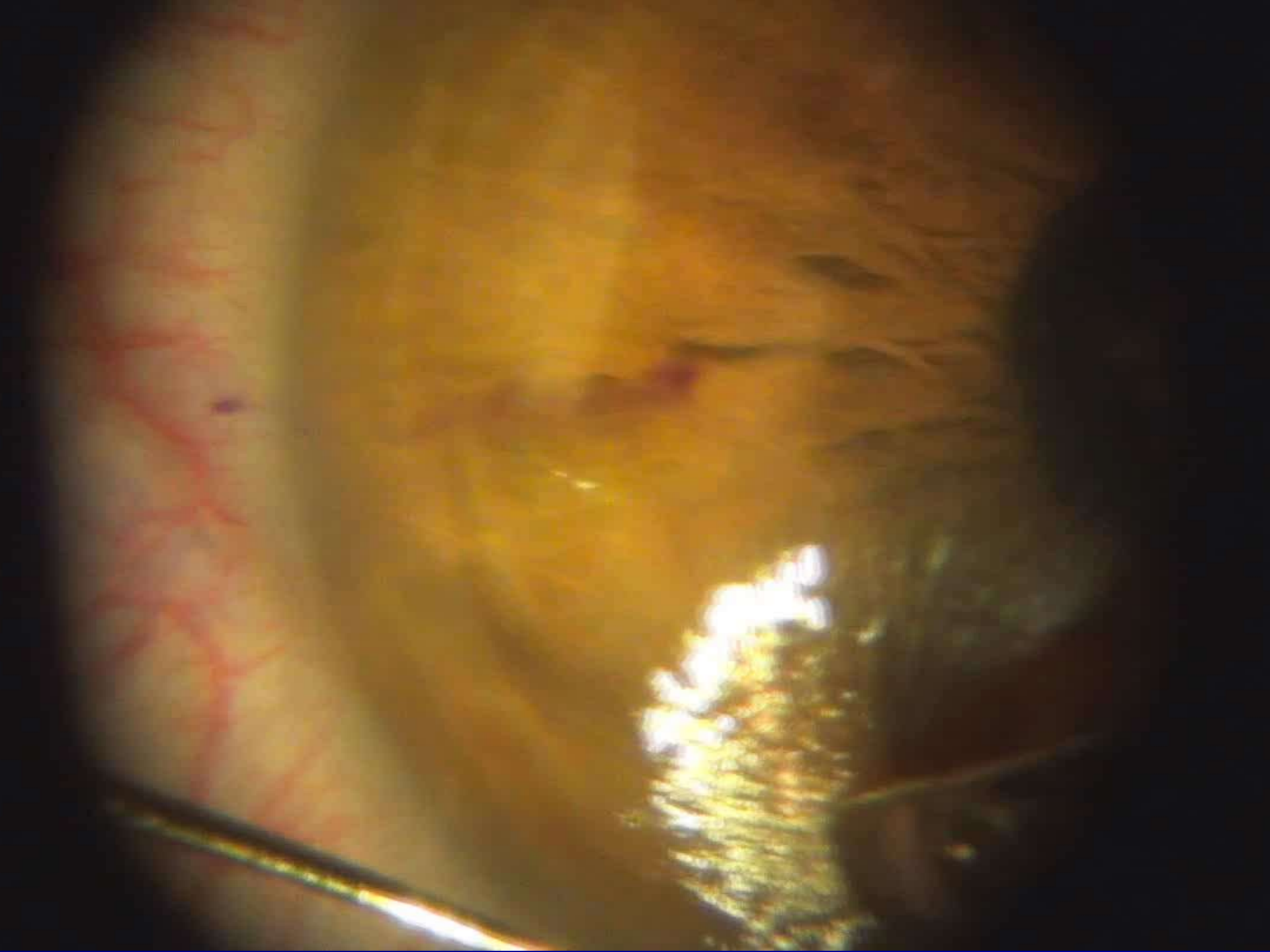

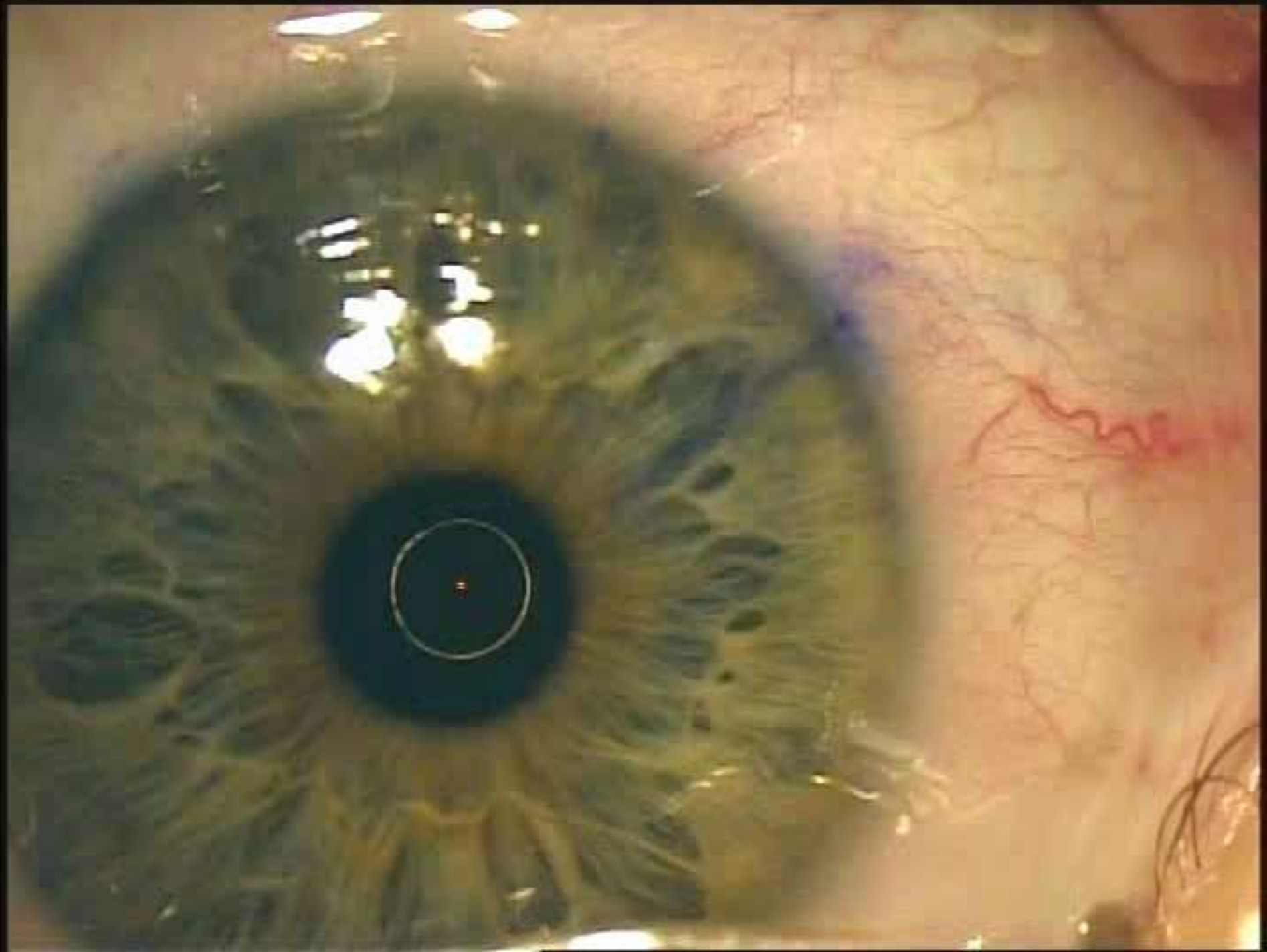

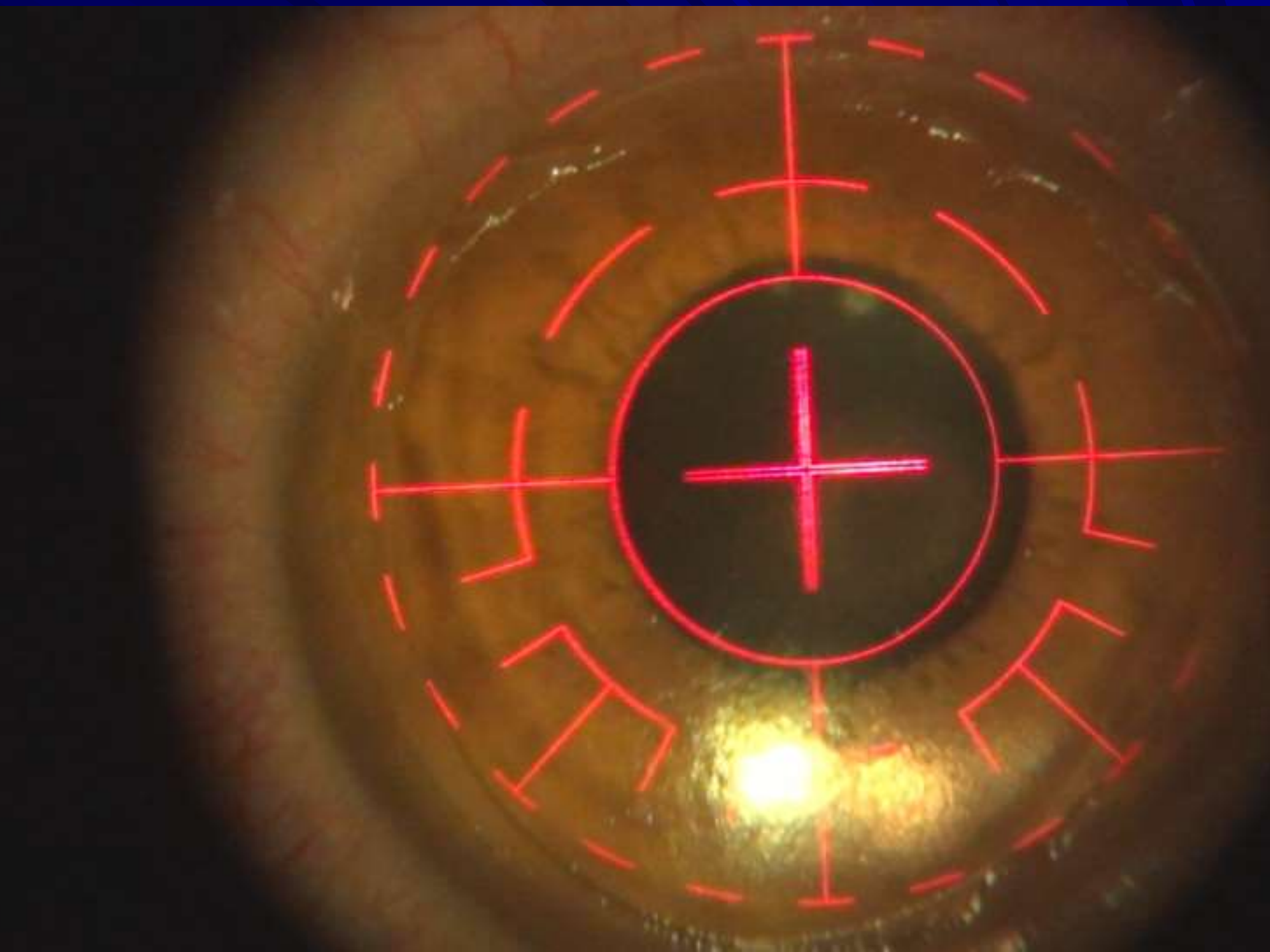

High cylinder with large angle K
Limbus truncated at 4:30

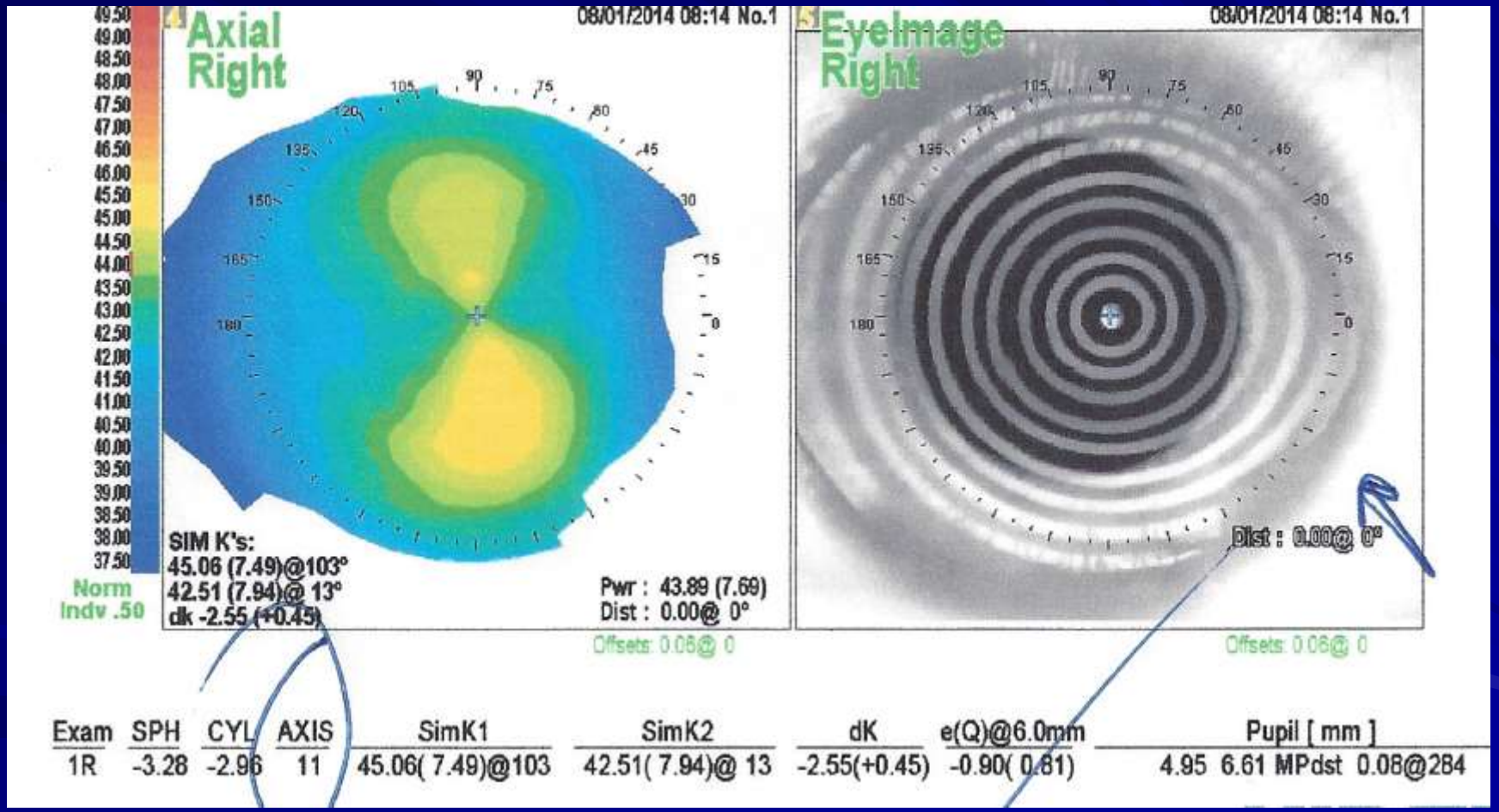

PRK: History of a Partial flap secondary to suction loss

Incomplete flap (suction loss)

- Of eyes with an incomplete flap, that achieved a CDVA of 20/20

  – 7 (87.5%) in the microkeratome laser group
  – 9 (90.0%) in the femtosecond laser group

  – JCRS,November 2010 Volume 36, Issue 11, Pages 1925–1933